UNIVERSITY
OF MICHIGAN
JUL 8 1957
ENGINEERING
LIBRARY

JOURNAL OF FLUID MECHANICS

VOLUME 2 PART 4

JUNE 1957

Printed and Published by

TAYLOR & FRANCIS LTD

RED LION COURT, FLEET STREET, LONDON, E.C.4

The JOURNAL OF FLUID MECHANICS exists for the publication of theoretical and experimental investigations of all aspects of the mechanics of fluids, and is issued in six parts per volume.

Editor:

Dr. G. K. BATCHELOR, Cavendish Laboratory, University of Cambridge, Cambridge, England.

Assistant Editors:

Dr. T. B. BENJAMIN, Dr. I. PROUDMAN.

Associate Editors:

Prof. G. F. CARRIER, Pierce Hall, Harvard University, Cambridge 38, Massachusetts, U.S.A.

Prof. W. C. GRIFFITH, Palmer Physical Laboratory, Princeton University, Princeton, New Jersey, U.S.A.

Prof. M. J. LIGHTHILL, Department of Mathematics, The University, Manchester, England.

Authors wishing to have papers published in the JOURNAL should communicate them to any one of the persons named above, choosing one in their own country where possible.

Authors are urged to ensure that their papers are written clearly and attractively, in order that their work will be readily accessible to readers.

Manuscripts should be typed in double spacing on one side of the paper only, with references listed at the end in alphabetical order of authors. Drawings should be done on a large scale in Indian ink on tracing cloth or drawing paper, captions being typed on a separate sheet. Proofs of papers from overseas will usually be despatched to authors by airmail. Authors are entitled to receive 50 offprints of a paper in the JOURNAL free of charge, and additional offprints can be purchased from the publisher.

PRICE £1 ($2.80) per part

Subscription, £5 10s. 0d. per volume of six parts, post free ($15.40 in U.S.A. and Canada)

Agents for U.S.A. and Canada:

Academic Press Inc., 111 Fifth Avenue, New York 3, N.Y., U.S.A.

Space-time double correlations and spectra in a turbulent boundary layer

By A. J. FAVRE, J. J. GAVIGLIO, and R. DUMAS
Laboratoire de Mécanique de l'Atmosphère, Université de Marseille

(*Received* 3 *September* 1956 *and in revised form* 30 *January* 1957)

SUMMARY

This paper describes the results of an experimental investigation of the turbulent boundary layer on a flat plate with zero pressure gradient, carried out at the Laboratoire de Mécanique de l'Atmosphère (I.M.F. Marseille). Transition to turbulent flow was obtained either by increasing the preturbulence upstream of the plate by means of a grid, or by a series of emery paper roughness elements beginning at the leading edge. The measurements were of the space-time double correlations, i.e. double velocity correlations with both spatial separation and time delay, from which isocorrelation lines for optimum delay can be drawn, and of the spectrum function, all for the longitudinal component of the velocity fluctuation.

1. EXPERIMENTAL APPLIANCES

Most of these have been described in previous papers (Favre, Gaviglio & Dumas, 1952, 1953 b, 1954 a, 1954 b).

The wind-tunnel has a complete return circuit, and is operated by two contra-rotating fans whose pitch is adjustable during operation. The fans are driven by two direct-current motors, fed by a 60 H.P. regulated ignitron rectifier, making it possible to change the rotation speed. The test section is 80 cm × 80 cm × 270 cm. There is a smooth contraction with an area ratio of 15; it is preceded by a settling chamber, in which five damping screens are set, and by a rapid expansion diffuser, with a screen analogous to that of the low-turbulence wind-tunnel of the R.A.E. (Squire, Winter & Barnes 1947). The natural intensity ratio of the turbulence in the test section is 0·00038 for a speed of 12·20 m/sec.

A flat plate made of glass (Favre, Gaviglio & Dumas 1954 a), 210 cm in length and 80 cm in width, and with a profiled leading edge, was hung in the test section. The measurements have been made, as previously, under the lower side of the plate at distances from the leading edge of about 80 cm and 194 cm.

y' and y are distances from the walls of the wires A (fixed) and B (adjustable); $X_3 = y' - y$ (figure 1); $CB = X_1$ is their separation in the direction of the general stream velocity; their separation X_2 parallel to the plate and normal to the stream is zero. T is the interval of time added to the instant of the signal corresponding to the fixed wire A.

The hot-wire probes used were either of an old pattern (diameter of the body 10 mm—see figure 1) or of a new type (diameter of the body 8 mm, with holders thinned and lengthened); the holders of the upstream probe were made lozenge-shaped in order to lessen the effects of the wake.

The platinum hot wire was made by the wollaston process with an etched length 7 μ in diameter and about 1 mm in length. In the position $z = 194$ cm, the new type of probe holder was used. This holder, fixed to the upper side of the plate, passed round the trailing edge and was supported on the lower side. It allowed variation of X_1, X_2, X_3.

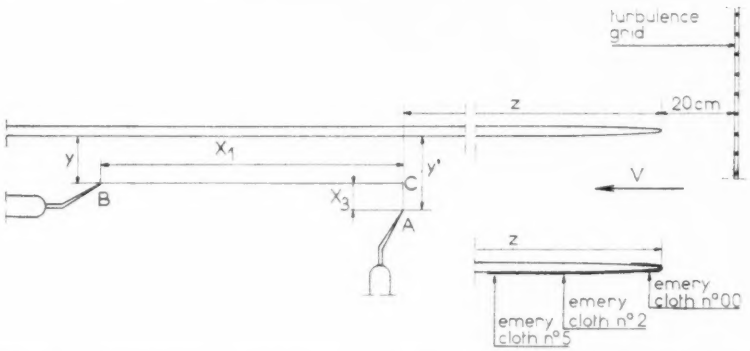

Figure 1. Experimental arrangement: transition by roughness on leading edge, or by preturbulence downstream of a grid.

Transition to turbulent flow in the boundary layer was obtained either by increasing the preturbulence of the stream by means of a biplane grid of mesh $M = 1$ in. with rods of circular section ($d = 0{\cdot}5$ cm) (Favre, Gaviglio & Dumas 1952) set at 20 cm upstream of the leading edge of the plate (figure 1), or by inserting, starting at this leading edge (figure 1), roughness in the form of emery cloth (no. 00 up to $z = 20$ cm, then no. 2 to $z = 30$ cm, and then no. 5 to $z = 40$ cm).

The principal measuring appliances were the hot-wire anemometers reproducing the oscillations, within $\pm 4\%$ in energy from 1 to 3500 hertz, the spectral analyser with a selectivity of 4·5% of the median frequency and a measuring band extending from 1 to 5000 hertz, and the apparatus for measurement of time and space correlations (Favre 1946, 1948; Favre, Gaviglio & Dumas 1953 a) with a band-pass extending from 1 to 2500 hertz. This latter apparatus records simultaneously, and reproduces with a relative delay, the two voltages coming from the two anemometers, and measures the time-correlation coefficient.

2. Checks on the measurements

We tried to check the influence of the disturbances due to the upstream wire (platinum wire, silver coating, needles, body of the probe) on the precision of measurements of the intensities of turbulence, the local mean

velocity and the space-time correlation (Favre, Gaviglio & Dumas 1955). With the old type of probes the disturbances in unfavourable conditions (upstream wire near the wall) may have reached 10% of the turbulence intensities, 5% of the mean velocity, and 0·05% of the space-time correlation. With the new type probes these disturbances seemed to be reduced to 4% for intensities and to 1% for the mean velocity.

We have verified, thanks to a method proposed by H. W. Liepmann (1952), that the length of the hot wires had a negligible influence on the measurements of space-time correlation (for these experimental investigations, the minimum value of the dissipation length λ was 2·5 mm).

3. Mean velocities

The velocity $V_{\max}$ outside the boundary layer was 12·00 m/sec. In the case of the measurements made at $x = 79$ cm, with hot-wire holders, the mean gradient of static pressure is negative and less than 4% per metre. For the measurements made at $x = 194$ cm, with the new holders, the mean gradient is negative and less than 1% per metre downstream of the roughness.

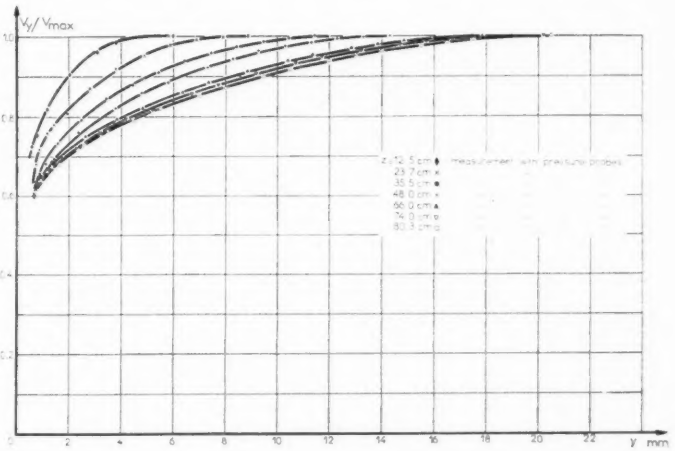

Figure 2. Mean velocity in the boundary layer on a flat plate downstream of a grid.

In the case of the boundary layer on a flat plate downstream of a turbulence grid, the relative velocities $V_y/V_{\max}$ were determined as a function of the distance y from the wall, for $x = 12{\cdot}5$, 23·7, 35·5, 48·0, 66·0, 74·0, 80·3 cm, and the results are shown in figure 2. The thickness of the boundary layer at 79 cm from the leading edge was 16·8 mm.

In the case of the boundary layer on a flat plate with a rough leading edge, the velocity profiles were measured, in the absence of the hot-wire holders, at $x = 58{\cdot}5$, 79·0, 167·5 and 194·0 cm, and are given in figure 3. A supplementary curve has been drawn to show the effect of the presence

of the holders. The velocity V_y in the vicinity of the wall was determined at $z = 194$ cm by means of a hot wire. The thickness of boundary layer in this case was 17·5 mm at $z = 79$ cm, and 34 mm at $z = 194$ cm.

In figure 4 we have represented the displacement thickness δ^* and the momentum thickness θ as functions of the distance z from the leading edge. The roughness set on the leading edge brings about a marked increase in the thickness of the boundary layer.

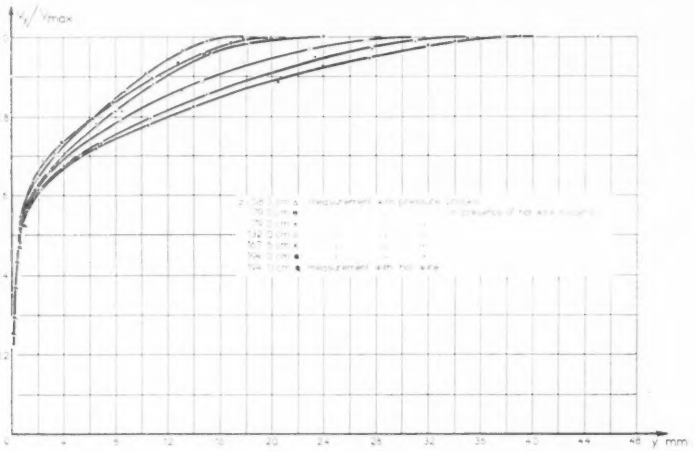

Figure 3. Mean velocity in the boundary layer on a flat plate with a rough leading edge.

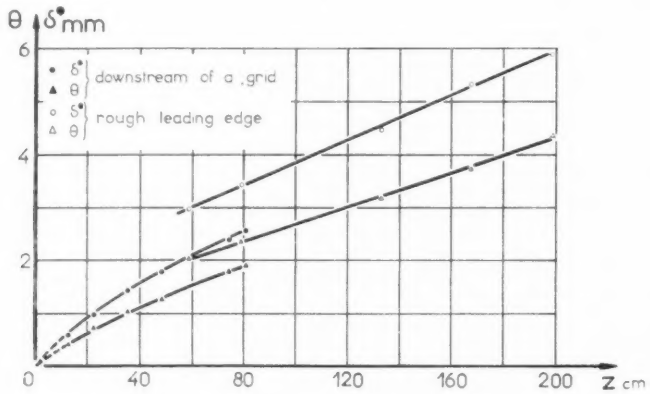

Figure 4. Displacement thickness δ^* and momentum thickness θ.

Figure 5 shows Clauser's universal velocity profile (Clauser 1954). In this figure, $V_* = \sqrt{(\tau_0/\rho)}$ with $\tau_0 = \rho V_{\max}^2 \, d\theta/dz$, and the value of δ corresponds to $V_y/V_{\max} \doteq 1$. In the case of transition obtained by preturbulence (in the presence of the old type of wire holders, the mean

pressure gradient being 4% per metre) the data are not wholly consistent with the curve, but in the case of transition obtained by roughness (with the new type of holders, the mean pressure gradient being 1% per metre) the agreement between the data and the curve is fairly good.

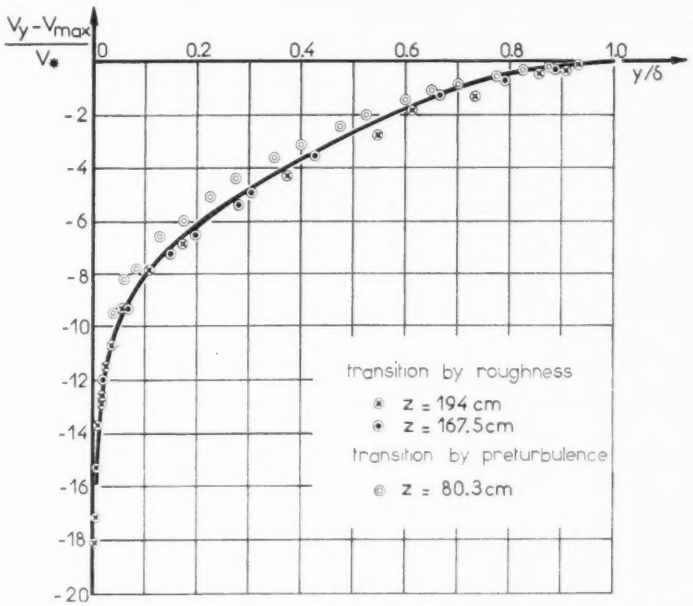

Figure 5. Comparison of measured velocities with Clauser's universal profile.

4. Intensities and spectra

In the case of transition by preturbulence, the intensities as functions of the distance y/δ have been given previously (Favre, Gaviglio & Dumas 1954a). The intensity $\sqrt{(\overline{\tau_1^2})}/U_y$ reaches 15% for $y/\delta = 0{\cdot}06$, which may be compared with the value 1·8% for the intensity of free turbulence at a great distance from the wall. In the case of the transition by roughness, two series of measurements have been made, at $z = 79$ cm and $z = 194$ cm. The intensity, as a fraction of the local mean velocity, seems to decrease more rapidly at $z = 194$ cm than at $z = 79$ cm when y/δ increases. At $z = 79$ cm, it reaches 18% for $y/\delta = 0{\cdot}06$, that of the free turbulence being of the order of 0·045%.

The spectral functions of turbulence energy $F(n)$ (Taylor 1938) are obtained as functions of the frequency n; directly by selective amplification, and indirectly by Fourier transformation of the auto correlation curves.

The areas of the curves $F(n)$ have been chosen so as to be equal for the common intervals of frequencies.

In the case of transition by preturbulence, the spectra have been published previously (Favre, Gaviglio & Dumas 1954a). They correspond

to $z = 79$ cm. The difference between these spectra inside and outside the boundary layer is small, except for low frequencies (less than 40 hertz) where they change markedly as functions of the distance from the wall, thus disclosing an increase of energy in the boundary layer.

In the case of transition by roughness, unlike the previous case, the intensity of turbulence is very low outside the boundary layer (0·045%). Figure 6 shows the spectra measured at 79 cm from the leading edge for

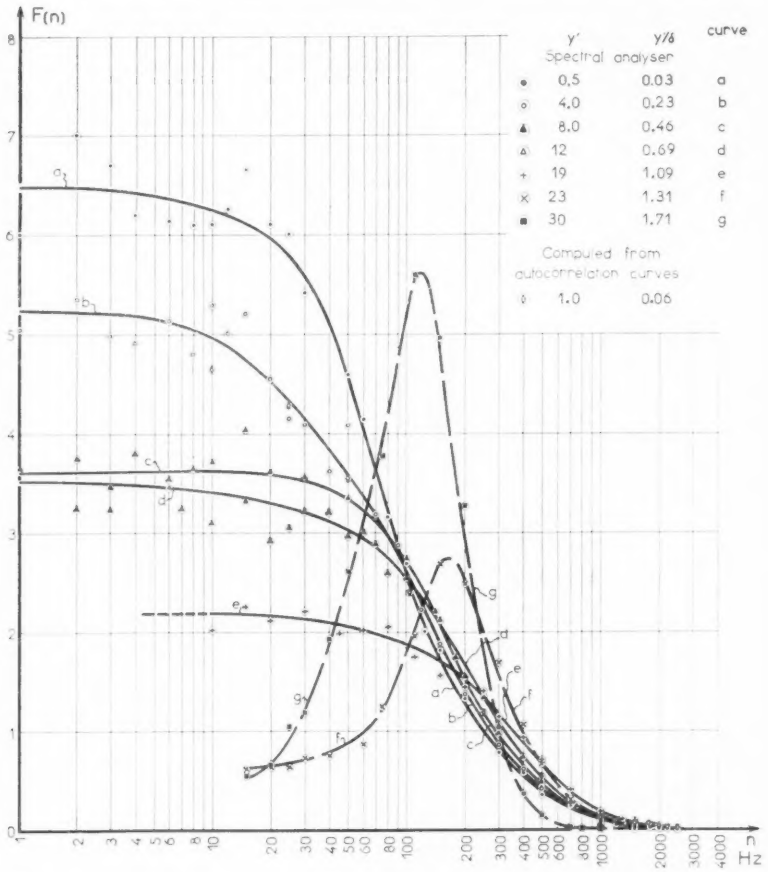

Figure 6. Turbulence spectra in the boundary layer on a flat plate with rough leading edge. ($R_\delta = 14\,500$, $z = 79$ cm).

different distances y from the plate. Inside the boundary layer the evolution at frequencies greater than 80 hertz is slight; for the lower frequencies the curves show an increase of energy as y/δ decreases. Outside the conventional boundary layer, at $y/\delta = 1{\cdot}31$ and $y/\delta = 1{\cdot}71$ (the factor of intermittance there being markedly smaller than 0·04 according to

Corrsin & Kistler (1954)), the spectra become different; each of them presents a marked maximum. At the distance $z = 194$ cm from the leading edge (figure 7) the results are qualitatively the same, but with lower frequencies, which corresponds to the increase of the scale of turbulence with the thickness of the boundary layer. Outside the boundary layer, for instance, at $y/\delta = 1{\cdot}35$ and $y/\delta = 1{\cdot}77$, a marked maximum was found as in the previous case.

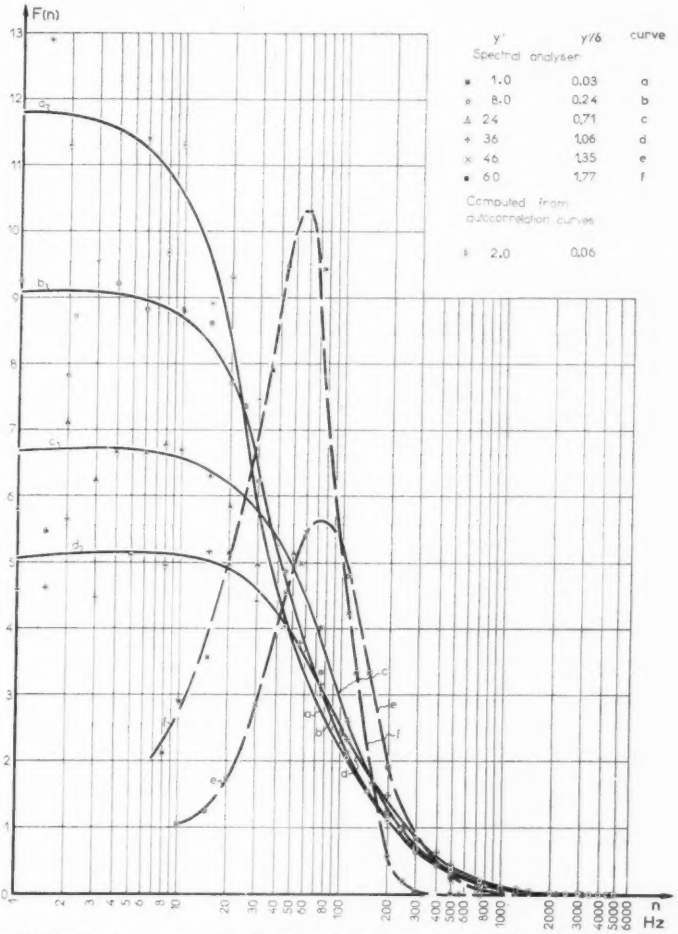

Figure 7. Turbulence spectra in the boundary layer on a flat plate with rough leading edge. ($R_\delta = 28\,000$, $z = 194$ cm).

The intensities of these fluctuations outside the boundary layer are 0·47% and 0·17% respectively for $y/\delta = 1{\cdot}31$ and 1·71 ($z = 79$ cm), and 0·38% and 0·13% for $y/\delta = 1{\cdot}35$ and 1·77 ($z = 194$ cm). Thus, they do not seem to be due to the preturbulence, the intensity of which is of 0·045%.

When we inserted a small thin plate (4·2 cm × 12·5 cm) parallel to the wall, at $y/\delta = 1{\cdot}25$, between the hot wire placed at $y/\delta = 1{\cdot}8$ ($z = 79$ cm) and this wall, the intensity was reduced by more than half and this phenomenon was no longer detected.

It may be that these fluctuations are induced by random motion at the edge of the boundary layer (Phillips 1954).

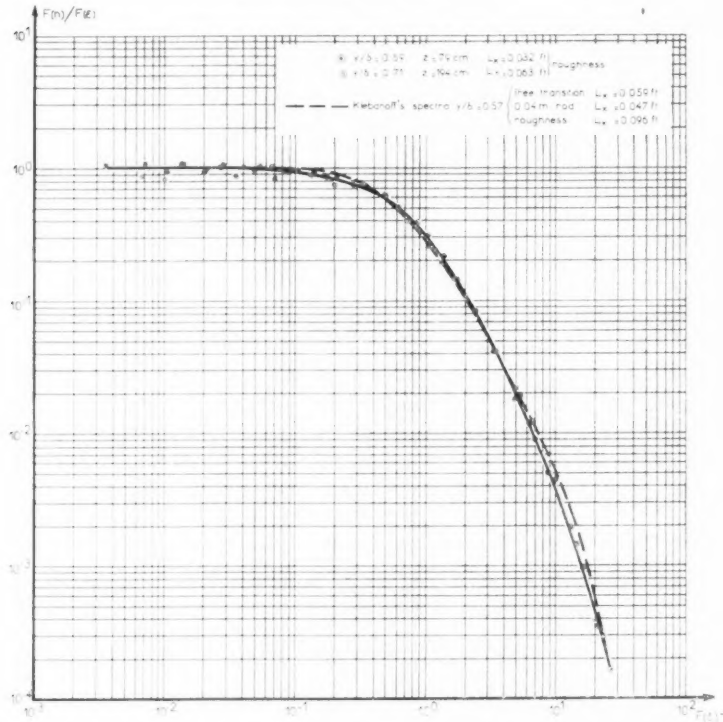

Figure 8. Comparison of turbulence spectra in several boundary layers on flat plates.

We have compared (figure 8) the spectra obtained for $z = 79$ cm and $z = 194$ cm (y/δ having respectively the neighbouring values 0·69 and 0·71), with Klebanoff & Diehl's (1952) spectra. The ordinates and abscissae in figure 8 are $F(n)/F(\epsilon)$ and $nF(\epsilon)/F(\epsilon)$, $F(\epsilon)$ being the average value corresponding to the lowest frequencies. The results are fairly consistent.

5. Measurements of space-time correlations

First consider the measurements of transverse space-time correlations $R_{11}(T, X_1 = 0, X_2 = 0, X_3)$.

In the case of transition by preturbulence, the transverse space-time correlation $R_{11}(T, X_1 = 0, X_2 = 0, X_3)$ is represented in figures 9 to 12.

The data for these figures are:

figure 9, $y'/\delta = 0{\cdot}06$, $y' = 1$ mm, $z = 79$ cm;
figure 10, $y'/\delta = 0{\cdot}06$, $y' = 1$ mm, $z = 74$ cm;
figure 11, $y'/\delta = 0{\cdot}24$, $y' = 4$ mm, $z = 79$ cm;
figure 12, $y'/\delta = 0{\cdot}71$, $y' = 12$ mm, $z = 79$ cm.

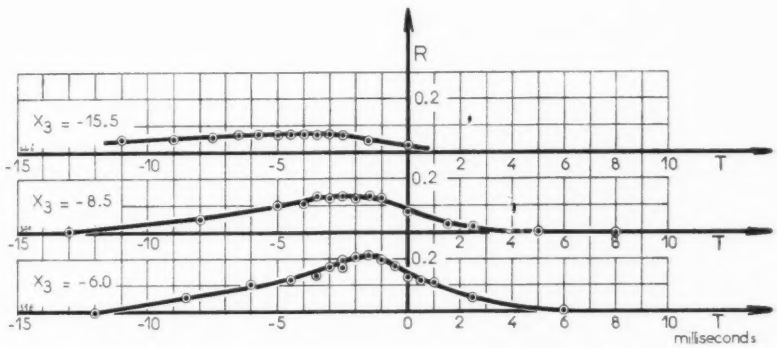

Figure 9. Transverse space-time correlations in the boundary layer on a flat plate downstream of a grid. ($y' = 1$ mm, $z = 79$ cm, $\delta = 16{\cdot}8$ mm).

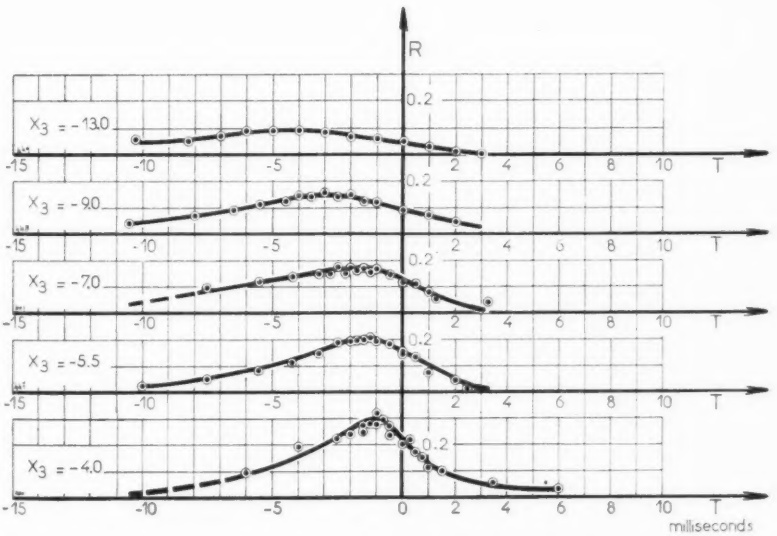

Figure 10. Transverse space-time correlations in the boundary layer on a flat plate downstream of a grid. ($y' = 1$ mm, $z = 74$ cm, $\delta = 16{\cdot}0$ mm).

One finds that the correlation reaches a maximum for a value T_i of the delay which is a function of X_3. Figure 13 summarizes the values of T_i. Note that for the distances from the leading edge $z = 74$ cm and $z = 79$ cm, which differ only by 3δ, the values of T_i are very little different. Note also that T_i changes sign with $X_3 = y' - y$.

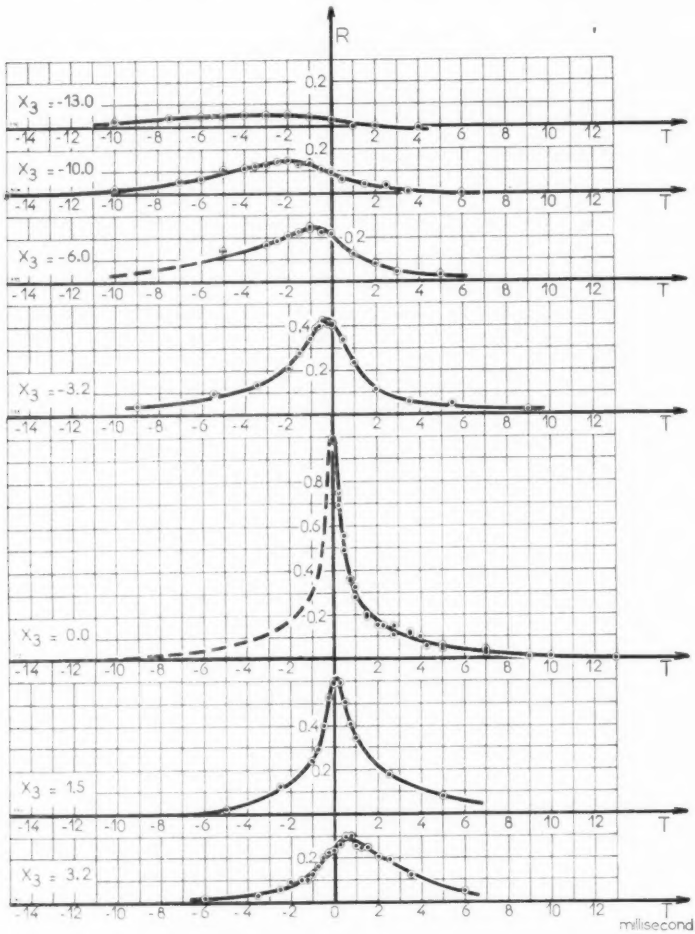

Figure 11. Transverse space-time correlations in the boundary layer on a flat plate downstream of a grid. ($y' = 4$ mm, $z = 79$ cm, $\delta = 16{\cdot}8$ mm).

In the case of the transition by roughness, the measurements have been made at two different stations, at distances $z = 79$ cm and $z = 194$ cm from the leading edge. The measurements of $R_{11}(T, X_1 = 0, X_2 = 0, X_3)$ at

the distance $x = 79$ cm are represented in figures 14 to 16, for which the data are:

figure 14, $y'/\delta = 0{\cdot}06$, $y' = 1$ mm;
figure 15, $y'/\delta = 0{\cdot}23$, $y' = 4$ mm;
figure 16, $y'/\delta = 0{\cdot}69$, $y' = 12$ mm.

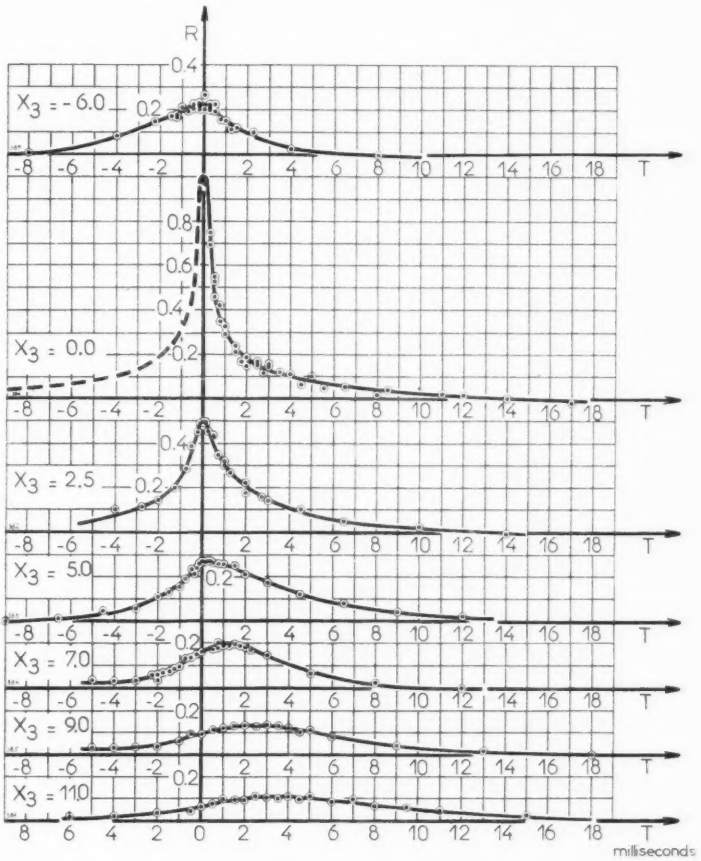

Figure 12. Transverse space-time correlations in the boundary layer on a flat plate, downstream of a grid. ($y' = 12$ mm, $x = 79$ cm, $\delta = 16{\cdot}8$ mm).

The measurements at the distance $x = 194$ cm are represented in figures 17 to 19, for which the data are:

figure 17, $y'/\delta = 0{\cdot}06$, $y' = 2$ mm;
figure 18, $y'/\delta = 0{\cdot}23$, $y' = 8$ mm;
figure 19, $y'/\delta = 0{\cdot}69$, $y' = 24$ mm.

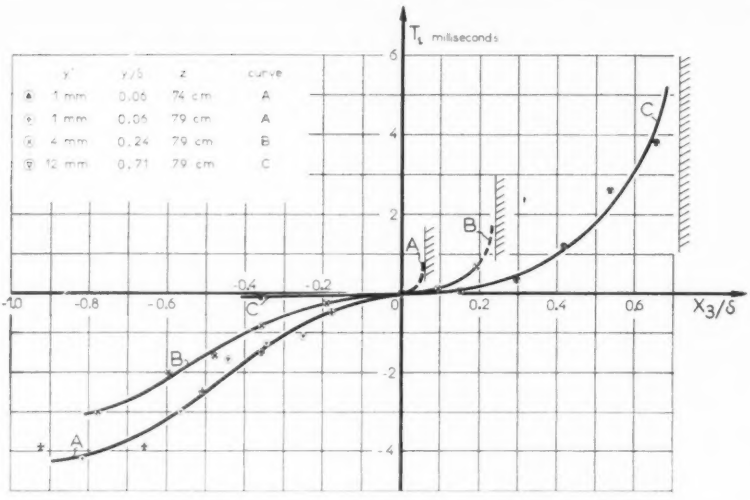

Figure 13. Optimum delays $T = T_i$ for transverse space-time correlations in the boundary layer on a flat plate downstream of a grid.

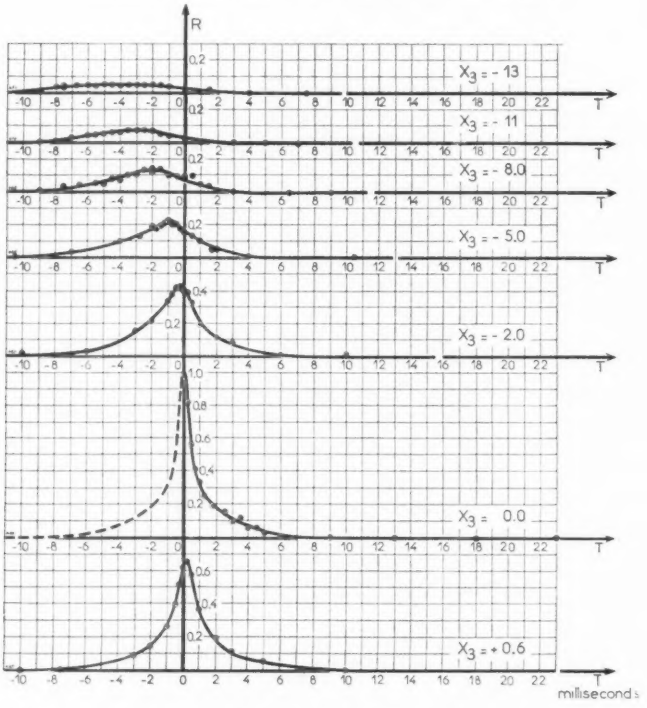

Figure 14. Transverse space-time correlations in the boundary layer on a flat plate with rough leading edge ($y' = 1$ mm $z = 79$ cm, $\delta = 17{\cdot}5$ mm).

As in the case of transition by preturbulence, one finds that the correlation reaches a maximum for a value T_i of the delay which is a function of X_3. Figure 20 summarizes the values of T_i which change sign with X_3.

The values of T_i obtained at the distances $z = 74$ cm and $z = 79$ cm from the leading edge and for a thickness of the boundary layer of the same order are only slightly different, whether the transition is due to preturbulence (figure 13) or roughness (figure 20). Also, the curves for the distribution of the corresponding mean velocities are also only slightly different.

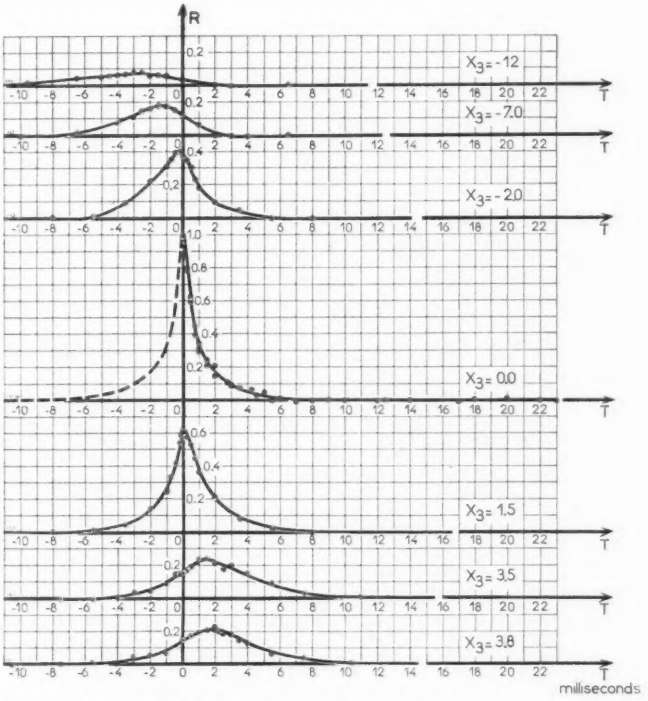

Figure 15. Transverse space-time correlations in the boundary layer on a flat plate with rough leading edge ($y' = 4$ mm, $z = 79$ cm, $\delta = 17{\cdot}5$ mm).

The measurements of T_i made at the two distances $z = 79$ cm and $z = 194$ cm (distances which differ by about 45 times the average thickness of the boundary layer) show that, X_3 being fixed, the delay T_i generally increases with the distance z from the leading edge, in the direction of increasing thickness of the boundary layer. Moreover, this increase of T_i is much smaller than the differences of the delays τ_y corresponding to the transport due to the mean motion, if one considers this transport over the distance separating the position $z = 79$ cm from the position $\dot{z} = 194$ cm (this delay, along the isochronous lines is $\tau_{y'} - \tau_y = (\dot{z} - z)(1/V' - 1/V)$).

y'/δ	y/δ	$\tau_{y'}-\tau_y$ (ms)	$(T_i)_z-(T_i)_z$ (ms)	$\frac{\tau_{y'}-\tau_y}{(T_i)_z-(T_i)_z}$
0·06	0·76	68	3·2	21
	0·46	56	2·2	25
	0·26	43	1·3	33
0·23	0·63	23	1·3	18
	0·43	13·5	0·6	32
	0·13	9·4	0·3	31
	0·03	54	0·05	1000
0·69	0·49	8·5	0·45	19
	0·29	22	1·25	18
	0·09	47	1·6	29

Table 1.

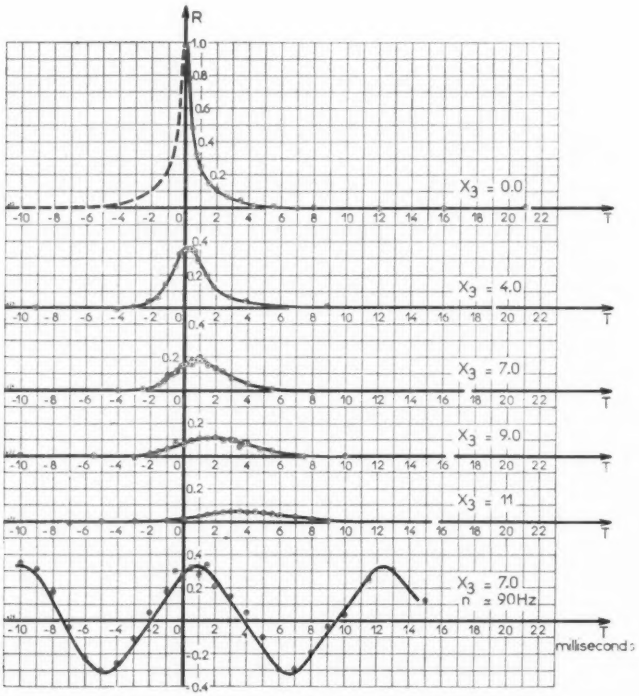

Figure 16. Transverse space-time correlations in the boundary layer on a flat plate with rough leading edge ($y' = 12$ mm, $z = 79$ cm, $\delta = 17{\cdot}5$ mm).

Table 1 gives this comparison, in the case of the distances z mentioned above.

Measurements of $R_{11}(T, X_1 = 0, X_2 = 0, X_3)$ have also been made by means of a double analyser which admitted only the waves of frequencies of about 90 hertz. When $z = 79$ cm, $y'/\delta = 0{\cdot}69$, $X_3/\delta = 0{\cdot}40$ ($nF(\epsilon) \doteqdot 0{\cdot}32$), we see from figure 16 that the maximum correlation 0·33 is reached for a delay T_i of about 0·95 ms. When $z = 194$ cm, $y'/\delta = 0{\cdot}71$, $X_3/\delta = 0{\cdot}38$ ($nF(\epsilon) \doteqdot 0{\cdot}60$), figure 19 shows that the maximum correlation 0·22 is reached for a delay T_i of about 2·2 ms. So, in both cases, the value of T_i is not practically modified, and that of the correlation is increased by filtering, but this is not very significant because these frequencies are in the middle of the spectrum.

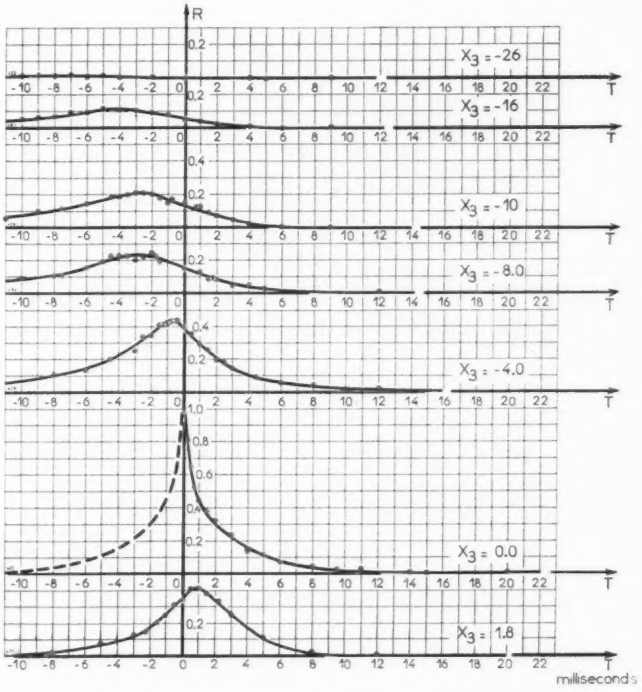

Figure 17. Transverse space-time correlations in the boundary layer on a flat plate with rough leading edge ($y' = 2$ mm, $z = 194$ cm, $\delta = 34$ mm).

We turn now to the longitudinal space-time correlations $R_{11}(T, X_1, X_2 = 0, X_3 = 0)$. Let us recall that we tried (Favre, Gaviglio & Dumas 1953 b) to obtain a verification of Taylor's hypothesis for the turbulence downstream of a grid, and found a satisfactory concordance of the autocorrelation curves with the curves of longitudinal space correlation, established up to a distance X_1/M of about 8, with the

correspondence $T = X_1/V$; but for distances $X_1/M > 1{\cdot}5$, the correlations being smaller than 0·1, the comparison is no longer conclusive.

Further verification, including measurements of the longitudinal space-time correlations (up to $X_1/M = 8$) with optimum delay to compensate for the transport due to the mean flow, has shown that these correlations retain high values, of the order of 0·5, up to great distances $X_1/M = 5$ to 8, these values not being, however, equal to unity.

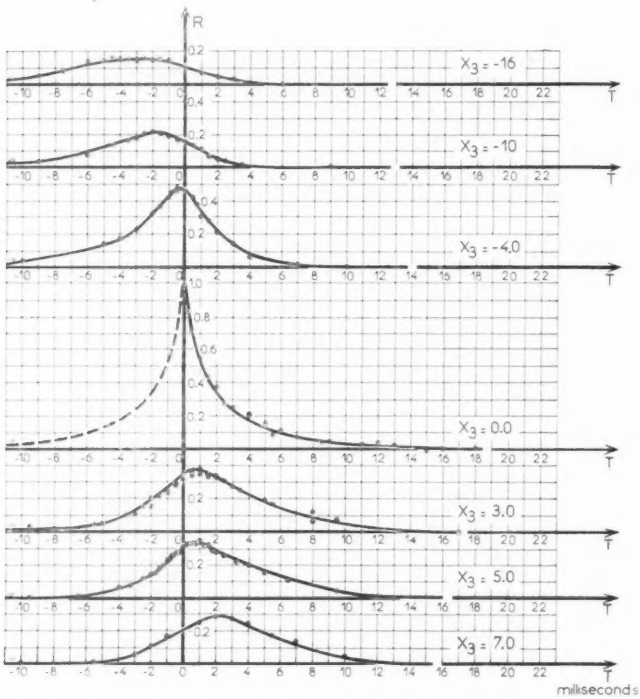

Figure 18. Transverse space-time correlations in the boundary layer on a flat plate with rough leading edge ($y' = 8$ mm, $x = 194$ cm, $\delta = 34$ mm).

In the conditions of the present experiments relating to the boundary layer, with transition by preturbulence, we have attempted a similar comparison, with a view to a possible extension of Taylor's hypothesis.

Figure 21 presents, for $y'/\delta = 0{\cdot}24$, the comparison of the two auto-correlation curves $R_{11}(T, X_1 = X_2 = X_3 = 0)$ (at positions $x = 74$ cm and $x = 79$ cm) with the longitudinal correlation curve $R_{11}(T = 0, X_1, X_2 = X_3 = 0)$ obtained along a line $X_3 = 0$, which here is not very different from the streamline. In this case there is still a satisfactory concordance between

the autocorrelation and the longitudinal space correlation, established up to X_1/M of about 2·5 (i.e. $X_1/V = 5{\cdot}2$ ms), but for $X_1/M \geqslant 2$ (or $X_1/V \geqslant 4$ ms), the correlations being smaller than 0·1, the comparison is no longer conclusive.

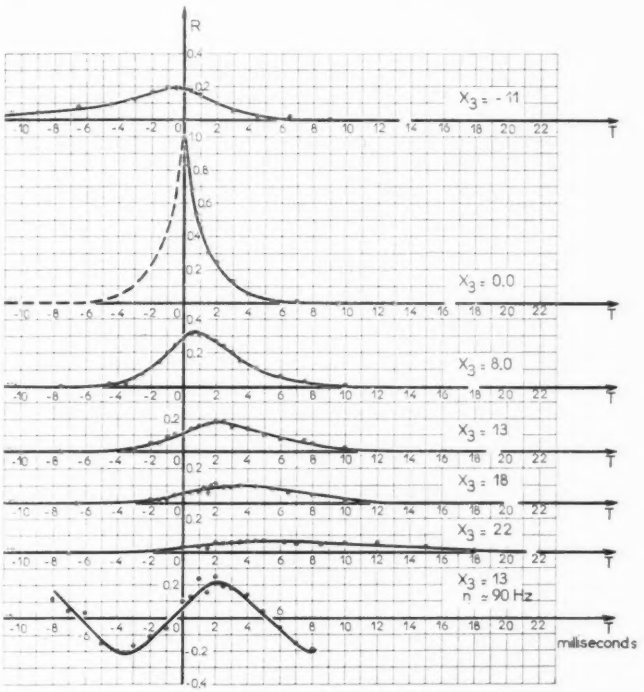

Figure 19. Transverse space-time correlations in the boundary layer on a flat plate with rough leading edge ($y' = 24$ mm, $z = 194$ cm, $\delta = 34$ mm).

y'/δ	1	0·71	0·24	0·06
$(X_1/M)_{R=0{\cdot}5}$	5 to 8	5·0	1·6	0·8
$(X_1/\delta)_{R=0{\cdot}5}$	7·5 to 12	7·5	2·4	1·2

Table 2.

Further verification, including the measurement of the longitudinal and transverse space-time correlations $R_{11}(T, X_1, X_2 = 0, X_3)$ along the line of maximum correlation, with an optimum delay $T = T_m$ (see below), shows (figure 30) that this correlation retains high values of the order of 0·5 up to the distances $(X_1/\delta)_{R=0{\cdot}5}$ or $(X_1/M)_{R=0{\cdot}5}$ given in table 2, but these distances decrease rapidly with the distance y'/δ of the upstream wire from the wall.

Measurements of the longitudinal and transverse space-time correlations $R_{11}(T, X_1, X_2 = 0, X_3)$ have been made in the case of the transition by preturbulence, using the old type of probes. The upstream hot wire A was fixed, at a distance $x = 74$ cm from the leading edge, and at a distance y' from the wall. The hot wire B was placed at the distance X_1 downstream

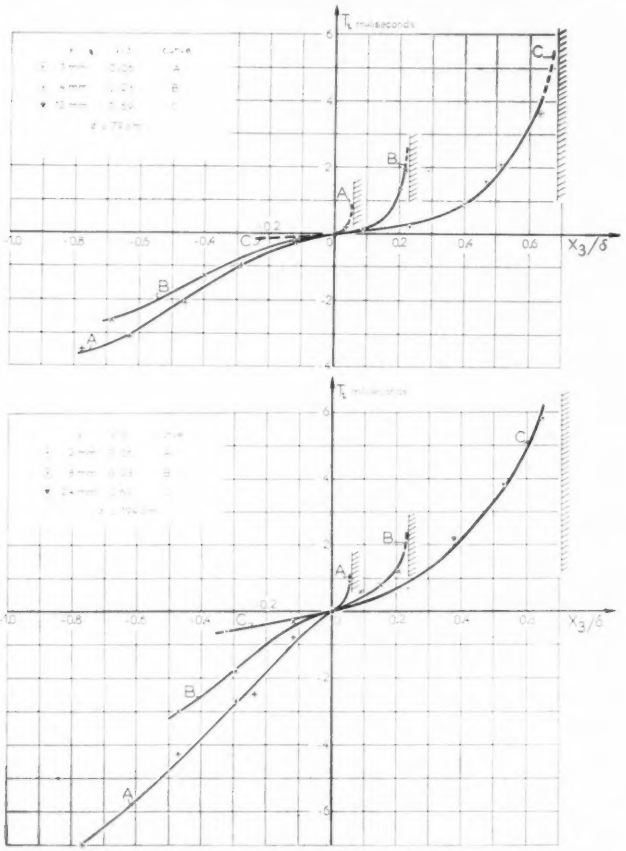

Figure 20. Optimum delays $T = T_i$ for transverse space-time correlations in the boundary layer on a flat plate with rough leading edge.

of A. Its distance y to the wall and consequently X_3, was varied. The delay T was also varied. The results are presented in figures 22 to 25, which correspond to the following conditions:

figure 22, $y'/\delta = 0{\cdot}06$, $y' = 1$ mm, $X_1 = 25{\cdot}4$ mm;
figure 23, $y'/\delta = 0{\cdot}06$, $y' = 1$ mm, $X_1 = 50{\cdot}8$ mm;
figure 24, $y'/\delta = 0{\cdot}24$, $y' = 4$ mm, $X_1 = 25{\cdot}4$ mm;
figure 25, $y'/\delta = 0{\cdot}24$, $y' = 4$ mm, $X_1 = 50{\cdot}8$ mm.

They follow the results published (Favre, Gaviglio & Dumas 1954b) for the conditions $y'/\delta = 0{\cdot}71$, $y' = 13$ mm, $X_1 = 49$ mm. The correlation is found to reach a maximum for an optimum value T_m of the delay, which is a function of X_3.

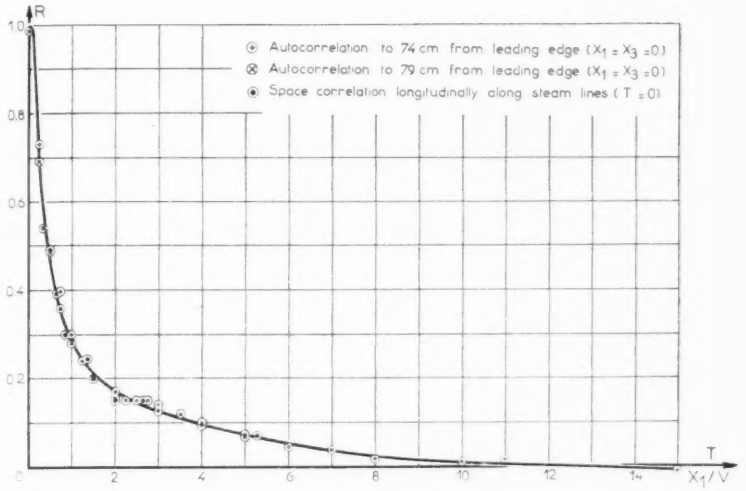

Figure 21. Check on Taylor's hypothesis for the boundary layer on a flat plate downstream of a grid ($y' = 4$ mm, $y/\delta = 0{\cdot}24$).

Figure 26 gives the values of T_m and their comparison with the computed values. The computation is made as previously (Favre, Gaviglio & Dumas 1954b), that is, by assuming (as a first approximation in the case of these experiments) that *the optimum delays T_m differ from the delays T_i by time intervals which are equal to the delays T_c compensating for the transport due to the mean flow** ;

$$T_m \sim T_i + T_c.$$

This relation is still satisfactory when, the upstream wire being at a distance from the wall $y'/\delta = 0{\cdot}24$, the downstream wire itself is at a distance $y/\delta \geqslant 0{\cdot}04$; also when $y'/\delta = 0{\cdot}06$ for $y/\delta \geqslant 0{\cdot}09$. For shorter distances, the relation is less satisfactory, either on account of the disturbances brought about by the probe or because supplementary terms should be introduced.

Figures 27 and 28 indicate that, as we have shown elsewhere (Favre, Gaviglio & Dumas 1954b), the introduction of the optimum delay T_m increases the correlation in a large proportion (of the order of 2·55 to 5·5 in the cases examined). The ***maximum maximorum*** of the space-time correlations, $R_{\max}(T = T_m, X_1, X_2 = 0, X_3)$, corresponding to given X_1, is

* T_c is given, to a sufficient approximation, by $T_c = 2X_1/(V_A + V_B)$.

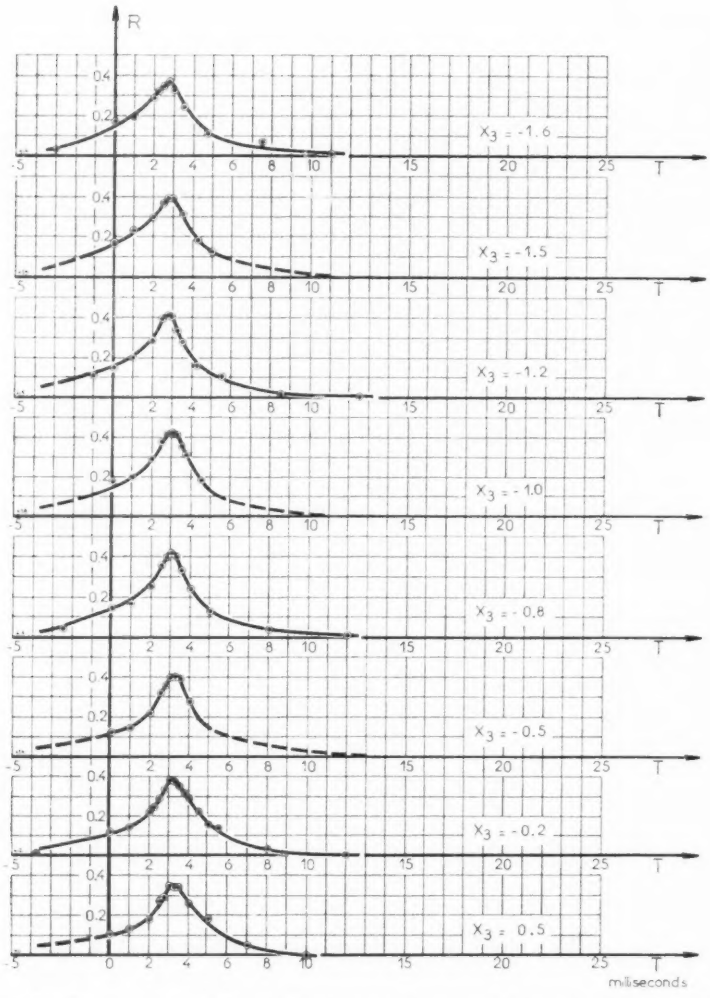

Figure 22. Transverse and longitudinal space-time correlations in the boundary layer on a flat plate downstream of a grid ($y' = 1$ mm, $y'/\delta = 0{\cdot}06$, $X_1 = 25{\cdot}4$ mm).

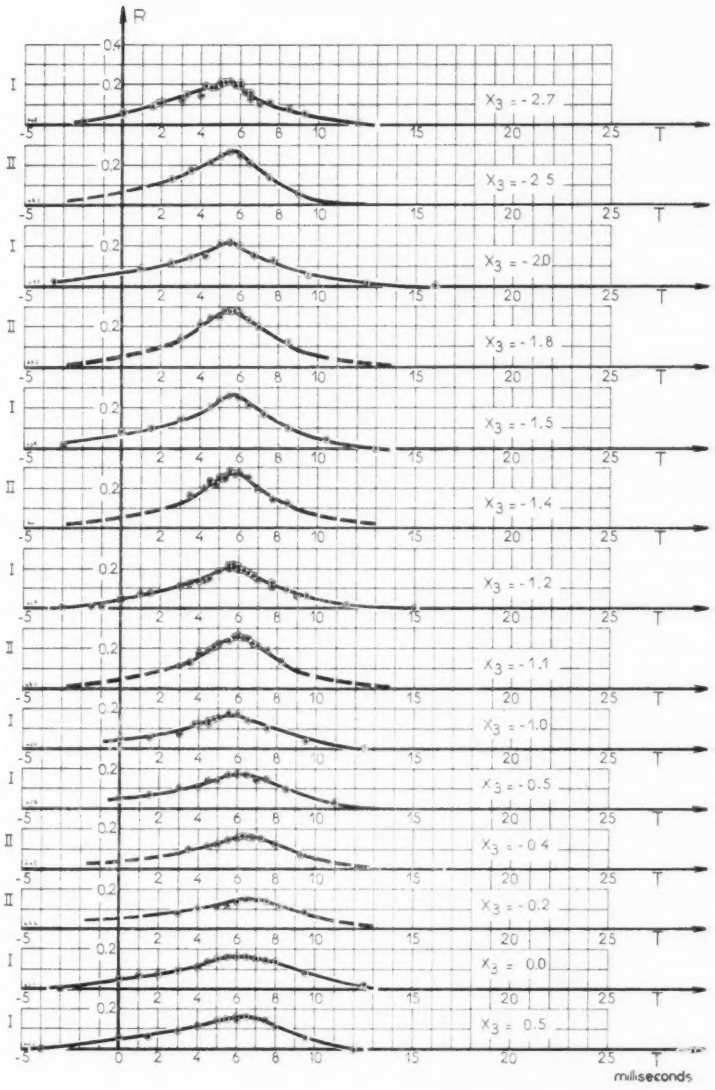

Figure 23. Transverse and longitudinal space-time correlations in the boundary layer on a flat plate downstream of a grid ($y' = 1$ mm, $y'/\delta = 0{\cdot}06$, $X_1 = 50{\cdot}8$ mm). I. First series of measurements. II. Second series of measurements.

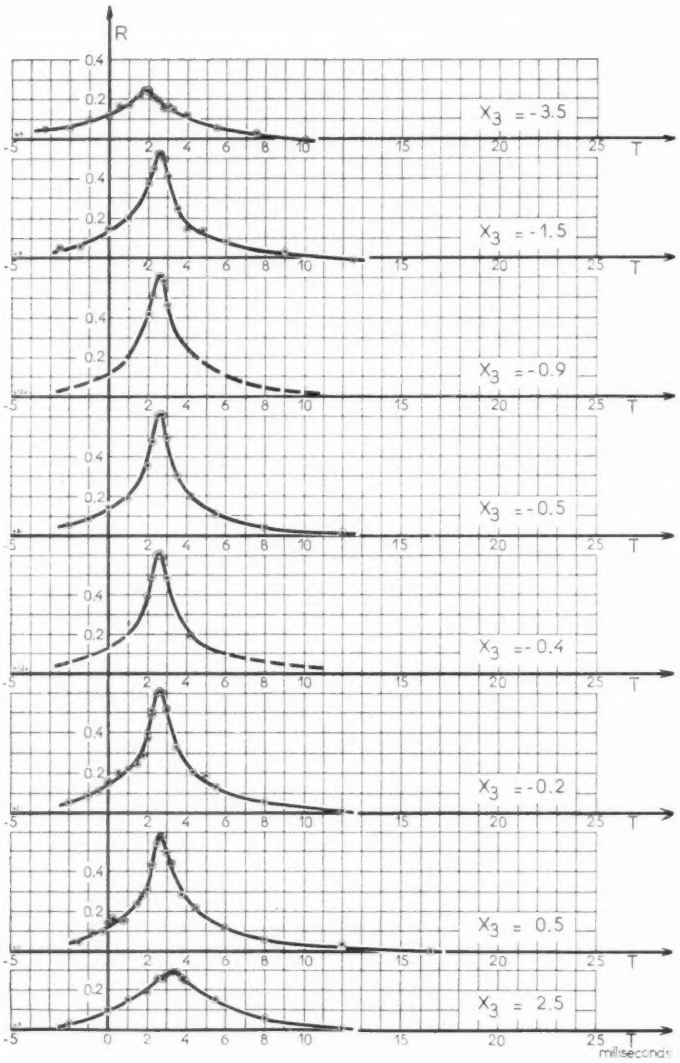

Figure 24. Transverse and longitudinal space-time correlations in the boundary layer on a flat plate downstream of a grid ($y' = 4$ mm, $y'/\delta = 0{\cdot}24$, $X_1 = 25{\cdot}4$ mm).

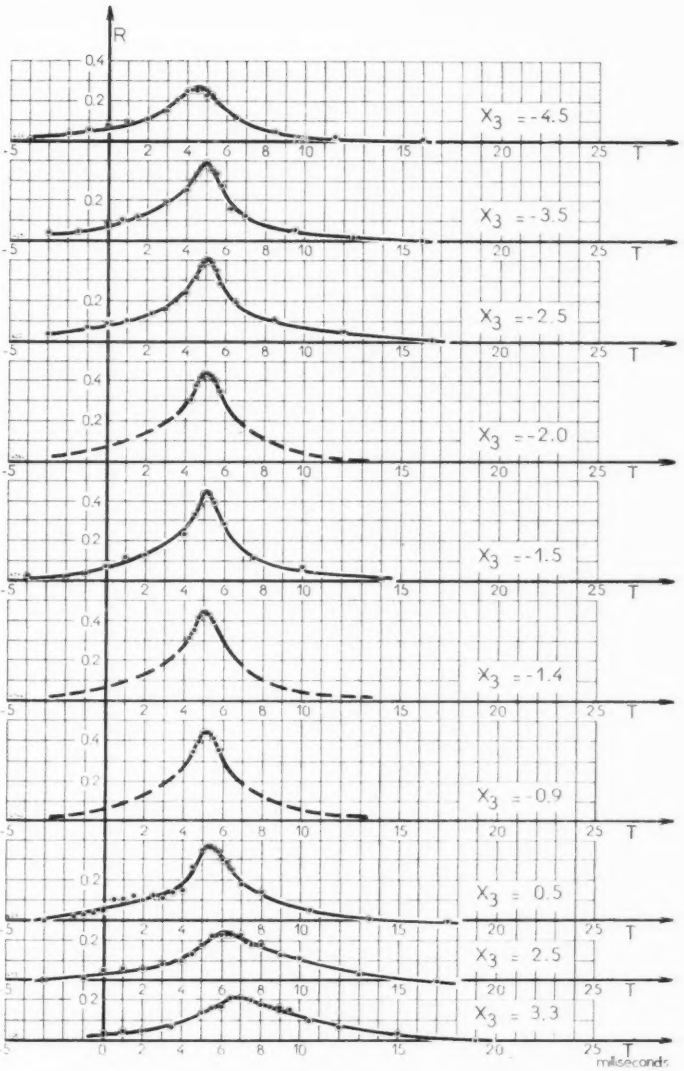

Figure 25. Transverse and longitudinal space-time correlations in the boundary layer on a flat plate downstream of a grid ($y' = 4$ mm, $y'/\delta = 0{\cdot}24$, $X_1 = 50{\cdot}8$ mm).

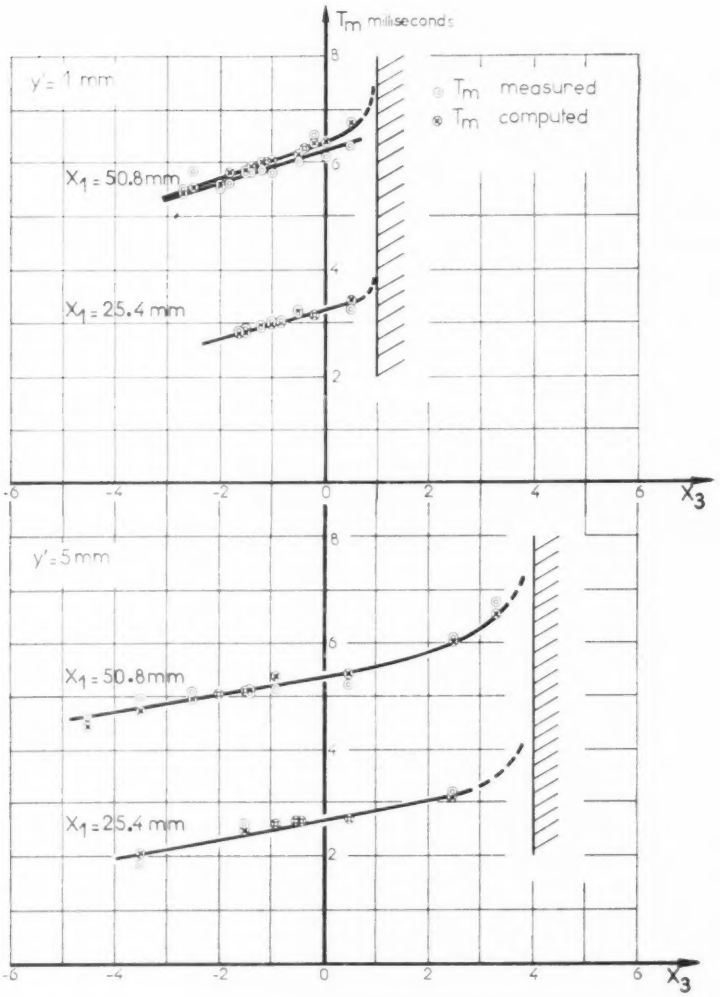

Figure 26. Optimum delays $T = T_m$ for transverse and longitudinal correlations. Transition by preturbulence.

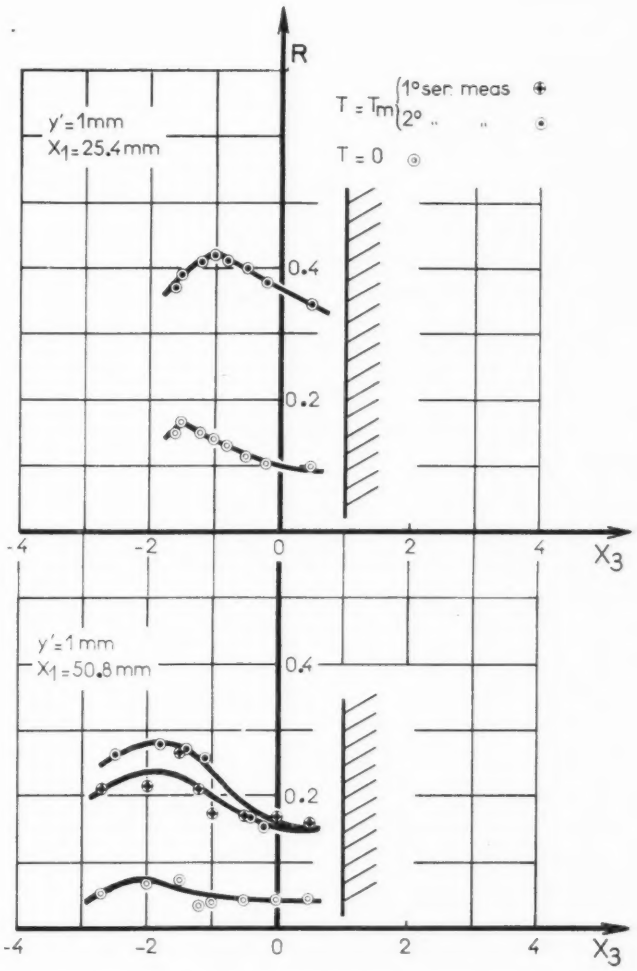

Figure 27. Comparison between transverse and longitudinal correlations with zero delay ($T = 0$) and transverse and longitudinal correlations with optimum delay ($T = T_m$). Transition by preturbulence ($z = 74$ cm).

obtained for a certain value of X_3. Likewise the maximum of the space-time correlations, $R_{\max}(T = 0, X_1, X_2 = 0, X_3)$, corresponding to given X_1, is obtained for $T = 0$ and for a certain value of X_3, different from the previous one. In figure 29 have been drawn the lines of maximum space-time

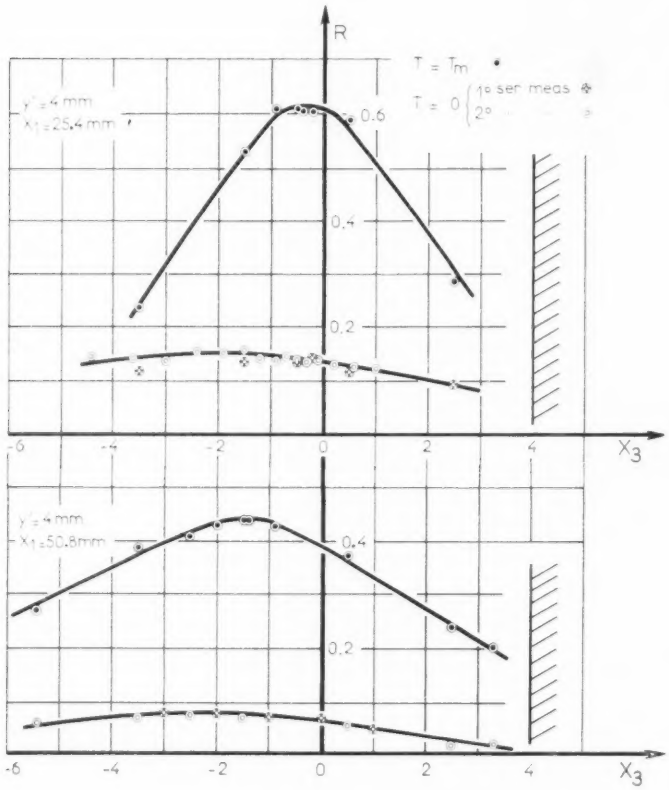

Figure 28. Comparison between transverse and longitudinal space-time correlations with zero delay ($T = 0$) and transverse and longitudinal space-time correlations with optimum delays ($T = T_m$). Transition by preturbulence ($x = 74$ cm.).

correlations with optimum delay ($T = T_m$), and also the lines of maximum correlations with zero delay ($T = 0$). Outside the boundary layer, these lines coincide with the mean streamlines (Favre, Gaviglio & Dumas 1953 b), but inside the boundary layer, they are markedly different from the streamlines. Table 3 summarizes the results.

Figure 30 shows the space-time correlations outside the boundary layer ($y'/\delta \geqslant 1$) and inside the boundary layer ($y'/\delta = 0{\cdot}71$, $0{\cdot}24$, $0{\cdot}06$), along the line of maximum space-time correlations, relative to the upstream wire position. $S_{y'}$ and S_y represent the curvilinear abscissae of the upstream

y'/δ	X_1	X_3	$R_{11\max}$ $(T = T_m, X_1, X_2 = 0, X_3)$	$R_{11\max}$ $(T = 0, X_1, X_2 = 0, X_3)$
0·06	25·4	−1	0·42	
		−1·6		0·165
	50·8	−1·8	0·28 or 0·24	
		−2·0		0·070
0·24	25·4	−0·5	0·62	
		−1·6		0·160
	50·8	−1·5	0·44	
		−2·2		0·080
0·71	49·0	−1·3	0·705	
		−2·8		0·160

Table 3.

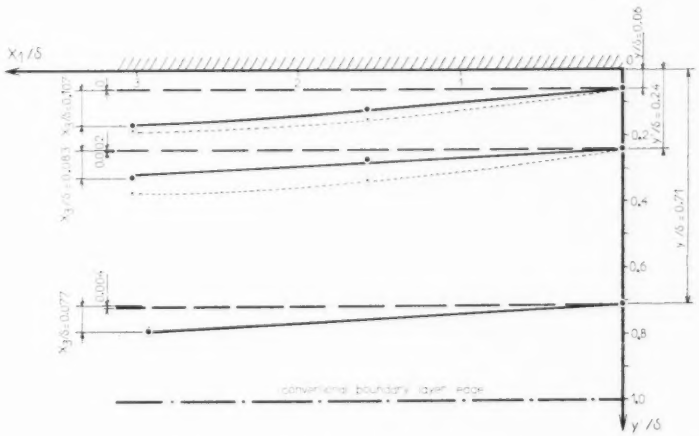

Figure 29. Lines of maximum correlation with optimum delay ($T = T_m$) —⊙— Lines of maximum correlation with zero delay ($T = 0$) – – – –⊗– – – – Stream-lines ——— ——— ——— (downstream of a grid).

and downstream wires along this line. When $T = T_m$ one gets the curves of space-time correlation along the line of maximum space-time correlation, with optimum delay. As we have noted above these curves show that the correlation retains high values of the order of 0·5 up to distances $(X_1/\delta)_{R=0{\cdot}5}$ which decrease rapidly with the distance y'/δ of the upstream wire from the wall.

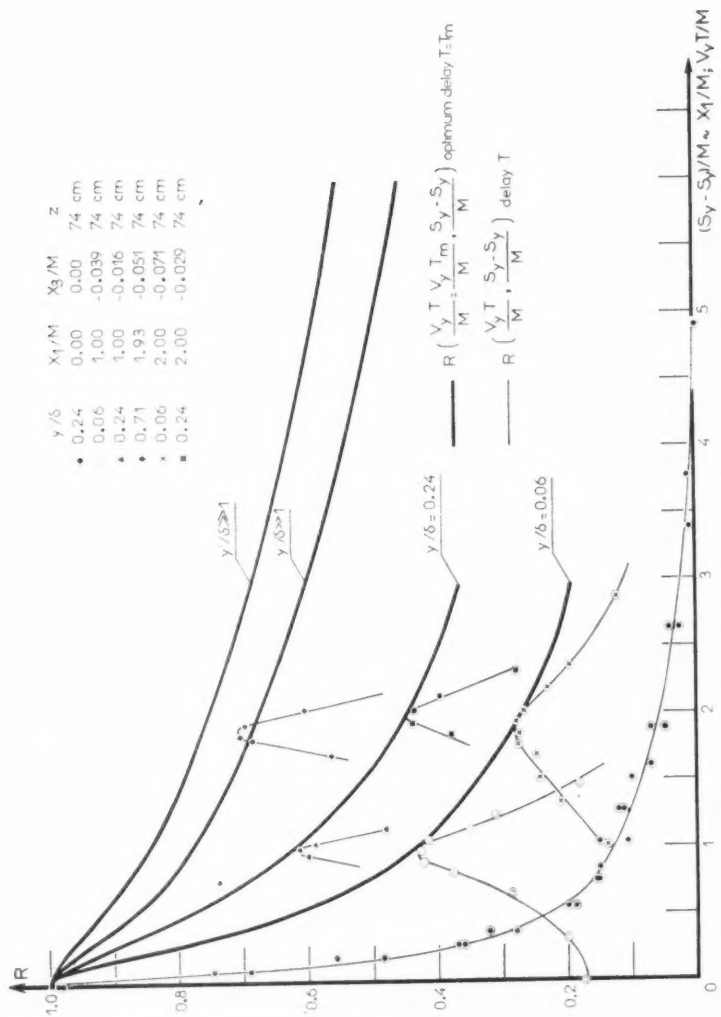

Figure 30. Space-time correlations along the line of maximum correlation with delay T, and with optimum delay $T = T_m$, in the boundary layer on a flat plate downstream of a grid

In figure 31 are reproduced the space-time isocorrelation curves with optimum delay $T = T_m$, for the distances to the wall of the upstream wire $y'/\delta = 0{\cdot}06$, $0{\cdot}24$ and $0{\cdot}71$.

Measurements are being continued, with improved accuracy.

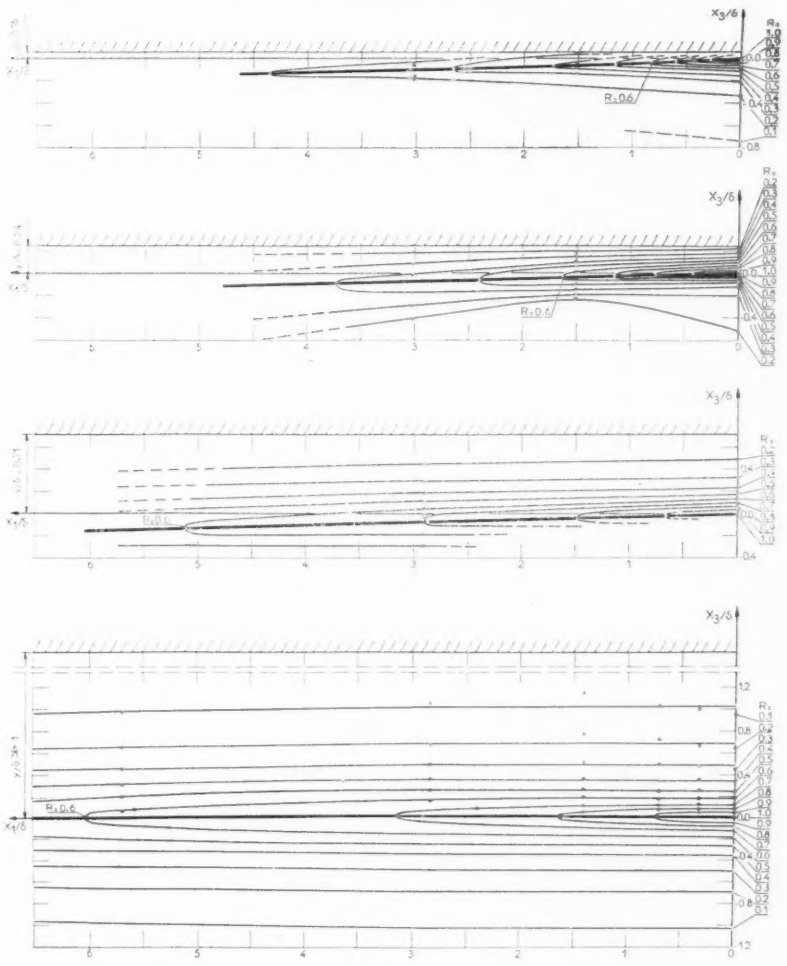

Figure 31. Space-time isocorrelation with optimum delay, in the boundary layer on a flat downstream of a grid.

These researches were made at the Laboratoire de Mécanique de l'Atmosphère (I.M.F. Marseille) for the Office National d'Etudes et de Recherches Aéronautiques (O.N.E.R.A.) with the aid of the Ministère de l'Air and of the Centre National de la Recherche Scientifique.

References

Clauser, F. H. 1954 *J. Aero. Sci.* **21,** 91.

Corrsin, S. & Kistler, A. L. 1954 *Nat. Adv. Comm. Aero., Wash., Tech. Note* no. 3133.

Favre, A. 1946 *Proc. 6th Inter. Congr. Appl. Mech.*

Favre, A. 1948 *Proc. 7th Inter. Congr. Appl. Mech.*

Favre, A., Gaviglio, J. & Dumas, R. 1952 *Publ. Sci. Tech. Minist. de l'Air,* no. 296.

Favre, A., Gaviglio, J. & Dumas, R. 1953 a *La Rech. Aéro.*, no. 31.

Favre, A., Gaviglio, J. & Dumas, R. 1953 b *La Rech. Aéro.*, no. 32.

Favre, A., Gaviglio, J. & Dumas, R. 1954 a *La Rech. Aéro.*, no. 38.

Favre, A., Gaviglio, J. & Dumas, R. 1954 b *La Rech. Aéro.*, no. 39.

Favre, A., Gaviglio, J. & Dumas, R. 1955 *La Rech. Aéro.* no. 48.

Klebanoff, P. S. & Diehl, Z. W. 1952 *Nat. Adv. Comm. Aero., Wash., Rep.* no. 1110.

Liepmann, H. W. 1952 *Z. angew. Math. Phys.* **3,** 321 and 407.

Phillips, O. M. 1954 *Proc. Camb. Phil. Soc.* **51,** 220.

Squire, H. B., Winter, K. G. & Barnes, E. G. 1947 *Royal Aircraft Establishment, Rep. Aero.* no. 2182.

Taylor, G. I. 1948 *Proc. Roy. Soc.* A, **164,** 476.

On the hydrodynamic stability of two viscous incompressible fluids in parallel uniform shearing motion

By SAUL FELDMAN
AVCO Research Laboratory, Everett, Massachusetts

(*Received* 15 *November* 1956)

SUMMARY

A new problem in hydrodynamic stability is investigated. Given two contiguous viscous incompressible fluids, the fluid on one side of the plane interface being bounded by a solid wall and that on the other side being unbounded, the problem is to determine the hydrodynamic stability when the fluids are in steady unidirectional motion, parallel to the interface, with uniform rate of shear in each fluid. The mathematical analysis, based on small disturbance theory, leads to a characteristic value problem in a system of two linear ordinary differential equations. The essential dimensionless parameters that appear in the present problem are the viscosity ratio m, the density ratio r, the Froude number F, and the Weber number W, as well as the parameters α, R (which is proportional here to the flow rate of the inner fluid) and c, that occur in the study of hydrodynamic stability of a single fluid. The results obtained are presented graphically for most fluid combinations of possible interest. The neutral stability curve in the (α, R)-plane is single-looped, as in the boundary layer case. The calculated critical Reynolds numbers are higher than the values observed in liquid film cooling experiments. (In these experiments, the outer fluid is usually a turbulent gas, in which the thickness of the laminar sublayer is of the same order of magnitude as the liquid film thickness.) General agreement between the theoretical and experimental values exists for all critical quantities except the Reynolds number. Gravity and surface tension are found here to have a destabilizing effect on the flow, in agreement with experimental evidence. Semi-infinite plane Couette flow is a special case of the present problem and the known stability of this flow is recovered. The linear velocity profile of two adjacent fluids with the same viscosity, but different densities, is shown to be unstable for high enough Reynolds numbers. The Reynolds stress distribution for a neutral oscillation in the general case is discussed qualitatively.

I. INTRODUCTION

The interest in the present problem stems from the desire to understand what happens when a liquid film flows over a flat surface, dragged along by a high speed gas. For certain liquid flow rates, the film surface becomes

wavy, and detached parcels of liquid from the main body are entrained by the gas and carried downstream. This situation arises, among numerous engineering applications, in connection with film cooling of a solid boundary, as reported by Knuth (1954).

A classical problem related to the one mentioned above is the generation of ocean waves by wind. This problem has recently been investigated theoretically by Lock (1954), who was the first to have included in the analysis all the physical properties of the air and water. His calculations are incomplete, and the results obtained are quite different from the usual single-fluid results.

The problem of the stability of stratified motion of different fluids has been studied by Taylor (1931) and Goldstein (1931), who did not include viscosity in their analyses. Taylor investigated continuous and discontinuous density and velocity distributions. Goldstein treated similar problems, his investigations being a generalization to heterogeneous stratified fluids of Rayleigh's (1887) work on the homogeneous case.

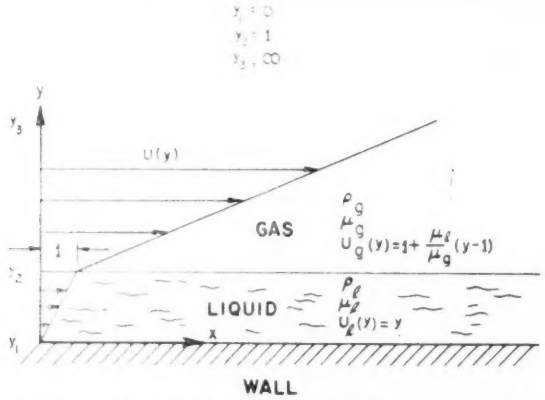

Figure 1. Undisturbed velocity profile to be investigated.

The problem of liquid film stability has been investigated experimentally by Kinney, Abramson & Sloop (1952) and by Knuth (1954), who were concerned with liquid film cooling applications where the gas stream was always turbulent. York, Stubbs & Teck (1953) studied the mechanism of disintegration of liquid sheets experimentally, and they proposed an inviscid model based on an extension of Lamb's work (1932).

The aim of this investigation is to solve the hydrodynamic stability problem when two viscous incompressible fluids, in two-dimensional, laminar, uniform shearing motion (figure 1) are perturbed by a small arbitrary disturbance. One of the fluids, from now on called the liquid, is bounded in the direction normal to the flow by a solid wall and by the second fluid, called the gas, of semi-infinite extent in the direction normal to the flow.

By 'solving the problem' is meant finding the relationships satisfied by certain parameters when neutral stability exists. This implies that a neutral-stability hypersurface, whose coordinates are the physical variables involved, could be constructed that would separate regions of stability and instability. In other words, if the physical properties of the fluids are given, we wish to determine the minimum critical Reynolds number* at which instability begins.

It will be realized from the above remarks that the chosen model is an idealization of the physical situation. The most serious criticism is that the gas motion, in the actual case, is turbulent in most cases of interest, and the velocity profile is not a linear function of the distance away from the wall. Some justification for the present approach lies in the fact that, at least in the laminar sublayer of the turbulent flow, the gas is laminar with an almost linear velocity profile. (The ratio of gas laminar sublayer thickness to liquid film thickness in existing experiments is of the order of unity.) There is still one other reason for the approach used (besides the obvious one of greater tractability when the turbulence is ignored), for it has been definitely shown by Zondek & Thomas (1953) that semi-infinite plane Couette flow is always stable. Now, this situation is a special case of the present model, and it is interesting in this connection to know how a discontinuity in density or viscosity affects the stability of uniform shearing motion.

II. The boundary value problem and its solution

1. *The Orr–Sommerfeld differential equation and its general solution for plane Couette flow*

The task now is to formulate mathematically the problem of stability of two-dimensional laminar motion. This has been done in the past by numerous authors (e.g. Lin 1945). For the sake of completeness, however, a brief description of the derivation of the disturbance equation will be given here.

Let all coordinates and velocities be made dimensionless by the use of a reference length δ, and a reference velocity $\bar{U}_2$. Consider a basic flow in the x-direction with a velocity profile $U(y)$. The Navier–Stokes and continuity equations in the xy-plane can be perturbed by assuming the velocities in the x- and y-directions and the pressure to have the form

$$U(y)+u(x,y,t), \qquad v(x,y,t), \qquad P+p(x,y,t), \tag{1}$$

where the lower-case symbols indicate small quantities, and t is the dimensionless time (i.e. time $\times\, \bar{U}_2/\delta$). The introduction of (1) into the Navier–Stokes equations leads to two linear partial differential equations from which the pressure can be eliminated by cross differentiation and subtraction. The result is a linear partial differential equation containing

* Defined, for given flow physical properties, as the smallest value of R for which incipient disturbances will become amplified, i.e. the smallest value of R of the neutral stability curve in the (α, R)-plane.

u and v as the dependent variables, with x, y and t as the independent variables. The equation of continuity guarantees the existence of a stream function $\psi(x, y, t)$, such that

$$u = \frac{\partial \psi}{\partial y}, \qquad v = -\frac{\partial \psi}{\partial x},$$

and which, when used in the differential equation last mentioned, reduces it to a linear partial differential equation in terms of only one dependent variable $\psi(x, y, t)$. The fact that this equation is linear is very important, since this means that superposition of solutions is allowable. This implies that if any arbitrary disturbance is decomposed into its Fourier components, it is then sufficient to solve the problem for one general sinusoidal oscillation. After the solution is obtained, it will be necessary to consider all possible frequencies and see how they affect the behaviour of the solution.

In order to separate the variables in the partial differential equation for ψ, let

$$\psi(x, y, t) = \phi(y)e^{i\alpha(x-ct)}, \tag{2}$$

where α is the wave number, assumed positive without any loss of generality, and c is the complex wave velocity which may be expressed as

$$c = c_r + ic_i, \tag{3}$$

where c_r is the wave velocity and c_i allows for amplification of disturbances if $c_i > 0$, damping of disturbances if $c_i < 0$, and neutral disturbances if $c_i = 0$. The partial differential equation for ψ then reduces to the Orr–Sommerfeld equation

$$(U-c)(\phi'' - \alpha^2\phi) - U''\phi = -\frac{i}{\alpha R}(\phi^{iv} - 2\alpha^2\phi'' + \alpha^4\phi), \tag{4}$$

where the primes indicate derivatives with respect to y, and R is the Reynolds number $\rho\delta\overline{U}_2/\mu$ (ρ is the density of the fluid and μ the viscosity).

If the velocity profile of the undisturbed flow is a linear function of y, as in the case of interest, $U'' = 0$, and (4) becomes

$$(U-c)(\phi'' - \alpha^2\phi) = -\frac{i}{\alpha R}(\phi^{iv} - 2\alpha^2\phi'' + \alpha^4\phi), \tag{5}$$

which is a linear fourth-order total differential equation in the complex y-plane. As first pointed out by Lin (1945), equation (5) has four linearly independent solutions, which are analytic functions of y and entire functions of the parameters c, α and αR. We will now solve (5). A transformation which was first pointed out by Orr (1906) and later independently by Sommerfeld (1909) is

$$\phi''(y) - \alpha^2\phi(y) = \zeta(y), \tag{6}$$

which when used in (5) yields

$$\zeta'' - [i\alpha R(U-c) + \alpha^2]\zeta = 0. \tag{7}$$

Now, let

$$\zeta(y) = h(z), \qquad z = \left\{\frac{\alpha^2}{(\alpha R)^{2/3}} + i(\alpha R)^{1/3}[U(y)-c]\right\}[U'(y)]^{-2/3}, \tag{8}$$

so that (7) can be written as

$$h''(z) + zh(z) = 0, \tag{9}$$

which is the so-called Stokes equation. The solution can be obtained in terms of contour integrals by using Laplace's method (Morse & Feshbach 1953, pp. 582–585). The result is

$$h(z) = 2k_3 h_1(z) + 2k_4 h_2(z), \tag{10}$$

where the factor 2 is introduced for convenience in later calculations, k_3 and k_4 are arbitrary constants, and

$$h_1(z) = \frac{k}{i\pi} \int_{L_1} \exp(zt + \tfrac{1}{3}t^3)\, dt, \qquad k = (12)^{1/6} e^{-i\pi/6}, \tag{11}$$

$$h_2(z) = -\frac{k^*}{i\pi} \int_{L_2} \exp(zt + \tfrac{1}{3}t^3)\, dt, \quad k^* = (12)^{1/6} e^{-i\pi/6}, \tag{12}$$

in which L_1 and L_2 are the contours of integration shown in figure 2, h_1 and h_2 are entire functions of z, and t is a complex variable of integration.

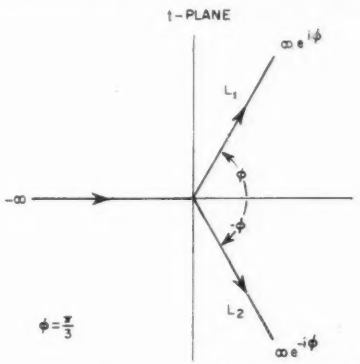

Figure 2. Paths for contour integrals in the solution of Stokes' equation.

The functions $h_1(z)$ and $h_2(z)$ may also be written in terms of Hankel functions of order one-third as

$$h_1(z) = (\tfrac{2}{3}z^{3/2})^{1/3} H^{(1)}_{1/3}(\tfrac{2}{3}z^{3/2}), \qquad h_2(z) = (\tfrac{2}{3}z^{3/2})^{1/3} H^{(2)}_{1/3}(\tfrac{2}{3}z^{3/2}). \tag{13}$$

It will be recalled (see, for instance, Copson (1935)) that the Hankel functions are of oscillatory nature, $H^{(1)}_{1/3}$, the function of the first kind, being damped exponentially as $|\frac{2}{3}z^{3/2}|$ becomes large, while $H^{(2)}_{1/3}$ increases exponentially under the same conditions.

From (8) and (10) we have

$$\zeta(y) = 2k_3 \zeta_1(y) + 2k_4 \zeta_2(y),$$

where

$$\zeta_1(y) = h_1(z), \qquad \zeta_2(y) = h_2(z), \tag{14}$$

which when inserted in (6) gives

$$\phi''(y) - \alpha^2 \phi(y) = 2k_3 \zeta_1(y) + 2k_4 \zeta_2(y). \tag{15}$$

The complete solution of (5) is then

$$\phi(y) = k_1 \phi_1(y) + k_2 \phi_2(y) + k_3 \phi_3(y) + k_4 \phi_4(y), \tag{16}$$

where
$$\left.\begin{aligned} &\phi_1(y) = e^{-\alpha y}, \qquad \phi_2(y) = e^{\alpha y}, \\ &\phi_3(y) = \frac{1}{\alpha}\left\{ \int^y e^{\alpha(y-t)}\zeta_1(t)\,dt - \int^y e^{-\alpha(y-t)}\zeta_1(t)\,dt \right\}, \\ &\phi_4(y) = \frac{1}{\alpha}\left\{ \int^y e^{\alpha(y-t)}\zeta_2(t)\,dt - \int^y e^{-\alpha(y-t)}\zeta_2(t)\,dt \right\}. \end{aligned}\right\} \tag{17}$$

t is a variable of integration and should not be confused with the notation used to denote time. ζ_1 and ζ_2 are given by (14).

2. *Differential equations for the present problem*

When the phenomenon under investigation involves the stratified motion of two fluids, an equation like (5) must be used for each fluid, with the proper boundary conditions at the interface. Let δ and $\overline{U}_2$ as used to render (5) dimensionless be, respectively, the height of the liquid sheet and its surface velocity. Lower-case and capital Greek letters will represent conditions in the liquid and gas respectively, and the subscripts l and g will denote quantities evaluated in the liquid and in the gas. We then choose

$$\psi = \phi(y)e^{i\alpha(x-ct)}, \qquad \Psi = \Phi(y)e^{i\alpha(x-ct)} \tag{18}$$

as our representation of the disturbance stream function in the liquid and gas respectively. The disturbance velocities then become

$$\left.\begin{aligned} u_l &= \frac{\partial\psi}{\partial y} = \phi'(y)e^{i\alpha(x-ct)}, & u_g &= \frac{\partial\Psi}{\partial y} = \Phi'(y)e^{i\alpha(x-ct)}, \\ v_l &= -\frac{\partial\psi}{\partial x} = -i\alpha\phi(y)e^{i\alpha(x-ct)}, & v_g &= -\frac{\partial\Psi}{\partial x} = -i\alpha\Phi(y)e^{i\alpha(x-ct)}, \end{aligned}\right\} \tag{19}$$

while the corresponding Orr–Sommerfeld equations are

$$(U_l - c)(\phi'' - \alpha^2\phi) = -\frac{i}{\alpha R_l}(\phi^{iv} - 2\alpha^2\phi'' + \alpha^4\phi), \qquad (0 \leqslant y \leqslant 1), \tag{20}$$

$$(U_g - c)(\Phi'' - \alpha^2\Phi) = -\frac{i}{\alpha R_g}(\Phi^{iv} - 2\alpha^2\Phi'' + \alpha^4\Phi), \quad (1 \leqslant y \leqslant \infty), \tag{21}$$

where
$$R_l = \frac{\rho_l \delta \overline{U}_2}{\mu_l}, \qquad R_g = \frac{\rho_g \delta \overline{U}_2}{\mu_g}, \qquad U_l = y. \tag{22}$$

Equating the shear stresses at the interface of the basic flow gives

$$U_g = 1 + \frac{\mu_l}{\mu_g}(y-1). \tag{23}$$

The solutions of (20) and (21) can now be written, from (16), as

$$\phi(y) = k_1\phi_1(y) + k_2\phi_2(y) + k_3\phi_3(y) + k_4\phi_4(y), \qquad (0 \leqslant y \leqslant 1), \tag{24}$$

$$\Phi(y) = K_1\Phi_1(y) + K_2\Phi_2(y) + K_3\Phi_3(y) + K_4\Phi_4(y), \quad (1 \leqslant y \leqslant \infty), \tag{25}$$

where the ϕ's are given by (17), and the Φ's can also be obtained from the same equation by using the appropriate value of z in the gas, given by (8).

3. *Boundary conditions*

The boundary conditions will be written in terms of dimensionless variables.

Let subscripts 1, 2 and 3 used with the coordinate y denote, respectively, the wall, interface and infinity, i.e. $y_1 = 0$, $y_2 = 1$ and $y_3 = \infty$.

At the wall ($y = y_1 = 0$), both components of the disturbance velocities must vanish; i.e.

$$v_l(y_1) = 0, \qquad u_l(y_1) = 0. \tag{26}$$

At the interface ($y = y_2 = 1$), the following conditions must hold:

(*a*) Both fluids move together with no vacuum layer between them; thus

$$v_l(y_2) - v_g(y_2) = 0. \tag{27}$$

(*b*) There is no slip between the fluids in the direction of flow; thus

$$u_l(y_2) - u_g(y_2) = 0. \tag{28}$$

(*c*) The shear stress must be continuous; thus

$$u_l\left(\frac{\partial v_l}{\partial x} + \frac{\partial u_l}{\partial y}\right) - \mu_g\left(\frac{\partial v_g}{\partial x} + \frac{\partial u_g}{\partial y}\right) = 0. \tag{29}$$

(*d*) Because of surface tension, the normal stress is discontinuous according to the relation

$$p_T - \sigma_{yyg} = -\sigma_{yyl},$$

where p_T is the effective pressure caused by surface tension. If σ is the surface tension coefficient and l_r the radius of curvature of the interface, p_T can be written as

$$p_T = \sigma / l_r,$$

where

$$\frac{1}{l_r} = -\frac{d^2\bar{y}}{d\bar{x}^2} \Big/ \left[1 + \left(\frac{d\bar{y}}{d\bar{x}}\right)^2\right]^{3/2},$$

the negative sign having been chosen because p_T is to be positive when $d^2\bar{y}/d\bar{x}^2$ is negative. The normal force equation can be rewritten as

$$p_g - 2\mu_g \frac{\partial v_g}{\partial y} - p_l + 2\mu_l \frac{\partial v_l}{\partial y} + p_T = 0. \tag{30}$$

At infinity ($y = y_3 = \infty$), the disturbance must vanish; i.e.

$$v_g(y_3) = 0, \qquad u_g(y_3) = 0. \tag{31}$$

Equations (26) to (31) are the eight boundary conditions necessary for solving the system of two-fourth order differential equations given by (24) and (25).

4. *The secular equation*

Equations (13), (14) and (17) show that when $y \to \infty$, $\Phi_2(y)$ and $\Phi_4(y) \to \infty$. In order to satisfy the boundary conditions given in (31), it is necessary that in (25)

$$K_2 = K_4 = 0, \tag{32}$$

which when used with (19) allows the boundary conditions (26) to (31) to be rewritten as

$$k_1\phi_{11} + k_2\phi_{21} + k_3\phi_{31} + k_4\phi_{41} = 0, \tag{33}$$

$$k_1\phi'_{11} + k_2\phi'_{21} + k_3\phi'_{13} + k_4\phi'_{41} = 0, \tag{34}$$

$$k_1\phi_{12} + k_2\phi_{22} + k_3\phi_{32} + k_4\phi_{42} - K_1\Phi_{12} - K_3\Phi_{32} = 0, \tag{35}$$

$$k_1\phi'_{12} + k_2\phi'_{22} + k_3\phi'_{32} + k_4\phi'_{42} - K_1\Phi'_{12} - K_3\Phi'_{32} = 0, \tag{36}$$

$$k_1(\alpha^2\phi_{12} + \phi''_{12}) + k_2(\alpha^2\phi_{22} + \phi''_{22}) + k_3(\alpha^2\phi_{32} + \phi''_{32}) + k_4(\alpha^2\phi_{42} + \phi''_{42}) - \frac{K_1}{m}(\alpha^2\Phi_{12} + \Phi''_{12}) - \frac{K_3}{m}(\alpha^2\Phi_{32} + \Phi''_{32}) = 0, \tag{37}$$

$$k_1\left\{\left[\frac{\alpha^2}{W} + \frac{1}{F(1-c)} + 1\right]R\phi_{12} - [(1-c)R - i3\alpha]\phi'_{12} - \frac{i}{\alpha}\phi'''_{12}\right\} + k_2\left\{\left[\frac{\alpha^2}{W} + \frac{1}{F(1-c)} + 1\right]R\phi_{22} - [(1-c)R - i3\alpha]\phi'_{22} - \frac{i}{\alpha}\phi'''_{22}\right\} + k_3\left\{\left[\frac{\alpha^2}{W} + \frac{1}{F(1-c)} + 1\right]R\phi_{32} - [(1-c)R - i3\alpha]\phi'_{32} - \frac{i}{\alpha}\phi'''_{32}\right\} + k_4\left\{\left[\frac{\alpha^2}{W} + \frac{1}{F(1-c)} + 1\right]R\phi_{42} - [(1-c)R - i3\alpha]\phi'_{42} - \frac{i}{\alpha}\phi'''_{42}\right\} - \frac{K_1}{m}\left\{\left[m + \frac{1}{F(1-c)}\right]Rrm\Phi_{12} - [(1-c)Rrm - i3\alpha]\Phi'_{12} - \frac{i}{\alpha}\Phi''_{12}\right\} - \frac{K_3}{m}\left\{\left[m + \frac{1}{F(1-c)}\right]Rrm\Phi_{32} - [(1-c)Rrm - i3\alpha]\Phi'_{32} - \frac{i}{\alpha}\Phi'''_{32}\right\} = 0, \tag{38}$$

where $\phi_{11} \equiv \phi_1(y_1)$, $\phi_{23} \equiv \phi_2(y_3)$, etc., and

$$m = \mu_l/\mu_g; \qquad r = \rho_g/\rho_l; \qquad R = R_l; \qquad F = \bar{U}_2^2/g\delta; \qquad W = \rho_l\delta\bar{U}_2^2/\sigma. \tag{39}$$

R_g does not enter in the relationships of this section because it is clear, from (25) and (26), that

$$R_g = R_l rm.$$

For the details of the derivation of (38), reference may be made to the author's thesis (Feldman 1955, Appendix A).

Thus, the essential dimensionless parameters of the problem have been defined as α, R, c, m, r, F and W, where F and W denote, respectively, the Froude and Weber numbers. It is seen that R_g has disappeared from the problem as an explicit parameter. This seems to be in line with experimental results (Knuth 1954, pp. 362–363), which show that the inception point of unstable disturbances is independent of the gas-stream Reynolds number.

If the preceding set of equations, (33) to (38), is to have a non-trivial solution for the k's and K's, the following relation, the so-called secular

equation, must hold:

$$\begin{vmatrix} \phi_{11} & \phi_{21} & \phi_{31} & \phi_{41} & 0 & 0 \\ \phi'_{11} & \phi'_{21} & \phi'_{31} & \phi'_{41} & 0 & 0 \\ \phi_{12} & \phi_{22} & \phi_{32} & \phi_{42} & -\Phi_{12} & -\Phi_{32} \\ \phi'_{12} & \phi'_{22} & \phi'_{32} & \phi'_{42} & -\Phi'_{12} & -\Phi'_{32} \\ f_{12} & f_{22} & f_{32} & f_{42} & -F_{12}/m & -F_{32}/m \\ g_{12} & g_{22} & g_{32} & g_{42} & -G_{12}/m & -G_{32}/m \end{vmatrix} = 0, \quad (40)$$

where

$$f_{n2} = \alpha^2\phi_{n2} + \phi''_{n2}, \qquad n = 1, 2, 3, 4;$$

$$F_{n2} = \alpha^2\Phi_{n2} + \Phi''_{n2}, \qquad n = 1, 3;$$

$$g_{n2} = \left[\frac{\alpha^2}{W} + \frac{1}{F(1-c)} + 1\right]R\phi_{n2} - [(1-c)R - i3\alpha]\phi'_{n2} - \frac{i}{\alpha}\phi'''_{n2}, \quad n = 1, 2, 3, 4;$$

$$G_{n2} = \left[m + \frac{1}{F(1-c)}\right]Rrm\Phi_{n2} - [(1-c)Rrm - i3\alpha]\Phi'_{n2} - \frac{i}{\alpha}\Phi'''_{n2}, \quad n = 1, 3.$$

5. *Solutions of the boundary value problem*

The purpose of our calculation from now on will be to find the function that the secular equation represents.

From (22), (23) and (38), it is clear that in the liquid

$$U = y, \qquad U' = 1, \quad (0 \leqslant y \leqslant 1),$$

and in the gas

$$U = 1 + m(y-1); \quad U' = m, \quad (1 \leqslant y \leqslant \infty). \quad (41)$$

The six solutions involved are, from (8), (11), (14), (17), (24), (25) and (32),

$$\phi_1(y) = e^{-\alpha y}, \quad (42)$$

$$\phi_2(y) = e^{\alpha y}, \quad (43)$$

$$\phi_3(y) = \frac{1}{\alpha}\left\{\int_1^y \exp\{\alpha(y-t_l)\}\zeta_1(t_l)\,dt_l - \int_1^y \exp\{-\alpha(y-t_l)\}\zeta_1(t_l)\,dt_l\right\}, \quad (44)$$

$$\phi_4(y) = \frac{1}{\alpha}\left\{\int_1^y \exp\{\alpha(y-t_l)\}\zeta_2(t_l)\,dt_l - \int_1^y \exp\{-\alpha(y-t_l)\}\zeta_2(t_l)\,dt_l\right\}, \quad (45)$$

$$\Phi_1(y) = e^{-\alpha y}, \quad (46)$$

$$\Phi_3(y) = \frac{1}{\alpha}\left\{\int_\infty^y \exp\{\alpha(y-t_g)\}\zeta_1(t_g)\,dt_g - \int_\infty^y \exp\{-\alpha(y-t_g)\}\zeta_1(t_g)\,dt_g\right\}, \quad (47)$$

where

$$\zeta_1(t_l) = h_1(z_l) = \frac{k}{i\pi}\int_{L_1} \exp(z_l t + \tfrac{1}{3}t^3)\,dt, \quad (48)$$

$$\zeta_2(t_l) = h_2(z_l) = -\frac{k^*}{i\pi}\int_{L_2} \exp(z_l t + \tfrac{1}{3}t^3)\,dt, \quad (49)$$

$$\zeta_1(t_g) = h_1(z_g) = \frac{k}{i\pi}\int_{L_1} \exp(z_g t + \tfrac{1}{3}t^3)\,dt, \quad (50)$$

$$z_l = \left[\frac{\alpha^2}{(\alpha R)^{2/3}} + i(\alpha R)^{1/3}(t_l - c)\right], \quad (51)$$

$$z_g = \left\{ \frac{\alpha^2}{(\alpha Rrm^2)^{2/3}} + i(\alpha Rrm^2)^{1/3} \left[(t_g - 1) + \frac{1}{m}(1 - c) \right] \right\}, \tag{52}$$

and for clarity, instead of using y in the liquid and gas, the variables t_l and t_g were introduced. In (44) and (45), the lower limit of integration was taken as $y = 1$ for convenience in later calculations. (For an alternative refer to discussion following (55).) Later on, many expressions will have to be evaluated at $y = y_2 = 1$. With the choice made here, the calculation is simplified since several integrals vanish, i.e. ϕ_{32}, ϕ'_{32}, ϕ''_{32}, ϕ_{42}, ϕ'_{42}, ϕ''_{42} and ϕ'''_{42}. In (47) the lower limit was taken as infinity, because two of the boundary conditions required the solutions to vanish there: no other choice would have been satisfactory. The functions needed in (40) will now be written down:

$$\begin{aligned}
&\phi_{11} = 1, \qquad \phi_{21} = 1, \\
&\phi'_{11} = -\alpha, \qquad \phi'_{21} = \alpha, \\
&\phi_{12} = e^{-\alpha}, \qquad \phi_{22} = e^{\alpha}, \qquad \Phi_{12} = e^{-\alpha}, \\
&\phi'_{12} = -\alpha e^{-\alpha}, \qquad \phi'_{22} = \alpha e^{\alpha}, \qquad \Phi'_{12} = -\alpha e^{-\alpha}, \\
&\phi''_{12} = \alpha^2 e^{-\alpha}, \qquad \phi''_{22} = \alpha^2 e^{\alpha}, \qquad \Phi''_{12} = \alpha^2 e^{-\alpha}, \\
&\phi'''_{12} = -\alpha^3 e^{-\alpha}, \qquad \phi'''_{22} = \alpha^3 e^{\alpha}, \qquad \Phi'''_{12} = -\alpha^3 e^{-\alpha}, \\
&\phi_{31} = \frac{1}{\alpha}\left\{ \int_1^0 \exp(-\alpha t_l)\zeta_1(t_l)\, dt_l - \int_1^0 \exp(\alpha t_l)\zeta_1(t_l)\, dt_l \right\}, \\
&\phi'_{31} = \int_1^0 \exp(-\alpha t_l)\zeta_1(t_l)\, dt_l + \int_1^0 \exp(\alpha t_l)\zeta_1(t_l)\, dt_l, \\
&\phi_{32} = 0, \qquad \phi'_{32} = 0, \\
&\phi''_{32} = 2\zeta_1(t_l = 1) = 2h_1(z_l(1)], \\
&\phi'''_{32} = 2\zeta'_1(t_l = 1) = 2h'_1[z_l(1)]i(\alpha R)^{1/3}, \\
&\phi_{41} = \frac{1}{\alpha}\left\{ \int_1^0 \exp(-\alpha t_l)\zeta_2(t_l)\, dt_l - \int_1^0 \exp(\alpha t_l)\zeta_2(t_l)\, dt_l \right\}, \\
&\phi'_{41} = \int_1^0 \exp(-\alpha t_l)\zeta_2(t_l)\, dt_l + \int_1^0 \exp(\alpha t_l)\zeta_2(t_l)\, dt_l, \\
&\phi_{42} = 0, \qquad \phi'_{42} = 0, \\
&\phi''_{42} = 2\zeta_2(t_l = 1) = 2h_2(z_l(1)], \\
&\phi'''_{42} = 2\zeta'_2(t_l = 1) = 2h'_2[z_l(1)]i(\alpha R)^{1/3}, \\
&\Phi_{32} = \frac{1}{\alpha}\left\{ \int_{-\infty}^{1} \exp\{-\alpha(t_g - 1)\}\zeta_1(t_g)\, dt_g - \int_{-\infty}^{1} \exp\{\alpha(t_g - 1)\}\zeta_1(t_g)\, dt_g \right\}, \\
&\Phi'_{32} = \int_{-\infty}^{1} \exp\{-\alpha(t_g - 1)\}\zeta_1(t_g)\, dt_g + \int_{-\infty}^{1} \exp\{\alpha(t_g - 1)\}\zeta_1(t_g)\, dt_g, \\
&\Phi''_{32} = 2\zeta_1(t_g = 1) + \alpha^2\Phi_{32} = 2h_1[z_g(1)] + \alpha^2\Phi_{32}, \\
&\Phi'''_{32} = 2\zeta'_1(t_g = 1) + \alpha^2\Phi'_{32} = 2h'_1[z_g(1)]i(\alpha Rrm^2)^{1/3}.
\end{aligned} \tag{53}$$

Here $z_l(1)$ and $z_g(1)$ denote the values for $t_l = 1$ and $t_g = 1$ respectively.

We shall next change the determinant of (40) into a form more convenient for calculation. The procedure is as follows:

(*a*) Divide the last row by R.

(*b*) Multiply the 3rd, 4th and 6th columns by $(\alpha R)^{1/2}/'\phi''_{32}$, $(\alpha R)^{1/2}/'\phi''_{42}$ and $(\alpha Rrm^2)^{1/2}/'\Phi''_{32}$ respectively, where the accent to the left of a symbol means the leading term in the asymptotic expansion ($\alpha R \gg 1$) of the corresponding function.

(*c*) From (60), insert all the zeros for the terms that vanish.

(*d*) Multiply the 5th column by -1, and rearrange the columns so that column 5 becomes 3, 3 becomes 4, and 4 becomes 5.

The result is then

$$\begin{vmatrix} \Lambda_1 & V_1 & 0 & a_1 & b_1 & 0 \\ \Lambda_2 & V_2 & 0 & a_2 & b_2 & 0 \\ \Lambda_3 & V_3 & T_3 & 0 & 0 & c_3 \\ \Lambda_4 & V_4 & T_4 & 0 & 0 & c_4 \\ \Lambda_5 & V_5 & T_5 & a_5 & b_5 & c_5 \\ \Lambda_6 & V_6 & T_6 & a_6 & b_6 & c_6 \end{vmatrix} = 0, \tag{54}$$

where the first three columns involve the inviscid terms (except for the last row, which has terms of $O(1/R)$ and will be neglected in comparison with the terms kept in the calculation), and the last three columns involve the viscous solutions. The term 'viscous solutions' refers to any of ϕ_3, ϕ_4, Φ_3, or their derivatives, regardless of where they are evaluated. The meaning of the symbols in (54) is given by the following relationships:

$$\left.\begin{aligned} &\Lambda_1 = \phi_{11}, \quad \Lambda_2 = \phi'_{11}, \quad \Lambda_3 = \phi_{12}, \quad \Lambda_4 = \phi'_{12}, \quad \Lambda_5 = \alpha^2\phi_{12} + \phi''_{12}, \\ &\Lambda_6 = \left[\frac{\alpha^2}{W} + \frac{1}{F(1-c)} + 1\right]\phi_{12} - (1-c)\phi'_{12} + i(3\alpha^2\phi'_{12} - \phi'''_{12})(\alpha R)^{-1}, \end{aligned}\right\} \tag{55}$$

$$\left.\begin{aligned} &V_1 = \phi_{21}, \quad V_2 = \phi'_{21}, \quad V_3 = \phi_{22}, \quad V_4 = \phi'_{22}, \quad V_5 = \alpha^2\phi_{22} + \phi''_{22}, \\ &V_6 = \left[\frac{\alpha^2}{W} + \frac{1}{F(1-c)} + 1\right]\phi_{22} - (1-c)\phi'_{22} + i(3\alpha^2\phi'_{22} - \phi'''_{22})(\alpha R)^{-1}, \end{aligned}\right\} \tag{56}$$

$$\left.\begin{aligned} &T_3 = \Phi_{12}, \quad T_4 = \Phi'_{12}, \quad T_5 = m^{-1}(\alpha^2\Phi_{12} + \Phi''_{12}), \\ &T_6 = r\left\{\left[m + \frac{1}{F(1-c)}\right]\Phi_{12} - (1-c)\Phi'_{12}\right\} + im^{-1}(3\alpha^2\Phi'_{12} - \Phi'''_{12})(\alpha R)^{-1}, \end{aligned}\right\} \tag{57}$$

$$\left.\begin{aligned} &a_1 = (\alpha R)^{1/2}\phi_{31}/'\phi''_{32}, \quad a_2 = (\alpha R)^{1/2}\phi'_{31}/'\phi''_{32}, \\ &a_5 = (\alpha R)^{1/2}\phi''_{32}/'\phi''_{32}, \quad a_6 = -i(\alpha R)^{-1/2}\phi'''_{32}/'\phi''_{32}, \end{aligned}\right\} \tag{58}$$

$$\left.\begin{aligned} &b_1 = (\alpha R)^{1/2}\phi_{41}/'\phi''_{42}, \quad b_2 = (\alpha R)^{1/2}\phi'_{41}/'\phi''_{42}, \\ &b_5 = (\alpha R)^{1/2}\phi''_{42}/'\phi''_{42}, \quad b_6 = -i(\alpha R)^{-1/2}\phi'''_{42}/'\phi''_{42}, \end{aligned}\right\} \tag{59}$$

$$
\left.\begin{aligned}
&c_3 = (\alpha Rrm^2)^{1/2}\Phi_{32}/'\Phi''_{32}, \quad c_4 = (\alpha Rrm^2)^{1/2}\Phi'_{32}/'\Phi''_{32},\\
&c_5 = m^{-1}[\alpha^2(\alpha Rrm^2)^{1/2}\Phi_{32}/'\Phi''_{32} + (\alpha Rrm^2)^{1/2}\Phi''_{32}/'\Phi''_{32}],\\
&c_6 = m^{-1}\left[\left\{m + \frac{1}{F(1-c)}\right\}mr(\alpha Rrm^2)^{1/2}\Phi_{32}/'\Phi''_{32} - \left[(1-c)mr - i\frac{3\alpha^2}{\alpha R}\right]\times\right.\\
&\qquad\left.\times(\alpha Rrm^2)^{1/2}\Phi'_{32}/'\Phi''_{32} - \frac{1}{\alpha R}(\alpha Rrm^2)^{1/2}\Phi''_{32}/'\Phi''_{32}\right\}.
\end{aligned}\right\} \tag{60}
$$

It is worth remarking that the lower limit for the integrals in (44) and (45) could alternatively have been taken as zero instead of unity. This would have lead to a fourth-order determinant instead of the sixth-order one in (54). Each element of the alternative determinant would have been not only more complicated than the one of (54), but the clear distinction between viscid and inviscid solutions (of which use is made for the calculations of the neutral stability lines) would not have been possible.

6. *Behaviour of the viscous solutions for* $\alpha R \gg 1$

Thus far, no restrictions of any kind have been made in the analysis. We will restrict the discussion to the case $\alpha R \gg 1$, this being sufficient to solve the problem. One of the major tasks is the evaluation of the integrals in (53). The only previous discussion of a similar integral is the one by Hopf (1914), who assumed $\alpha R \ll 1$; thus his discussion is not suited to the present study. In order to find out how the neutral stability curve (i.e. for given m, r, F and W) behaves for large values of the parameter αR, it will be sufficient to keep only the terms of highest order in αR in the asymptotic expansion of the pertinent functions. As will be shown later (following (71)), the case of interest for neutral stability (cf. (3)), is the one where $c = c_r < 1$. A detailed description of the method used for obtaining the integrals, the order of magnitude of the errors involved, and the calculation of ϕ_{31} as an example of the procedure used, is given in Appendix B of the author's thesis. If $\alpha R \gg 1$, from (51) and (52) it may be assumed that

$$
\begin{aligned}
&z_{l0} = z_l(0) = \alpha^2(\alpha R)^{-2/3} - i(\alpha R)^{1/3}c \sim -i(\alpha R)^{1/3}c,\\
&z_{l1} = z_l(1) = \alpha^2(\alpha R)^{-2/3} + i(\alpha R)^{1/3}(1-c) \sim i(\alpha R)^{1/3}(1-c),\\
&z_{g1} = z_g(1) = \alpha^2(\alpha Rrm^2)^{-2/3} + i(\alpha Rrm^2)^{1/3}(1-c)m^{-1} \sim i(\alpha Rrm^2)^{1/3}(1-c)m^{-1}.
\end{aligned} \tag{61}
$$

Now, let

$$
\left.\begin{aligned}
e^+ &= \exp[\tfrac{2}{3}(\alpha R)^{1/2}e^{(5/4)\pi i}(1-c)^{3/2}],\\
e^- &= \exp[-\tfrac{2}{3}(\alpha R)^{1/2}e^{(5/4)\pi i}(1-c)^{3/2}],\\
E &= \exp\{i\tfrac{2}{3}(\alpha R)^{1/2}[e^{-(3/4)\pi i}c^{3/2} - e^{(3/4)\pi i}(1-c)^{3/2}]\},
\end{aligned}\right\} \tag{62}
$$

so that (58), (59) and (60) become

$$
\left.\begin{aligned}
a_1 &= a_{11}(\alpha R)^{-1/2}E + O[(\alpha R)^{1/4}e^-],\\
a_2 &= a_{21}E + O[(\alpha R)^{1/4}e^-],\\
a_5 &= a_{51}(\alpha R)^{1/2} + a_{52} + O(\alpha R)^{-1/2},\\
a_6 &= a_{61} + a_{62}(\alpha R)^{-1/2} + O(\alpha R)^{-1},
\end{aligned}\right\} \tag{63}
$$

$$\left.\begin{aligned} b_1 &= b_{11} + b_{12}(\alpha R)^{-1/2} + O[(\alpha R)^{1/4} e^{+}], \\ b_2 &= b_{21} + b_{22}(\alpha R)^{-1/2} + O[(\alpha R)^{1/4} e^{+}], \\ b_5 &= b_{51}(\alpha R)^{1/2} + b_{52} + O[(\alpha R)^{-1/2}], \\ b_6 &= b_{61} + b_{62}(\alpha R)^{-1/2} + b_{63}(\alpha R)^{-1} + O[(\alpha R)^{-3/2}], \end{aligned}\right\} \tag{64}$$

$$\left.\begin{aligned} c_3 &= c_{31}(\alpha R)^{-1/2} + c_{32}(\alpha R)^{-1} + O[(\alpha R)^{-3/2}], \\ c_4 &= c_{41} + c_{42}(\alpha R)^{-1/2} + O[(\alpha R)^{-1}], \\ c_5 &= c_{51}(\alpha R)^{1/2} + c_{52} + c_{53}(\alpha R)^{-1/2} + O[(\alpha R)^{-1}], \\ c_6 &= c_{61}(\alpha R)^{-1/2} + c_{62}(\alpha R)^{-1} + O[(\alpha R)^{-3/2}], \end{aligned}\right\} \tag{65}$$

where

$$\left.\begin{aligned} a_{11} &= e^{i(3\pi/4)} c^{5/4}(1-c)^{1/4}, & a_{52} &= -\tfrac{5}{48} e^{-i(\pi/4)}(1-c)^{-3/2}, \\ a_{21} &= U e^{-i(\pi/2)} c^{-3/4}(1-c)^{1/4}, & a_{61} &= -e^{-i(\pi/4)}(1-c)^{1/2}, \\ a_{51} &= 1, & a_{62} &= \tfrac{7}{48} e^{i(\pi/2)}(1-c)^{-1}, \end{aligned}\right\} \tag{66}$$

$$\left.\begin{aligned} b_{11} &= e^{-i(\pi/4)} \frac{\sinh\alpha}{\alpha(1-c)^{1/2}}, & b_{51} &= 1, \\ b_{12} &= e^{i(\pi/2)} \frac{\cosh\alpha}{1-c}, & b_{52} &= -e^{-i(\pi/4)} \tfrac{5}{48}(1-c)^{-3/2}, \\ b_{21} &= -e^{-i(\pi/4)} \frac{\cosh\alpha}{(1-c)^{1/2}}, & b_{61} &= e^{-i(\pi/4)}(1-c)^{1/2}, \\ b_{22} &= -e^{i(\pi/2)} \frac{\alpha \sinh\alpha}{1-c}, & b_{62} &= \tfrac{17}{48} e^{i(\pi/2)}(1-c)^{-1}, \\ & & b_{63} &= -e^{i(\pi/4)}\left(\tfrac{35}{192} + \tfrac{385}{4608}\right)(1-c)^{-5/2}, \end{aligned}\right\} \tag{67}$$

$$\left.\begin{aligned} c_{31} &= -e^{i(\pi/2)}(rm^2)^{-1/2} \frac{m}{1-c}, & c_{51} &= r^{1/2}, \\ c_{32} &= e^{i(\pi/4)} \alpha (rm^2)^{-1} \left(\frac{m}{1-c}\right)^{3/2}, & c_{52} &= -\tfrac{5}{4} e^{-i(\pi/4)} \left(\frac{m}{1-c}\right)^{3/2}, \\ c_{41} &= -e^{-i(\pi/4)} \left(\frac{m}{1-c}\right)^{1/2}, & c_{53} &= -2e^{i(\pi/2)} \alpha^2 (rm^2)^{-1/2}(1-c)^{-1}, \\ c_{42} &= -\tfrac{41}{48} e^{i(\pi/2)}(rm^2)^{-1/2} \left(\frac{m}{1-c}\right)^{2}, & c_{61} &= -e^{i(\pi/2)} \frac{(rm^2)^{1/2}}{F(1-c)^2 m}, \\ c_{62} &= e^{i(\pi/4)} \frac{1}{m} \left(\frac{m}{1-c}\right)^{1/2} \left\{ \left[m + \frac{1}{F(1-c)} \right] \frac{\alpha}{1-c} - 2\alpha^2 + \frac{385}{4608} \left(\frac{m}{1-c}\right)^2 \right\}. \end{aligned}\right\} \tag{68}$$

The secular equation (54) can be expanded in terms of a sum of products of the viscid and inviscid terms. Equations (62) to (68) are then used for the purpose of determining the important terms to be kept in the final result.

7. *The eigenvalue problem for* $\alpha R \to \infty$

It can be shown that for $\alpha R \to \infty$, the secular equation reduces to

$$\mathcal{F}(\alpha, c, r, m, F, W) = 0,$$

or

$$(1-c)\alpha[g(\alpha, r, m)+r] - \left(\frac{\alpha^2}{W} + 1 - mr\right) - \frac{(1-r)}{F(1-c)} = 0, \tag{69}$$

which, when solved for c, gives*

$$c = 1 - \frac{(\alpha^2/W + 1 - rm) + \sqrt{\{(\alpha^2/W + 1 - rm)^2 + 4\alpha[g(\alpha, r, m)+r](1-r)/F\}}}{2\alpha[g(\alpha, r, m)+r]}, \tag{70}$$

where

$$g(\alpha, r, m) = \left[\frac{e^{\alpha}}{\sinh \alpha} + \frac{(m/r)^{1/2}}{\tanh \alpha} - 1\right]\frac{1}{1+(m/r)^{1/2}}, \tag{71}$$

the radicand being always positive, i.e. c is always real. This means that for $R \to \infty$, *the flow is neutrally stable*†. Also, since for cases of interest $rm < 1$, *c is always less than unity as* $R \to \infty$. This is quite an important conclusion, since for finite Reynolds numbers, the computation is different, depending on whether c is less or more than unity. It will therefore be assumed, in all the work for finite Reynolds number, that $c < 1$. The final calculations will bear out this assumption.

A different approach to the case of infinite Reynolds number would be to neglect viscosity at the outset, i.e. in the Orr–Sommerfeld equations. The differential equations then become of second order, and by relaxing the proper boundary conditions, the problem could again be solved. This has been done, and the equation obtained for c is the same as (70) except that the function $g(\alpha, r, m)$ is not given by (71) but by

$$g(\alpha, r, m) = \coth \alpha, \tag{72}$$

which agrees with (71) only when $m/r \gg 1$.

The limiting processes used to obtain (71) and (72) were different. Therefore it is not surprising that these results are not identical. From a physical point of view, the disagreement is inacceptable. Although no physical explanation of the discrepancy has been found as yet, the disagreement is immaterial from the present standpoint because for the fluid of interest, viz. a liquid–gas combination, $m/r \gg 1$ and the results agree.

8. *The case of finite Reynolds number*

The fundamental equations for the neutral stability curve in the αR-plane, for a given physical situation (i.e. for fixed gas–liquid density ratio r,

* The root with the negative sign in front of the radical can be proven to be an extraneous root introduced when solving (69).

† It is worth remarking that for the case of 'inviscid Couette flow' of a single fluid the Orr–Sommerfeld equation has no non-trivial solution, while for two layers of fluids there is only this one non-trivial solution for the eigenvalue problem.

liquid–gas viscosity ratio m, Froude number F, and Weber number W), are

$$\mathscr{G}(\alpha, c) - \mathscr{H}(\alpha, c) = 0, \qquad (\alpha R)^{1/2} = -\frac{\mathscr{H}(\alpha, c)}{\mathscr{F}(\alpha, c)}, \tag{73}$$

each point on the curve having a particular wave velocity. The functions $\mathscr{F}(\alpha, c)$, $\mathscr{G}(\alpha, c)$ and $\mathscr{H}(\alpha, c)$ are defined by

$$\mathscr{F}(\alpha, c) = \frac{1}{\sqrt{2}}\left\{2\alpha(1-c) + [e^{-\alpha}(\Lambda_6 - V_6) + 2T_6 \sinh\alpha]\left(\frac{m}{r}\right)^{1/2} + \right.$$
$$\left. + 2\sinh\alpha(T_6 - \Lambda_6)\right\}, \tag{74}$$

$$\mathscr{G}(\alpha, c) = -\frac{2\alpha}{(1-c)^{1/2}}\left[\frac{5}{4}\left(\frac{m}{r}\right)^{1/2} m + \frac{17}{48} + \frac{1}{F(1-c)}\right] +$$
$$+ 4\alpha^2 e^{-\alpha}\left(1 - \frac{1}{m}\right)\sinh\alpha\left(\frac{m}{r}\right)^{1/2}(1-c)^{1/2} -$$
$$- [e^{-\alpha}(\Lambda_6 - V_6) + 2T_6\sinh\alpha]\left(\frac{m}{r}\right)^{1/2}\frac{1}{48(1-c)^{3/2}}\left[5 + 41\left(\frac{m}{r}\right)^{1/2}\right] +$$
$$+ \frac{\alpha}{r(1-c)^{1/2}}[(V_6 - \Lambda_6)e^{-\alpha} + 2T_6\cosh\alpha] -$$
$$- \frac{2\alpha}{(1-c)^{1/2}}(T_6 - \Lambda_6)\left[\frac{5}{4}\frac{m}{1-c}\left(\frac{m}{r}\right)^{1/2}\frac{\sinh\alpha}{\alpha} + \cosh\alpha\right] +$$
$$+ 2\alpha\left(1 - \frac{1}{m}\right)(V_6 e^{-2\alpha} - \Lambda_6)\left(\frac{m}{r}\right)^{1/2}\frac{1}{(1-c)^{1/2}}\frac{\sinh\alpha}{\alpha}, \tag{75}$$

$$\mathscr{H}(\alpha, c) = c^{-1/2}\left\{-2\alpha^2(1-c) + \alpha[(\Lambda_6 + V_6)e^{-\alpha} - 2T_6\cosh\alpha]\left(\frac{m}{r}\right)^{1/2} - \right.$$
$$\left. - 2\alpha(T_6 - \Lambda_6)\cosh\alpha\right\}, \tag{76}$$

$$\Lambda_6 = \left[\frac{\alpha^2}{W} + \frac{1}{F(1-c)} + 1 + (1-c)\alpha\right]e^{-\alpha}, \tag{77}$$

$$V_6 = \left[\frac{\alpha^2}{W} + \frac{1}{F(1-c)} + 1 - (1-c)\alpha\right]e^{\alpha}, \tag{78}$$

$$T_6 = \left[m + \frac{1}{F(1-c)} + (1-c)\alpha\right]re^{-\alpha}. \tag{79}$$

The solution of (73) for c as a function of α has to be obtained numerically*, because of the impossibility of solving explicitly for c or α in terms of the other. Once a pair of values of α and c is known, straightforward calculation leads to the value of $(\alpha R)^{1/2}$, it being possible to evaluate R immediately.

A digression is permissible at this point in order to point out the meaning of Reynolds number $R = R_l$ in the present problem. Since the velocity profile is a linear function of distance, for given liquid physical properties R is proportional to the liquid flow rate, and therefore is a constant once the flow rate is specified.

* All the numerical work was carried out on an IBM card-programmed electronic calculator using an 8-digit floating decimal system.

Now that a method for determining the neutral stability curve has been described, it is necessary to decide which region, on either side of it, is stable or unstable. The calculations indicate, as is reasonable to expect, that for a disturbance of a given wavelength, the flow is stable for Reynolds numbers smaller than a Reynolds number R_n, corresponding to a neutral disturbance; and similarly the flow is unstable for $R > R_n$.

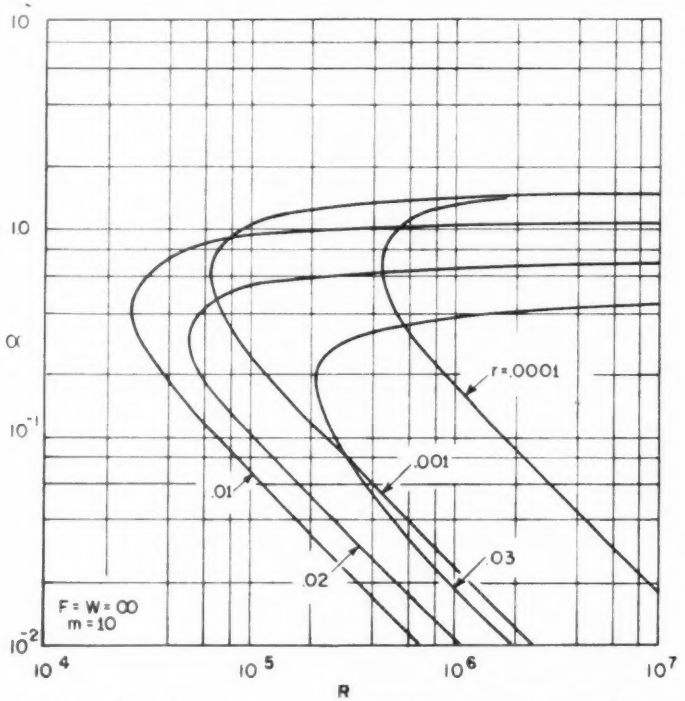

Figure 3. Neutral stability curves: wave number *vs* liquid Reynolds number. Gravity and surface tension forces are neglected. Liquid–gas viscosity ratio = 10.

The results obtained from the present analysis, of which figure 3 is a typical example with $F = W = 0$, indicate that the shape of the neutral stability curves in the αR-plane is similar to the boundary-layer case*. The effect of varying the gas–liquid density ratio r could be stabilizing or destabilizing, while increasing the liquid–gas viscosity ratio m always tends to stabilize the flow, provided m is not small compared with unity.

* The reason for obtaining only one solution to the problem, and not two as Lock (1954) found, is that in the present case each fluid is stable by itself, and the only reason for the existence of instability is the discontinuity in the physical properties of the fluids. In Lock's case each fluid is probably also unstable. On the other hand, in the present treatment instability regions which do not extend to $R = \infty$ have not necessarily been eliminated; this may occur when $c > 1$. The analysis would have to be extended to this case in order to investigate this possibility.

For $\alpha \to 0$, the equation for the lower branch of the neutral stability curve is

$$\alpha R = \text{const.}, \tag{80}$$

as can be derived analytically. The upper branch seems to have a nearly horizontal tangent for $R \to \infty$; this was obtained numerically.

The influences of non-vanishing gravity* or surface tension forces on the above results should be alike, since they enter as a sum in the secular relation (40). Figure 4 shows that for large Froude F and Weber numbers W,

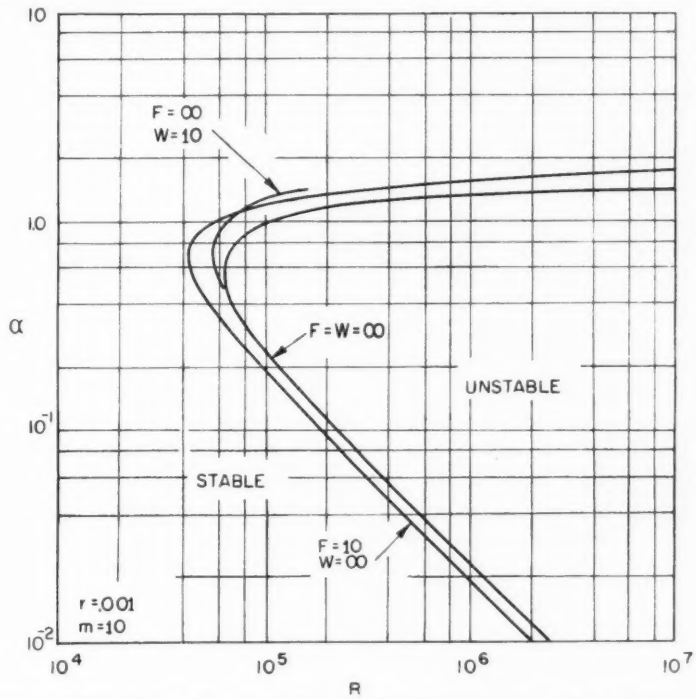

Figure 4. Effect of gravity and surface tension forces on neutral stability curves.

gravity and surface tension destabilize the flow. Obviously, surface tension effects are negligible when the disturbance frequency is small, but become very important at large frequencies. The effect on the neutral stability line is in this case to raise the upper branch so that its asymptote for $\alpha \gg 1$ is

$$\alpha/R = \text{const.}, \tag{81}$$

which can also be obtained analytically.

* The gravitational field was assumed to act downwards in the flow configuration indicated in figure 1.

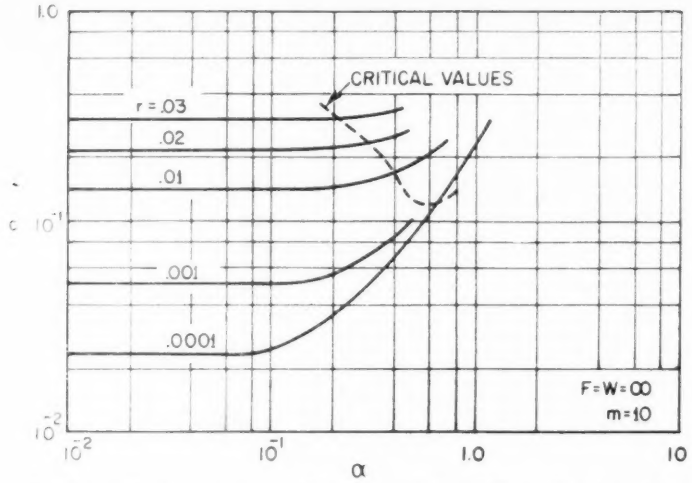

Figure 5. Wave velocity *vs* wave number for neutral stability. Gravity and surface tension forces are neglected. Liquid–gas viscosity ratio = 10.

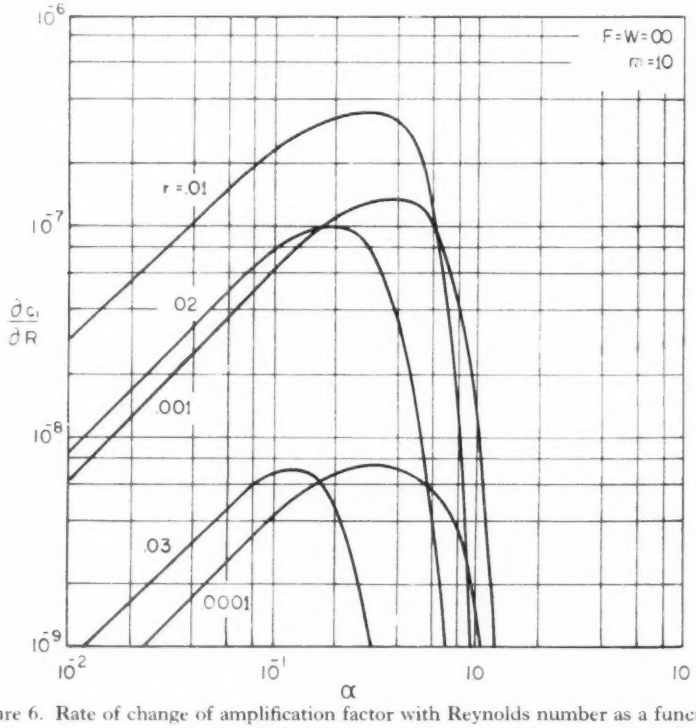

Figure 6. Rate of change of amplification factor with Reynolds number as a function of wave number and gas–liquid density ratio. Liquid–gas viscosity ratio = 10.

All the effects discussed thus far concern the stability of the flow, and the direction (left or right) in which the neutral stability curve moves in the αR-plane when the physical quantities are varied.

There are two or more items to be discussed before the results of our numerical calculations are summarized. They are (*a*) the behaviour of the magnitude of the wave velocity; (*b*) the amplification or damping rate of disturbances in the neighbourhood of the neutral stability line.

With respect to (*a*), it is enough to mention that all waves travel at speeds less than the velocity of the liquid–gas interface, a typical case being given in figure 5.

On the neutral stability curve, the imaginary part c_i of the complex velocity c vanishes. It is possible, nevertheless, to compute the rate of change of c_i with respect to Reynolds number. The important result is that this is always a positive quantity which, as a function of α (figure 6), has a peak near the critical Reynolds number. This means that the curves $c_i = \text{const.}$, in the αR-plane, would be packed close together when in the neighbourhood of the critical values of α and R.

Since the quantities of greatest interest are the parameters corresponding to the critical value of the Reynolds number, the large number of calculations which we have made may suitably be summarized as follows.

9. *Values of critical quantities and discussion of results. Comparison with experiments*

Since the physical case of interest is the one where gravity and surface tension forces are small, detailed calculations were carried out for $F = W = \infty$. The critical values are presented in figures 7 to 10, from which the following facts can be gathered:

(1) As m and $r \to 1$, the flow is completely stable.

(2) For a given gas–liquid density ratio r, an increase in the liquid–gas viscosity ratio m always increases the stability, and decreases the amplification or damping in the region away from the neutral stability curve.

(3) For very small r, the flow is completely stable.

(4) For a given m, there is always a value of r for which the flow is most unstable.

(5) As $r \to 0$, the wave number α tends to a value of 0·6 approximately, and the wave velocity c becomes 0·1 approximately.

(6) For the special case of air and water at a temperature of 100° C and a pressure of one atmosphere ($m \doteqdot 10$, $r \doteqdot 0{\cdot}001$), the value of the critical Reynolds number is 60 000.

(7) The critical conditions depend for given physical properties only on the liquid flow rate.

The significance of the results quoted as items (1) and (2) can be understood in terms of the known universal stability of plane Couette flow (from now on abbreviated as P.C.F.) between walls of arbitrary spacing. An explanation follows.

In the special case when the two fluids have the same density and viscosity (equivalent to the case of a single fluid), the velocity profile becomes a single straight line. Item (1) shows the flow then to be universally stable, in agreement with the known result for P.C.F.; a check on the analysis is thus obtained.

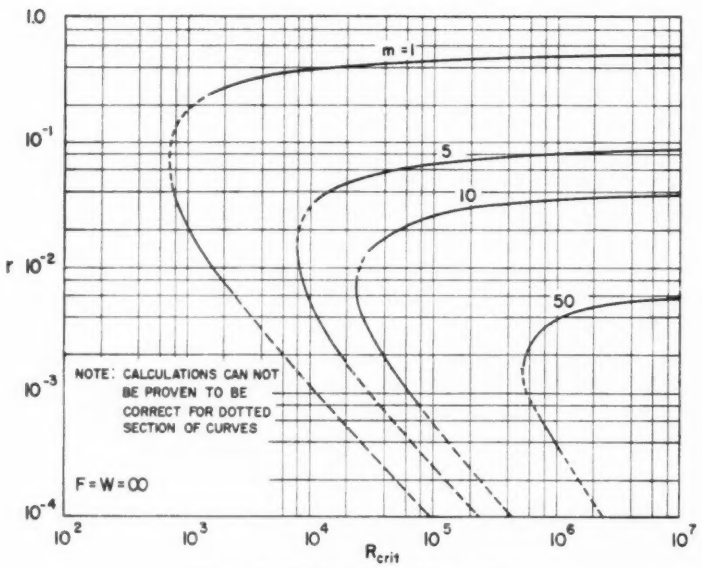

Figure 7. Critical Reynolds number.

When the result quoted as item (2) is interpreted for the limiting case of a very viscous liquid, the motion is again always stable. The very viscous liquid could just as well be considered as a solid and this case again reduces to P.C.F.

From item (2) and the above discussion, a result can be deduced which has not been obtained directly by any calculation. This is that, for an arbitrary density ratio, the flow is completely stabilized when $m \to 0$. The reason for stabilization is that this limiting case of the flow occurs when the gas becomes so viscous that it could be replaced by a solid wall, which again reduces to P.C.F. between two walls at a finite spacing.

Therefore, in figure 7 there would exist a curve for some small value of m that would be farthest to the left, and for smaller values of m the curves would again be displaced more and more to the right as the liquid–gas viscosity ratio is decreased.

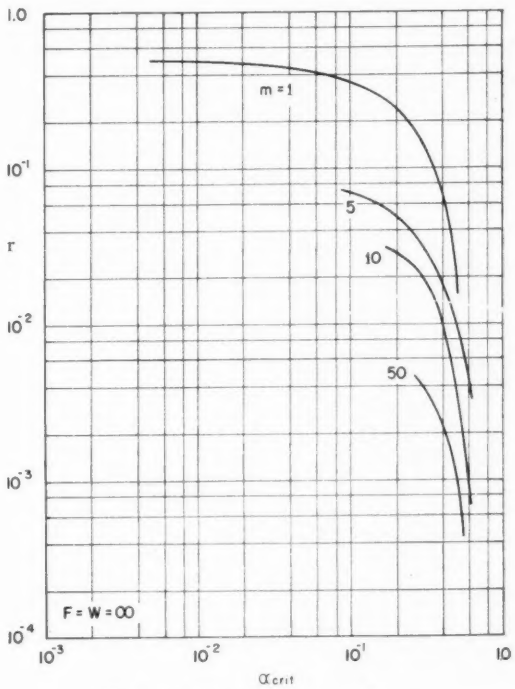

Figure 8. Critical wave number.

Items (5) and (6) will now be compared with some experimental observations. Most experiments with liquid films have been carried out in horizontal round tubes where the liquid flows along the inner surface dragged by a high-speed turbulent gas. It should be kept in mind that while the gas layer is of infinite thickness in the theoretical model, the ratio of laminar sublayer thickness in the gas to liquid film thickness in the experiments was of the order of unity.

The experimental neutral wavelength λ observed by Knuth (1954) for all liquid flow rates was about 10 film thicknesses. Considering that $\alpha = 2\pi/\lambda$, Knuth's findings check with the critical value of item (5). Since the wavelengths in the neighbourhood of the critical value are the most amplified, these might be the only ones visible in an experiment. Knuth might have observed these values, which, although seemingly neutral, could have been slightly amplified.

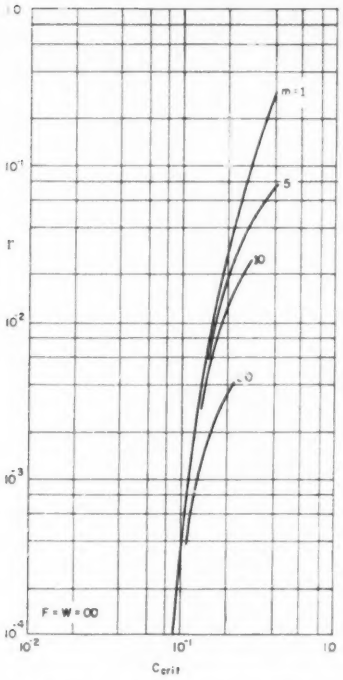

Figure 9. Critical wave velocity.

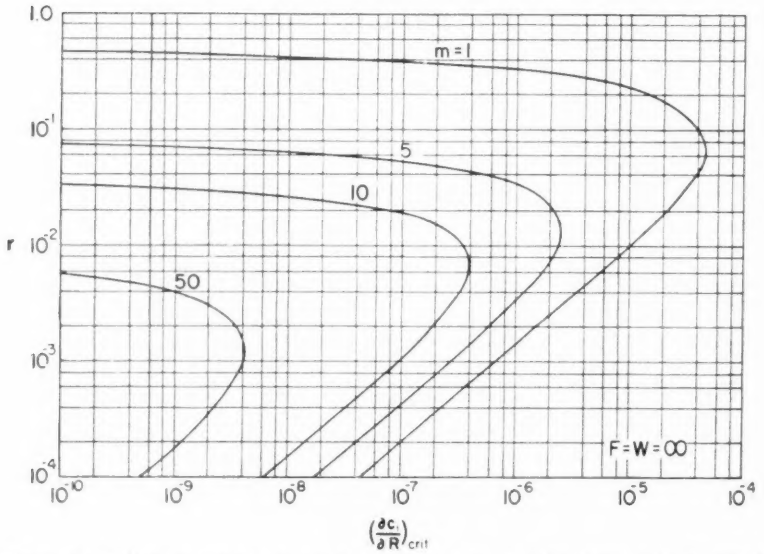

Figure 10. Critical values of the rate of change of amplification factor with Reynolds number.

Item (6) implies that for a liquid film 0·005 in. thick, the critical liquid–gas interface velocity is 100 ft/sec, which is one order of magnitude larger than the values obtained from experiments in liquid films. This discrepancy would seem to indicate that the observed instability is not simply laminar instability of uniform shearing motion. The fact that the computed critical Reynolds number is much higher than the experimental values could be due to the fact that the velocity profiles of both fluids in the analysis were assumed to be straight lines. If curved profiles were used it is conceivable that the critical Reynolds number could decrease. This possibility is suggested by the change in the value of critical Reynolds

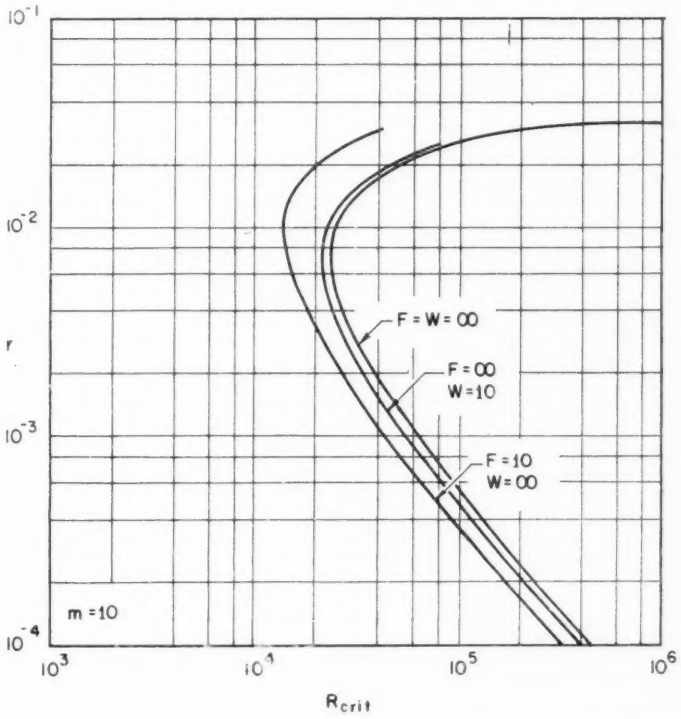

Figure 11. Influence of gravity and surface tension forces on critical Reynolds number.

number when going from plane Couette ($R_{crit} = \infty$) to plane Poiseuille flow ($R_{crit} = 11\,560$, based on the maximum velocity and width of the channel). Curvature in the velocity profile of the liquid could exist in the case of laminar flow when there is a pressure gradient in the flow direction. One of the things that has not been accounted for in the present or suggested analysis is the effect of turbulence of the gas stream, which also possibly influences the stability of the flow.

Gravity and surface tension have a destabilizing effect (see figures 11 and 12), as remarked in the discussion in §8. This influence of surface tension was observed by Kinney, Abramson & Sloop (1952, p. 10), the relative change in the critical Reynolds number being of the same order of magnitude (within a factor of at most 2) as the value found here analytically.

Item (7) agrees with the experimental fact reported by Knuth that the inception point of instability is a function of the liquid flow rate, and independent of the gas flow rate.

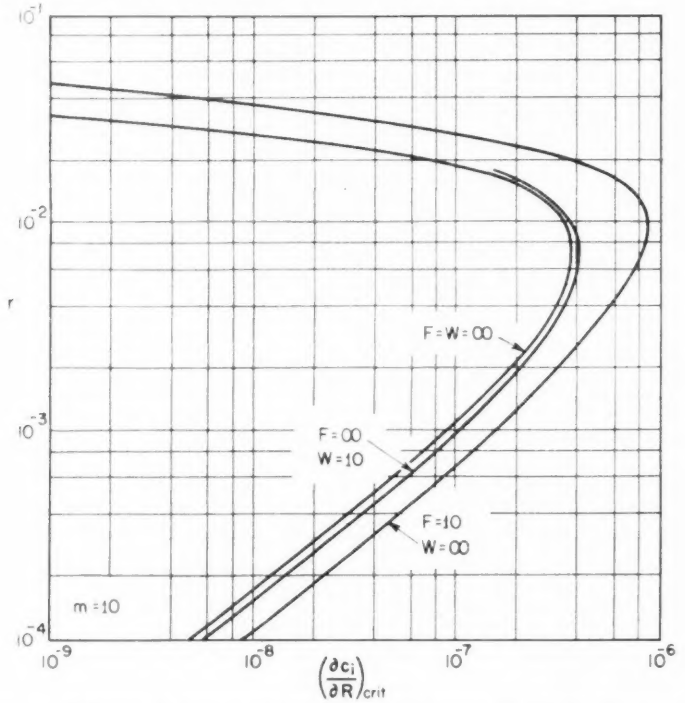

Figure 12. Influence of gravity and surface tension forces on critical rate of change of amplification factor with Reynolds number.

Before concluding, it will be helpful to try to gain some physical insight into the stability problem by looking at the energy of the disturbed motion. This will be done in Part III.

10. *Accuracy of calculations*

The accuracy of our calculations, based upon the viscous functions given in §6, Part II, is restricted by the fact that αR was assumed large. This was interpreted as meaning that in (61) the right-hand members are good approximations to the left-hand members, and permitted the use of

asymptotic methods. Terms of $O[(\alpha R)^{-1}]$ were neglected when compared with terms of $O[(\alpha R)^{-1.2}]$ in the secular equation. A check on the assumption mentioned was done for each calculation of a point on the neutral stability curve. The result of this checking showed that the assumption was incorrect for small values of r, shown dotted on figure 7 only. Nevertheless, the trends in that region are probably correct. This is inferred by comparing the dotted sections with the curve for $m = 50$, which is valid over almost all of the regions shown: they seem to form a reasonable family.

For small values of r, the last of equations (61) for z_{g1} should be approximated by the first term and not by the second, as for larger values of r. If this innovation were made, a valid calculation for the dotted part of figure 7 would then be possible.

III. The Reynolds shearing stress

A different way of looking at the stability problem, due to Lin (1954), consists of following the history of the disturbance energy, which, for damping or amplification, changes as a result of the action of the Reynolds shearing stress τ_s*. It is then enlightening to know its distribution across the stream.

Foote & Lin (1950) have shown that

$$\tau_s = -\rho\overline{uv} = -\frac{\rho\alpha}{4i}\exp\{2\alpha c_i t\}(\phi\bar{\phi}' - \bar{\phi}\phi'), \tag{82}$$

and

$$\frac{d\tau_s}{dy} = -\frac{\rho\alpha}{4i}\exp\{2\alpha c_i t\}\frac{d}{dy}(\phi\bar{\phi}' - \bar{\phi}\phi'), \tag{83}$$

where $\overline{uv}$ is the distance or time average of the product uv, and $\bar{\phi}$ and $\bar{\phi}'$ dicate complex conjugates of ϕ and ϕ'.

At the interface, for the viscous case,

$$\overline{u_l v_l} = \overline{u_g v_g} \tag{84}$$

$$(\tau_{sl}/\tau_{sg})_{\text{interface}} = \rho_l/\rho_g = 1/r. \tag{85}$$

The inviscid case

The amplitude functions ϕ and Φ for the inviscid case are real functions. Therefore (82) shows that

$$(\phi\bar{\phi}' - \bar{\phi}\phi') = \text{const.} = 0, \tag{86}$$

from which it follows that the Reynolds stresses are zero across the flow. This means that there is no mechanism for transferring energy between the basic flow and the disturbance, i.e. any disturbance will just subsist, without damping or amplification.

As can be seen, the method of this section is extremely useful, since the important result of § 7 regarding stability has now been rederived in a few lines without any calculation.

* The work done per unit volume per unit time by the basic flow is $\tau\, dU/dy$ (Schlichting 1950), and converts energy from the basic flow into the disturbance when $dU/dy > 0$.

The viscous case

We will start the study of this case by showing that the Reynolds stress is continuous across the layer where $U(y) = c_r$. The Orr–Sommerfeld equation (4) can be rewritten as (c is complex)

$$\phi'' - \alpha^2\phi = \frac{U''}{U-c}\phi - \frac{i}{\alpha R(U-c)}(\phi^{iv} - 2\alpha^2\phi'' + \alpha^4\phi), \tag{87}$$

which, on multiplying by $\bar{\phi}$, subtracting its complex conjugate and regrouping yields

$$\frac{d}{dy}(\bar{\phi}\phi' - \bar{\phi}'\phi) = \frac{2c_i U''\phi^2}{U-c^2} - \frac{i}{\alpha R}\left(\frac{\phi^{iv}\bar{\phi} - 2\alpha^2\phi''\bar{\phi} + \alpha^4\phi\bar{\phi}}{U-c} + \right.$$
$$\left. + \frac{\bar{\phi}^{iv}\phi - 2\alpha^2\phi''\bar{\phi} + \alpha^4\phi\bar{\phi}}{U-\bar{c}}\right). \tag{88}$$

Equation (88) can now be introduced into (83), and since $U'' = 0$, we have

$$\frac{d\tau_s}{dy} = \frac{\rho}{4R}e^{2\alpha c_i t}\left(\frac{\phi^{iv}\phi - 2\alpha^2\phi''\phi + \alpha^4\phi\phi}{U-c} + \frac{\bar{\phi}^{iv}\phi - 2\alpha^2\phi''\bar{\phi} + \alpha^4\phi\bar{\phi}}{U-\bar{c}}\right), \tag{89}$$

which can be integrated across the layer where $U = c$, and remembering that in our case $U = y$,

$$\int d\tau_s = (\tau_s)_{y=c+0} - (\tau_s)_{y=c-0} = [\tau_s]$$
$$= \frac{\rho}{4R}e^{2\alpha c_i t}\lim_{\epsilon\to 0}\{[\phi^{iv}\bar{\phi} - 2\alpha^2\phi''\bar{\phi} + \alpha^4\phi\bar{\phi}]_{y=c}[\log\epsilon - \log(-\epsilon)] +$$
$$+ [\bar{\phi}^{iv}\phi - 2\alpha^2\bar{\phi}''\phi + \alpha^4\phi\bar{\phi}]_{y=c}[\log(c-\bar{c}+\epsilon) - \log(c-\bar{c}-\epsilon)]\}. \tag{90}$$

Since $\log\epsilon - \log(-\epsilon) = \pm i\pi(2n+1), \qquad n = 0, 1, 2, \ldots,$

equation (90), with $c_i = 0$, gives for the jump in Reynolds stress $[\tau_s]$ across the layer where $U = c$

$$[\tau_s] = \frac{\rho}{4R}[\bar{\phi}^{iv}\phi + \bar{\phi}^{iv}\bar{\phi} - 2\alpha^2(\bar{\phi}''\bar{\phi} + \bar{\phi}''\phi) + 2\alpha^2\phi\bar{\phi}][\pm i\pi(2n+1)]. \tag{91}$$

where a particular n should be chosen for the branch of the logarithm being used. (Note that the quantity in the first bracket on the right-hand side of (91) is real, and the quantity in the second bracket is purely imaginary.) Since $[\tau_s]$ must be real, and $\rho/4R \neq 0$, we have at $y = c$

$$\phi^{iv}\bar{\phi} + \bar{\phi}^{iv}\phi - 2\alpha^2(\phi''\bar{\phi} + \bar{\phi}''\phi) + 2\alpha^4\phi\bar{\phi} = 0. \tag{92}$$

Therefore $$[\tau_s] = 0 \quad \text{at} \quad y = c_r = c. \tag{93}$$

Lin (1954) has shown that the Reynolds stress in a viscous fluid grows positively and very rapidly with distance away from the wall in a very thin layer, and then stays about constant.

We now have enough information to build the complete picture of stress distribution for the viscous case. Starting at the wall, the Reynolds stress is zero, and as we proceed outwards it grows at a rapid rate. It then levels off and since viscosity is not very important, (86) will be almost satisfied (i.e. $\tau_s \doteq$ const.). There is no jump across the layer where $U = c$. As we get to the liquid–gas interface, the stress is discontinuous, the ratio of the

values on both sides of the discontinuity being given by (85). The stress on the gas side cannot be zero, since by (84) this would mean that the stress in the liquid is zero. Far away in the gas stream, the Reynolds stress must vanish. Figure 13 shows qualitatively this stress distribution.

Lin (1954) found an important relationship in the theory of hydrodynamic stability in a very simple way. The principle used by him was to equate the stress in the fluid adjacent to the wall computed by two different methods, starting from the wall in one case, and from the main stream in the other. This method has not yet been made successful here, the reason being that the magnitude of the jump of stress across the interface is unknown, only the ratio being known. In order to compute the jump, one would have first to compute the stress at the interface, on the gas side, by calculating the function Φ. This would destroy the simplicity of Lin's method.

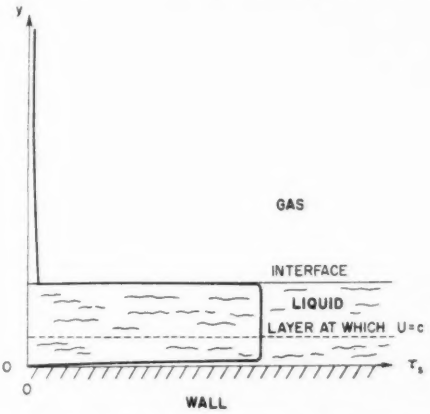

Figure 13. Distribution of Reynolds stress for a neutral oscillation.

Therefore, looking at the Reynolds stress in the present case was not as fruitful as in Lin's case. It would nevertheless be interesting to find the quantitative distribution of stress for a self-excited disturbance and for a neutral disturbance. This would show whether most of the energy input into the disturbance comes from the gas or the liquid. From the functions presented in this paper, it would be possible to calculate the Reynolds stress for a neutral disturbance. The case of a self-excited disturbance is much more complicated, and the necessary amount of numerical work, as envisaged at the present time, is prohibitive.

IV. Concluding remarks

The discrepancy between experiments on the stability of liquid films and the present theory is confined to the fact that the theoretical value of the critical Reynolds number is larger than the experimental one, all other quantities being in agreement. The results obtained here seem to indicate that a study of the hydrodynamic stability of two fluids with curved velocity profiles would be worth-while. Such a study might definitely settle the

question whether or not the large-scale disturbances observed in liquid-film cooling experiments are due to laminar instability.

The distribution of the Reynolds stress across the stream remains a problem of great importance to the physical understanding of hydrodynamic stability in the present example.

The model chosen for the analysis, although the simplest possible, has yielded a number of new and interesting results. The most important conclusion to be drawn from this investigation is that a discontinuity of viscosity or density has a destabilizing effect on uniform shearing motion.

This paper is based on the thesis submitted by the author in partial fulfilment of the requirements for the degree of Doctor of Philosophy at the California Institute of Technology, June 1955. The author wishes to express his gratitude to Professor W. D. Rannie, for suggesting this problem and for his critical guidance during the course of this investigation, and to Professor C. C. Lin for his very helpful suggestions and personal interest. The author is also grateful to the Daniel and Florence Guggenheim Foundation and to the California Institute of Technology for making possible his continuation of graduate study through the grants, respectively, of a Fellowship in Jet Propulsion and a Graduate Tuition Scholarship during the 1953–54 and 1954–55 academic years.

References

Copson, E. T. 1935 *An Introduction to the Theory of Functions of a Complex Variable*, 1st Ed. Oxford University Press.

Feldman, S. 1955 *On the hydrodynamic stability of two viscous incompressible fluids in parallel uniform shearing motion.* Ph.D. Thesis, California Institute of Technology.

Foote, J. R. & Lin, C. C. 1950 *Quart. Appl. Math.* **8,** 265.

Goldstein, S. 1931 *Proc. Roy. Soc.* A, **132,** 524.

Hopf, L. 1914 *Ann. Physik* **44,** 11.

Kinney, G. R., Abramson, A. E. & Sloop, J. L. 1952 *Nat. Adv. Comm. Aero., Wash., Rep.* no. 1087.

Knuth, E. H. 1954 *Jet Propulsion* **24,** 359.

Lamb, H. 1932 *Hydrodynamics*, 6th Ed., p. 456. New York : Dover Publications.

Lin, C. C. 1945 *Quart. Appl. Math.* **3,** 117.

Lin, C. C. 1954 *Proc. Nat. Acad. Sci.* **40,** 741.

Lock, R. C. 1954 *Proc. Camb. Phil. Soc.* **50,** 105.

Morse, P. M. & Feshbach, H. 1953 *Methods of Theoretical Physics*, Vol. 1. New York : McGraw-Hill Book Co., Inc.

Orr, W. Mc. F. 1906 *Proc. Roy. Irish Acad.* **27,** 9.

Rayleigh, Lord 1887 *Scientific Papers*, Vol. 3, 17.

Schlichting, H. 1950 *Nat. Adv. Comm. Aero., Wash., Tech. Mem.* no. 1265.

Sommerfeld, A. 1909 *Atti del IV Congresso Internazionale dei Matematici*, Vol. 3, p. 116, Roma.

Taylor, G. I. 1931 *Proc. Roy. Soc.* A, **132,** 499.

Thomas, L. H. 1953 *Phys. Rev.* **91,** 780.

York, J. L., Stubbs, H. E. & Teck, M. R. 1953 *Trans. Amer. Soc. Mech. Engrs.* **75,** 1279.

Zondek, B. & Thomas, L. H. 1953 *Phys. Rev.* **90,** 738.

Oscillations of tide and surge in an estuary of finite length

By J. PROUDMAN
Edgemoor, Verwood, Dorset

(*Received* 18 *February* 1957)

SUMMARY

This paper concerns a narrow basin of uniform cross-section open to the sea at one end and closed at the other. An incident long wave of prescribed general form is supposed to enter from the sea and to represent the combination of tide and surge as generated in the sea. The solution of the linear terms of the equations of continuity and motion gives the reflection of this wave at the head of the estuary. This paper gives the next approximation when the non-linear terms are retained, the second-order motion being made determinate by the condition that, at the mouth, it reduces to a progression towards the sea.

The chief results relate to the surface elevation at the head of the estuary. When the first order elevation there increases steadily to a maximum, the effect of the 'shallow water terms' is to make high water higher and earlier, while the effect of the 'frictional term' is to make high water lower and later. For a short estuary, the interaction of the tide on a surge, due to a given sequence of meteorological conditions over the sea, is to make it higher when its maximum occurs at the time of tidal high water than when its maximum occurs at the time of tidal low water. This is directly opposite to the corresponding result when the estuary is of infinite length.

1. INTRODUCTION

In two papers (Proudman 1955 a, b) I have discussed the dynamics of a progressive wave of tide and surge in an estuary, and particularly the interaction between the tide and the surge. For equal sequences of meteorological conditions over the sea, I showed that the apparent height of a surge whose maximum occurs near to the time of tidal high water is less than that of a surge at the same place whose maximum occurs near to the time of tidal low water. But the tides of the Thames Estuary, for example, constitute a standing oscillation much more nearly than they constitute a progressive wave.

In the first of the papers, I also gave an approximate solution of the differential equations relating to an estuary with a barrier, but without using end-conditions which would completely determine the motion. In 1956 Doodson considered the problem presented by a gulf, and gave numerical solutions for the cases of a tide prescribed at the mouth and of a surge prescribed at the head. Because of reflection from the head, it is

inappropriate to prescribe a surge at the mouth of an estuary. Also, any attempt to deal with discontinuities of basin at the mouth, involves reflections from the mouth, both on the seaward side and on the estuarial side.

In this paper, a prescribed incident wave is taken to progress up the estuary, and the remaining part of the motion is taken to reduce, at the mouth, to a wave travelling down the estuary. The incident wave is taken to represent the combined tide and surge which are generated in the sea, and the remainder of the motion is taken to represent the origin of the wave which, in the open sea, will diverge away from the mouth of the estuary.

In order to avoid a greater mathematical complication, I suppose the cross-section of the estuary to be uniform. I follow the same mathematical method as in my earlier paper, except that I now use the differential equation for the current, whereas previously I used that for the elevation of the water-surface. Because of the more precise end-conditions of the present paper, the results are more definite than those of that part of the earlier paper which relates to an estuary with a barrier.

It appears that the surface-elevation at the head of the estuary depends on the primary elevation there at the same time and for a previous interval during which a progressive wave could travel twice the length of the estuary. When, during this interval, the primary wave increases steadily to a maximum, the tendency of the shallow water terms of the differential equations is to make high water higher and earlier, while the tendency of the frictional term is to make high water lower and later. For a short estuary, the current in the estuary, and the time and height of high water at its head, are approximately independent of friction; while the interaction of the tide on a surge, due to a given sequence of meteorological conditions over the sea, is to make it higher when its maximum occurs at the time of tidal high water than when its maximum occurs at the time of tidal low water. This result is directly opposite to the corresponding result for a progressive wave.

2. Notation and differential equations

Denote by:

g the acceleration of gravity,
h the undisturbed depth of the water, supposed uniform,
a the length of the estuary,
x distance down the estuary, $x = 0$ being at the head and $x = a$ at the mouth,
t the time,
ζ the elevation of the water-surface,
u the current down the estuary,
k a numerical coefficient of friction, which will be taken as 0·0025;

and write

$$c = (gh)^{1/2}.$$

Take also
$$\xi = t + \frac{x}{c}, \qquad \eta = t - \frac{x}{c}, \tag{1}$$

so that
$$t = \tfrac{1}{2}(\xi + \eta), \qquad \frac{x}{c} = \tfrac{1}{2}(\xi - \eta), \tag{2}$$

and
$$\frac{\partial}{\partial t} = \frac{\partial}{\partial \xi} + \frac{\partial}{\partial \eta}, \qquad c\frac{\partial}{\partial x} = \frac{\partial}{\partial \xi} - \frac{\partial}{\partial \eta}, \tag{3}$$

so that
$$\frac{\partial^2}{\partial t^2} - c^2\frac{\partial^2}{\partial x^2} = 4\frac{\partial^2}{\partial \xi\, \partial \eta}. \tag{4}$$

Accents will be used to denote derivatives of functions with respect to their arguments. Suffixes 1 and 2 will be used respectively to denote terms which are of the first and second orders in the ratio of the primary surface-elevation to the depth of water.

The equation of continuity is
$$\frac{\partial}{\partial x}\{(h+\zeta)u\} + \frac{\partial \zeta}{\partial t} = 0, \tag{5}$$

and the equation of motion is
$$\frac{\partial u}{\partial t} + u\frac{\partial u}{\partial x} + g\frac{\partial \zeta}{\partial x} = -\frac{k}{h}\, u\, u \tag{6}$$

while $u = 0$ where $x = 0$.

The product terms on the left-hand sides of (5), (6) will be called the 'shallow water terms' of these equations.

3. General form of solution

The elimination of ζ from the first-order terms of (5) and (6) gives
$$\frac{\partial^2 u}{\partial t^2} - c^2\frac{\partial^2 u}{\partial x^2} = g\frac{\partial^2}{\partial x^2}(\zeta u) - \frac{1}{2}\frac{\partial^2 (u^2)}{\partial x\, \partial t} - \frac{k}{h}\frac{\partial}{\partial t}\, u\, u, \tag{7}$$

and the general solution of the first-order part of this equation, which makes $u_1 = 0$ where $x = 0$, is
$$u_1/c = -F\left(t + \frac{x}{c}\right) + F\left(t - \frac{x}{c}\right), \tag{8}$$

where $F(\,)$ denotes any function which is physically interpretable. It follows from the first-order part of (5) that
$$\frac{1}{h}\frac{\partial \zeta_1}{\partial t} = -\frac{\partial u_1}{\partial x} = F'\left(t + \frac{x}{c}\right) + F'\left(t - \frac{x}{c}\right),$$

so that
$$\frac{\zeta_1}{h} = F\left(t + \frac{x}{c}\right) + F\left(t - \frac{x}{c}\right), \tag{9}$$

no term independent of t being required.

The terms of (8), (9) in $F(t+x/c)$ are taken to represent the prescribed incident wave. The solution of the fundamental equations, as far as the second order, will be of the form

$$\frac{\zeta}{h} = F\left(t+\frac{x}{c}\right) + F\left(t-\frac{x}{c}\right) + \frac{\zeta_2}{h}, \tag{10}$$

$$\frac{u}{c} = -F\left(t+\frac{x}{c}\right) + F\left(t-\frac{x}{c}\right) + \frac{u_2}{c}. \tag{11}$$

The terms of (10), (11) in $F(t-x/c)$ represent a wave travelling down the estuary, and, to satisfy the condition prescribed in § 1, so must the terms in ζ_2, u_2 at $x = a$. The condition for this is

$$\frac{\zeta_2}{h} = \frac{u_2}{c}, \tag{12}$$

where $x = a$, and this will be used as the determining condition in this paper.

4. Second order terms

For the second approximation, the equations (5), (7) lead to

$$h\frac{\partial u_2}{\partial x} + \frac{\partial \zeta_2}{\partial t} = -\frac{\partial}{\partial x}(\zeta_1 u_1), \tag{13}$$

$$\frac{\partial^2 u_2}{\partial t^2} - c^2\frac{\partial^2 u_2}{\partial x^2} = g\frac{\partial^2}{\partial x^2}(\zeta_1 u_1) - \frac{1}{2}\frac{\partial^2(u_1^2)}{\partial x\,\partial t} - \frac{k}{h}\frac{\partial}{\partial t}|u_1|u_1 \tag{14}$$

respectively, and the transformation (3), (4) applied to (14) gives

$$4\frac{\partial^2 u_2}{\partial\xi\,\partial\eta} = \frac{1}{h}\left(\frac{\partial^2}{\partial\xi^2} - 2\frac{\partial^2}{\partial\xi\,\partial\eta} + \frac{\partial^2}{\partial\eta^2}\right)(\zeta_1 u_1) - \\ - \frac{1}{2c}\left(\frac{\partial^2}{\partial\xi^2} - \frac{\partial^2}{\partial\eta^2}\right)u_1^2 - \frac{k}{h}\left(\frac{\partial}{\partial\xi} + \frac{\partial}{\partial\eta}\right)|u_1|u_1. \tag{15}$$

Now (9), (8) may be written respectively as

$$\frac{\zeta_1}{h} = F(\xi) + F(\eta), \tag{16}$$

$$\frac{u_1}{c} = -F(\xi) + F(\eta), \tag{17}$$

and substitution from these into (15) gives

$$\frac{4}{c}\frac{\partial^2 u_2}{\partial\xi\,\partial\eta} = -\left(\frac{\partial^2}{\partial\xi^2} - 2\frac{\partial^2}{\partial\xi\,\partial\eta} + \frac{\partial^2}{\partial\eta^2}\right)\{F^2(\xi) - F^2(\eta)\} - \\ - \frac{1}{2}\left(\frac{\partial^2}{\partial\xi^2} - \frac{\partial^2}{\partial\eta^2}\right)\{F(\xi) - F(\eta)\}^2 + \\ + \frac{kc}{h}\left(\frac{\partial}{\partial\xi} + \frac{\partial}{\partial\eta}\right)\{|F(\xi) - F(\eta)|\,[F(\xi) - F(\eta)]\}. \tag{18}$$

The general solution of (18) is of the form

$$4u_2/c = \phi + \psi + X + Y, \tag{19}$$

where

$$\frac{\partial^2\phi}{\partial\xi\,\partial\eta} = \frac{\partial^2}{\partial\xi^2}\{-\tfrac{3}{2}F^2(\xi) + F(\xi)F(\eta)\} + \frac{kc}{h}\frac{\partial}{\partial\xi}\{|F(\xi) - F(\eta)|\,[F(\xi) - F(\eta)]\},$$

$$\frac{\partial^2\psi}{\partial\xi\,\partial\eta} = \frac{\partial^2}{\partial\eta^2}\{\tfrac{3}{2}F^2(\eta) - F(\eta)F(\xi)\} + \frac{kc}{h}\frac{\partial}{\partial\eta}\{|F(\xi) - F(\eta)|\,[F(\xi) - F(\eta)]\},$$

and X, Y are arbitrary functions of ξ, η respectively. One integration of each of these equations gives

$$\frac{\partial\phi}{\partial\eta} = -\tfrac{3}{2}[F^2(\xi)]' + F'(\xi)F(\eta) + \frac{kc}{h}|F(\xi)-F(\eta)|[F(\xi)-F(\eta)],$$

$$\frac{\partial\psi}{\partial\xi} = \tfrac{3}{2}[F^2(\eta)]' - F'(\eta)F(\xi) + \frac{kc}{h}|F(\xi)-F(\eta)|[F(\xi)-F(\eta)],$$

no additional arbitrary functions being required. Further integrations give

$$\phi = \tfrac{3}{2}(\xi-\eta)[F^2(\xi)]' + F'(\xi)\int_\xi^\eta F(\theta)\,d\theta + \\ + \frac{kc}{h}\int_\xi^\eta |F(\xi)-F(\theta)|[F(\xi)-F(\theta)]\,d\theta, \quad (20)$$

$$\psi = \tfrac{3}{2}(\xi-\eta)[F^2(\eta)]' - F'(\eta)\int_\eta^\xi F(\theta)\,d\theta + \\ + \frac{kc}{h}\int_\eta^\xi |F(\theta)-F(\eta)|[F(\theta)-F(\eta)]\,d\theta, \quad (21)$$

the additive functions of ξ and η respectively in these integrals being so chosen that $\phi = \psi = 0$ where $\xi-\eta = 0$.

From (19), (20), (21), and on taking

$$X = -4f(\xi), \qquad Y = 4f(\eta),$$

it follows that

$$\frac{u_2}{c} = \tfrac{3}{8}(\xi-\eta)\{[F^2(\xi)]' + [F^2(\eta)]'\} - \tfrac{1}{4}\{F'(\xi)+F'(\eta)\}\int_\eta^\xi F(\theta)\,d\theta - \\ - \frac{1}{4}\frac{kc}{h}\int_\eta^\xi \{F(\xi)-F(\theta)[F(\xi)-F(\theta)] - |F(\theta)-F(\eta)|[F(\theta)-F(\eta)]\}\,d\theta - \\ - f(\xi)+f(\eta). \quad (22)$$

In (22), $u_2 = 0$ where $\xi-\eta = 0$, whatever the function $f(\ )$ may be.

Transformation of (22) back to the independent variables x, t, by using the equations (1), (2), gives

$$\frac{u_2}{c} = \frac{3}{4}\frac{x}{c}\left\{\left[F^2\left(t+\frac{x}{c}\right)\right]' + \left[F^2\left(t-\frac{x}{c}\right)\right]'\right\} - \\ - \frac{1}{4}\left\{F'\left(t+\frac{x}{c}\right)+F'\left(t-\frac{x}{c}\right)\right\}\int_{t-x/c}^{t+x/c} F(\theta)\,d\theta - \\ - \frac{1}{4}\frac{kc}{h}\int_{t-x/c}^{t+x/c}\left\{\left|F\left(t+\frac{x}{c}\right)-F(\theta)\right|\left[F\left(t+\frac{x}{c}\right)-F(\theta)\right] - \right. \\ \left. - \left|F(\theta)-F\left(t-\frac{x}{c}\right)\right|\left[F(\theta)-F\left(t-\frac{x}{c}\right)\right]\right\}d\theta - \\ - f\left(t+\frac{x}{c}\right)+f\left(t-\frac{x}{c}\right); \quad (23)$$

and then substitution from (8), (9), (23) into (13) gives

$$\frac{1}{h}\frac{\partial \zeta_2}{\partial t} = \frac{1}{4}\left\{\left[F^2\left(t+\frac{x}{c}\right)\right]' + \left[F^2\left(t-\frac{x}{c}\right)\right]'\right\} -$$
$$- \frac{3}{4}\frac{x}{c}\left\{\left[F^2\left(t+\frac{x}{c}\right)\right]'' - \left[F^2\left(t-\frac{x}{c}\right)\right]''\right\} +$$
$$+ \frac{1}{4}\left\{F\left(t+\frac{x}{c}\right) + F\left(t-\frac{x}{c}\right)\right\}\left\{F'\left(t+\frac{x}{c}\right) + F'\left(t-\frac{x}{c}\right)\right\} +$$
$$+ \frac{1}{4}\left\{F'\left(t+\frac{x}{c}\right) - F'\left(t-\frac{x}{c}\right)\right\}\int_{t-x/c}^{t+x/c} F(\theta)\, d\theta +$$
$$+ \frac{1}{4}\frac{kc^2}{h}\int_{t-x/c}^{t+x/c}\frac{\partial}{\partial\theta}\left\{\left|F\left(t+\frac{x}{c}\right) - F(\theta)\right|\left[F\left(t+\frac{x}{c}\right) - F(\theta)\right] -\right.$$
$$\left. - \left|F(\theta) - F\left(t-\frac{x}{c}\right)\right|\left[F(\theta) - F\left(t-\frac{x}{c}\right)\right]\right\} d\theta +$$
$$+ f'\left(t+\frac{x}{c}\right) + f'\left(t-\frac{x}{c}\right), \quad (24)$$

since the terms due to differentiation with respect to the upper and lower bounds of the integrals in (23) balance. Integration of (24) gives

$$\frac{\zeta_2}{h} = \frac{1}{4}\left\{F\left(t+\frac{x}{c}\right) + F\left(t-\frac{x}{c}\right)\right\}^2 - \frac{3}{4}\frac{x}{c}\left\{\left[F^2\left(t+\frac{x}{c}\right)\right]' - \left[F^2\left(t-\frac{x}{c}\right)\right]'\right\} +$$
$$- \frac{1}{4}\left\{F'\left(t+\frac{x}{c}\right) - F'\left(t-\frac{x}{c}\right)\right\}\int_{t-x/c}^{t+x/c} F(\theta)\, d\theta +$$
$$- \frac{1}{4}\frac{kc}{h}\int_{t-x/c}^{t+x/c}\left\{\left|F\left(t+\frac{x}{c}\right) - F(\theta)\right|\left[F\left(t+\frac{x}{c}\right) - F(\theta)\right] +\right.$$
$$\left. + \left|F(\theta) - F\left(t-\frac{x}{c}\right)\right|\left[F(\theta) - F\left(t-\frac{x}{c}\right)\right]\right\} d\theta +$$
$$+ f\left(t+\frac{x}{c}\right) + f\left(t-\frac{x}{c}\right). \quad (25)$$

Substitution from (23), (25) into the condition (12) gives

$$2f\left(t+\frac{a}{c}\right) = -\frac{1}{4}\left\{F\left(t+\frac{a}{c}\right) + F\left(t-\frac{a}{c}\right)\right\}^2 +$$
$$- F'\left(t+\frac{a}{c}\right)\left\{\frac{3a}{c}F\left(t+\frac{a}{c}\right) - \frac{1}{2}\int_{t-a/c}^{t+a/c} F(\theta)\, d\theta\right\} -$$
$$- \frac{1}{2}\frac{kc}{h}\int_{t-a/c}^{t+a/c}\left|F\left(t+\frac{a}{c}\right) - F(\theta)\right|\left[F\left(t+\frac{a}{c}\right) - F(\theta)\right] d\theta$$

for all values of t, so that

$$f(t) = -\frac{1}{8}\left\{F(t) + F\left(t-\frac{2a}{c}\right)\right\}^2 + F'(t)\left\{\frac{3}{2}\frac{a}{c}F(t) - \frac{1}{4}\int_{t-2a/c}^{t} F(\theta)\, d\theta\right\} -$$
$$- \frac{1}{4}\frac{kc}{h}\int_{t-2a/c}^{t} F(t) - F(\theta)\,[F(t) - F(\theta)]\, d\theta. \quad (26)$$

Substitution from (26) into (25) gives

$$\begin{aligned}\frac{\zeta_2}{h} = {} & \frac{1}{8}F^2\left(t+\frac{x}{c}\right)+\frac{1}{8}F^2\left(t-\frac{x}{c}\right)-\frac{1}{8}F^2\left(t+\frac{x}{c}-\frac{2a}{c}\right)-\frac{1}{8}F^2\left(t-\frac{x}{c}-\frac{2a}{c}\right)+\\ & +\frac{1}{2}F\left(t+\frac{x}{c}\right)F\left(t-\frac{x}{c}\right)-\frac{1}{4}F\left(t+\frac{x}{c}\right)F\left(t+\frac{x}{c}-\frac{2a}{c}\right)-\\ & -\frac{1}{4}F\left(t-\frac{x}{c}\right)F\left(t-\frac{x}{c}-\frac{2a}{c}\right)+\frac{3}{2}\frac{a-x}{c}F\left(t+\frac{x}{c}\right)F'\left(t+\frac{x}{c}\right)+\\ & +\frac{3}{2}\frac{a+x}{c}F\left(t-\frac{x}{c}\right)F'\left(t-\frac{x}{c}\right)-\frac{1}{4}F'\left(t+\frac{x}{c}\right)\int_{t+x/c-2a/c}^{t-x/c}F(\theta)\,d\theta-\\ & -\frac{1}{4}F'\left(t-\frac{x}{c}\right)\int_{t-x/c-2a/c}^{t+x/c}F(\theta)\,d\theta\\ & -\frac{1}{4}\frac{kc}{h}\int_{t+x/c-2a/c}^{t-x/c}\left|F\left(t+\frac{x}{c}\right)-F(\theta)\right|\left[F\left(t+\frac{x}{c}\right)-F(\theta)\right]d\theta+\\ & +\frac{1}{4}\frac{kc}{h}\int_{t-x/c-2a/c}^{t+x/c}\left|F(\theta)-F\left(t-\frac{x}{c}\right)\right|\left[F(\theta)-F\left(t-\frac{x}{c}\right)\right]d\theta, \quad (27)\end{aligned}$$

and a similar formula may be obtained for u_2/c.

For the second approximation to be a valid approximation, it is necessary for $|\zeta_2|$ to be small compared with the maximum value of $|\zeta_1|$.

5. Elevation at head of estuary

At the head of the estuary, where $x = 0$, it follows from (10), (27) that

$$\begin{aligned}\frac{\zeta}{h} = {} & 2F(t)+\tfrac{3}{4}F^2(t)-\tfrac{1}{4}F^2(t-2a/c)-\tfrac{1}{2}F(t)F(t-2a/c)+\\ & +F'(t)\left\{3\frac{a}{c}F(t)-\frac{1}{2}\int_{t-2a/c}^{t}F(\theta)\,d\theta\right\}-\\ & -\frac{1}{2}\frac{kc}{h}\int_{t-2a/c}^{t}|F(t)-F(\theta)|[F(t)-F(\theta)]\,d\theta. \quad (28)\end{aligned}$$

It is then seen that the elevation of the water-surface at the head of the estuary depends upon the first-order elevation there at the same time and for a previous interval during which a first-order progressive wave could travel twice the length of the estuary.

When the first-order elevation at the head of the estuary has a positive maximum at $t = 0$, then $F'(0) = 0$ and $F''(0)$ is negative. The formula (28) then gives, for that time,

$$\begin{aligned}\frac{\zeta}{h} = {} & 2F(0)+\tfrac{3}{4}F^2(0)-\tfrac{1}{4}F^2(-2a/c)-\tfrac{1}{2}F(0)F(-2a/c)-\\ & -\frac{1}{2}\frac{kc}{h}\int_{-2a/c}^{0}|F(0)-F(\theta)|[F(0)-F(\theta)]\,d\theta, \quad (29)\end{aligned}$$

$$\begin{aligned}\frac{1}{h}\frac{\partial\zeta}{\partial t} = {} & -\tfrac{1}{2}F'(-2a/c)\{F(0)+F(-2a/c)\}+\\ & +F''(0)\left\{\frac{3a}{c}F(0)-\frac{1}{2}\int_{-2a/c}^{0}F(\theta)\,d\theta\right\}+\\ & +\frac{1}{2}\frac{kc}{h}|F(0)-F(-2a/c)|\{F(0)-F(-2a/c)\}, \quad (30)\end{aligned}$$

and (30) is of the second order in F.

Now
$$\frac{\partial\zeta}{\partial t} = \left(\frac{\partial\zeta}{\partial t}\right)_{t=0} + t\left(\frac{\partial^2\zeta}{\partial t^2}\right)_{t=0},$$
to the first order in t, and, as high water occurs when $\partial\zeta/\partial t = 0$, it follows from (30) that the time of high water is given, to the first order in F, by

$$t = -\frac{3}{2}\frac{a}{c}F(0) + \frac{1}{4}\frac{F'(-2a/c)}{F''(0)}\{F(0)+F(-2a/c)\} + \frac{1}{4}\int_{-2a/c}^{0} F(\theta)\,d\theta - \\ - \frac{1}{4}\frac{kc}{h}\frac{1}{F''(0)}\,F(0)-F(-2a/c)\,\{F(0)-F(-2a/c)\}. \quad (31)$$

Also,
$$\zeta = (\zeta)_{t=0} + t\left(\frac{\partial\zeta}{\partial t}\right)_{t=0},$$
so that, to the second order in F, the height of high water is given by (29).

Suppose now that
$$0 < F(-2a/c) < F(\theta) < F(0), \quad \text{for } -2a/c < \theta < 0,$$
so that $F'(-2a/c)$ is positive. Then from (29), (31) it can be shown that the tendency of the shallow water terms of the fundamental equations is to make high water higher and earlier, and that the tendency of the frictional term is to make high water lower and later.

When there is no surge and the first-order tide is harmonic of amplitude $2hA$ and period $2\pi/\sigma$ so that
$$F(t) = A\cos\sigma t,$$
then the formulae (29), (31) for the height and time of high water at the head of the estuary become respectively

$$\frac{\zeta}{h} = 2A + A^2\left\{\frac{5}{8} - \frac{1}{2}\cos\frac{2\sigma a}{c} - \frac{1}{8}\cos\frac{4\sigma a}{c} - \right. \\ \left. - \frac{1}{2}\frac{kc}{h\sigma}\left(\frac{3\sigma a}{c} - 2\sin\frac{2\sigma a}{c} + \frac{1}{4}\sin\frac{4\sigma a}{c}\right)\right\},$$

$$t = \frac{A}{\sigma}\left\{-\frac{3}{2}\frac{\sigma a}{c} - \frac{1}{8}\sin\frac{4\sigma a}{c} + \frac{1}{8}\frac{kc}{h\sigma}\left(3 - 4\cos\frac{2\sigma a}{c} + \cos\frac{4\sigma a}{c}\right)\right\}.$$

In the tidal example taken by Doodson, $h = 128$ ft, $2\pi/\sigma = 12$ hours, $\sigma a/c = 2\pi/5$, $2hA = 5$ ft, so that $A = 0{\cdot}0195$, $kc/h\sigma = 6{\cdot}9$, $\frac{1}{4}Akc/h\sigma = 0{\cdot}034$. These figures indicate that the method of the present paper should give an approximation to the motion. But for an estuary, the depths are smaller, so that the values of $kc/h\sigma$ are larger, and the values of A may be much larger. In these circumstances the approximation will only be valid if $\sigma a/c$ be small.

6. Short estuary

Now suppose that, during the time taken by a progressive wave to travel the length of the estuary, the elevation at any one place changes by only a small fraction of its maximum value. Then aF'/c will be small compared with the maximum value of F.

On expanding the second-order terms in ascending powers of x/c as far as x^3/c^3, it follows that

$$\int_{t-x/c}^{t+x/c} F(\theta)\,d\theta = \int_{t-x/c}^{t+x/c} \{F(t)+(\theta-t)F'(t)+\tfrac{1}{2}(\theta-t)^2F''(t)\}\,d\theta$$
$$= 2\frac{x}{c}F(t)+\frac{1}{3}\frac{x^3}{c^3}F''(t),$$

and similarly it may be shown that

$$\int_{t-2a/c}^{t} F(\theta)\,d\theta = \frac{2a}{c}F(t)-\frac{2a^2}{c^2}F'(t)+\frac{4}{3}\frac{a^3}{c^3}F''(t).$$

Also

$$\int_{t-x/c}^{t+x/c} F(t+x/c)-F(\theta)\,[F(t+x/c)-F(\theta)]\,d\theta$$
$$= F'(t)\,F'(t)\int_{t-x/c}^{t+x/c}(t+x/c-\theta)^2\,d\theta$$
$$= \frac{8}{3}\frac{x^3}{c^3}F'(t)\,F'(t),$$

and similarly it may be shown that

$$\int_{t-x/c}^{t+x/c} F(\theta)-F(t-x/c)\,[F(\theta)-F(t-x/c)]\,d\theta = \frac{8}{3}\frac{x^3}{c^3}F'(t)\,F'(t),$$

$$\int_{t-2a/c}^{t} F(t)-F(\theta)\,[F(t)-F(\theta)]\,d\theta = \frac{8}{3}\frac{a^3}{c^3}F'(t)\,F''(t).$$

It then follows, from (25), (23), (26) respectively, and on omitting the argument t of F and f, that

$$\frac{\zeta_2}{h} = F^2-\frac{x^2}{c^2}(FF''+3F'^2)+\frac{4}{3}\frac{kx^3}{hc^2}F'\,F''+2f+\frac{x^2}{c^2}f'', \tag{32}$$

$$\frac{u_2}{c} = 2\frac{x}{c}FF'+\frac{x^3}{c^3}\left(FF'''+\frac{13}{3}F'F''\right)-2\frac{x}{c}f'-\frac{1}{3}\frac{x^3}{c^3}f''', \tag{33}$$

$$f = -\tfrac{1}{2}F^2+\frac{2a}{c}FF'-\frac{a^2}{c^2}FF''+\frac{2}{3}\frac{a^3}{c^3}(FF'''+F'F'')-\frac{2}{3}\frac{ka^3}{hc^2}F'F'. \tag{34}$$

From (10), (32), (33), (34), it then follows that

$$\frac{\zeta}{h} = F\left(t+\frac{x}{c}\right)+F\left(t-\frac{x}{c}\right)+\frac{4a}{c}FF'-\frac{2a^2}{c^2}FF''-\frac{2x^2}{c^2}(FF''+2F'^2)+$$
$$+\frac{4}{3}\frac{a^3}{c^3}(FF'''+F'F'')+\frac{2ax^2}{c^3}(FF'''+3F'F'')-$$
$$-\frac{4}{3}\frac{k}{hc^2}(a^3-x^3)F'F', \tag{35}$$

$$\frac{u}{c} = -F\left(t+\frac{x}{c}\right)+F\left(t-\frac{x}{c}\right)+\frac{4x}{c}FF'-\frac{4ax}{c^2}(FF''+F'^2)+$$
$$+\frac{2a^2x}{c^3}(FF'''+F'F'')+\frac{4}{3}\frac{x^3}{c^3}(FF'''+4F'F'''), \tag{36}$$

the argument of F being t, except where otherwise shown.

It will be seen that, to the order x^3/c^3, the current is independent of friction.

When $\qquad F(0) > 0, \qquad F'(0) = 0, \qquad F''(0) < 0,$

the formulae (29), (31), for the approximate height and time of high water at the head of the estuary, become

$$\frac{\zeta}{h} = 2F(0)\left\{1 - \frac{a^2}{c^2}F''(0) + \frac{2}{3}\frac{a^2}{c^3}F'''(0)\right\}, \tag{37}$$

$$t = -\frac{2a}{c}F(0) + \frac{a^2}{c^2}\frac{F(0)}{F''(0)}\left\{F'''(0) - \frac{2}{3}\frac{a}{c}F^{iv}(0)\right\} - \frac{2}{3}\frac{a^3}{c^3}F'''(0). \tag{38}$$

Both these results are independent of friction.

When again $\qquad F(t) = A\cos\sigma t$

A, σ being constants, the formulae (35), (36) become

$$\frac{\zeta}{h} = 2A\cos\frac{\sigma x}{c}\cos\sigma t + A^2\left\{\left[-\frac{2\sigma a}{c} + \frac{4\sigma^3}{c^3}\left(\tfrac{1}{3}a^3 + ax^2\right)\right]\sin 2\sigma t + \frac{\sigma^2}{c^2}(a^2 - x^2)\right.$$
$$\left. + \frac{\sigma^2}{c^2}(a^2 + 3x^2)\cos 2\sigma t + \frac{4}{3}\frac{k\sigma^2}{hc^2}(a^3 - x^3)\sin\sigma t\,|\sin\sigma t\right\},$$

$$\frac{u}{c} = 2A\sin\frac{\sigma x}{c}\sin\sigma t +$$
$$+ A^2\left\{\left[-\frac{2\sigma x}{c} + \frac{2\sigma^3}{c^3}\left(a^2x + \frac{5}{3}x^3\right)\right]\sin 2\sigma t + \frac{4\sigma^2 ax}{c^2}\cos 2\sigma t\right\},$$

respectively. The formulae (37), (38), for the height and time of high water at the head of the estuary, become

$$\frac{\zeta}{h} = 2A\left(1 + \frac{\sigma^2a^2}{c^2}A^2\right),$$

$$t = -\frac{2a}{c}A\left(1 - \frac{2}{3}\frac{\sigma^2a^2}{c^2}\right),$$

respectively.

The validity of the expansions in x/c requires that $\sigma a/c < 1$. For the above formulae to give a valid approximation to a solution of the fundamental equations, it is necessary for $(\sigma a/c)A$, $(k\sigma^2a^3/hc^2)A$ to be small.

As an example, take $h = 40$ ft and a semi-diurnal tide. Then $c = 24{\cdot}5$ miles per hour, $\sigma = 2\pi/12$ hours^{-1}, so that $c/\sigma = 47$ miles. With $a = 20$ miles and $A = \frac{1}{3}$, this gives

$$\frac{\sigma a}{c}A = 0{\cdot}14, \qquad \frac{k\sigma^2a^3}{hc^2}A = 0{\cdot}39.$$

7. Separation of tide and surge

Take $\qquad F(t) = T(t) + S(t), \tag{39}$

where $T(\,)$ denotes a tide and $S(\,)$ a surge. Equal sequences of meteorological conditions over the sea may be regarded as giving rise to equal functions $S(t)$. Since the timing of the meteorological conditions which generate surges

is independent of the timing of the astronomical forces which generate the tides, the frequency-distribution of the first-order surges S will be independent of the phases of the first order tides T.

Substitution from (39) into (35) with $x = 0$, gives for the height of the combination of tide and surge at the head of the estuary

$$\frac{\zeta}{h} = 2(T+S) + \frac{4a}{c}(T+S)(T'+S') - \frac{2a^2}{c^2}(T+S)(T''+S'') + \\ + \frac{4}{3}\frac{a^3}{c^3}\{(T+S)(T'''+S''') + (T'+S')(T''+S'')\} - \\ - \frac{4}{3}\frac{ka^3}{hc^2}\,T'+S'\,(T'+S'), \quad (40)$$

the argument of T and S being t.

The predicted tide would be given by

$$\frac{\zeta}{h} = 2T + \frac{4a}{c}TT' - \frac{2a^2}{c^2}TT'' + \frac{4}{3}\frac{a^3}{c^3}(TT''' + T'T'') - \frac{4}{3}\frac{ka^3}{hc^2}\,T'\,T', \quad (41)$$

so that the apparent surge is given by subtracting (41) from (40). The formula for the apparent surge is thus

$$\frac{\zeta}{h} = 2S + \frac{4a}{c}SS' - \frac{2a^2}{c^2}SS'' + \frac{4}{3}\frac{a^3}{c^3}(SS''' + S'S'') + \frac{4a}{c}(TS' + T'S) - \\ - \frac{2a^2}{c^2}(TS'' + T''S) + \frac{4}{3}\frac{a^3}{c^3}(TS''' + T'''S + T'S'' + T''S' - \\ - \frac{4}{3}\frac{ka^3}{hc^2}\{T'+S'(T'+S') - |T'|T'\}. \quad (42)$$

When the first-order surge has either a maximum or a minimum so that $S' = 0$, the formula (42) reduces to

$$\frac{\zeta}{h} = 2S\left(1 - \frac{a^2}{c^2}S'' + \frac{2}{3}\frac{a^3}{c^3}S''' + \frac{2a}{c}T' - \frac{a^2}{c^2}T'' + \frac{2}{3}\frac{a^3}{c^3}T'''\right) - \\ - \frac{2a^2}{c^2}TS'' + \frac{4}{3}\frac{a^3}{c^3}(TS''' + T'S''), \quad (43)$$

and this is free from frictional influence.

When the terms in a^3/c^3 are negligible, and, at the same time, the first-order tide is either at high water or low water, so that $T' = 0$, the formula (43), for the apparent surge at the head of the estuary, reduces to

$$\frac{\zeta}{h} = 2S\left(1 - \frac{a^2}{c^2}S''\right) - \frac{2a^2}{c^2}(T''S + TS''). \quad (44)$$

Now suppose that

$$S > 0, \qquad S'' < 0,$$

so that the first-order surge has a positive maximum. When the first-order tide is at high water,

$$T = A, \qquad T'' = -\sigma^2 A,$$

hA denoting the amplitude of the tide and $2\pi/\sigma$ its period, and the apparent surge (44) is given by

$$\frac{\zeta}{h} = 2S\left(1 - \frac{a^2}{c^2}S''\right) + \frac{2a^2}{c^2}A(\sigma^2 S - S''). \tag{45}$$

When the first-order tide is at low water,

$$T = -A, \qquad T'' = \sigma^2 A,$$

and the apparent surge (44) is given by

$$\frac{\zeta}{h} = 2S\left(1 - \frac{a^2}{c^2}S''\right) - \frac{2a^2}{c^2}A(\sigma^2 S - S''). \tag{46}$$

The excess of (45) over (46) is

$$\frac{4a^2}{c^2}A(\sigma^2 S - S''), \tag{47}$$

and this is positive.

It is thus seen that, at the head of a very short estuary, the effect of the interaction of the tide on the surge is to make the apparent surge higher when its maximum occurs at the time of tidal high water than when its maximum occurs at the time of tidal low water. This result, which is due to the shallow water terms of the differential equations, is directly opposite to the corresponding result for a progressive wave. That result, in the case of an estuary of uniform cross-section, is due to the frictional term.

To examine the order of magnitude of the difference (47), take the particular case in which, when the first-order surge is at its maximum, $S'' = -\sigma^2 S$. The difference in the heights of the apparent surges is then equal to the height of the first-order surge multiplied by $(8\sigma^2 a^2/c^2)A$. With the figures at the end of § 6, this factor is 0·47.

References

Doodson, A. T. 1956 *Proc. Roy. Soc.* A, **237,** 325.

Proudman, J. 1955 a *Proc. Roy. Soc.* A, **231,** 8.

Proudman, J. 1955 b *Proc. Roy Soc.* A, **233,** 407.

An electronic analogue for supersonic flow

By LESLIE S. G. KOVÁSZNAY

Department of Aeronautics, The Johns Hopkins University, Baltimore

(*Received* 28 *January* 1957)

SUMMARY

An analogue method for solving certain quasi-linear hyperbolic partial differential equations is presented. The characteristic lines are formed by scanning electronically the screen of a cathode-ray tube. The boundary conditions are introduced in the form of an opaque mask. The solution appears as a picture on the screen of a second cathode-ray tube. The experiments demonstrate the feasibility of the approach, but the development of the machine has not been carried beyond this stage.

GENERAL DESCRIPTION OF THE METHOD

There are well-established analogue methods for solving Laplace's equation, such as the use of an electrolytic tank or of a soap film, to mention just two. An extensive bibliography of such methods has been given by Higgins (1956). On the other hand, there has not been comparable progress in finding analogue methods for solving the wave equation. Step-by-step numerical or graphical solutions are available. For example, for two-dimensional flows that are hyperbolic everywhere, the method of characteristics is applicable. It is essential to recapitulate certain features of the method of characteristics for the present point of view.

In the case of steady two-dimensional supersonic flow, there are two families of characteristic lines which can be regarded as a curvilinear coordinate system. In the case of a uniform supersonic flow, these characteristic lines become two sets of parallel straight lines each forming the Mach angle with the flow direction. If the departures from uniform flow are small, these characteristics will differ only little from the straight 'undisturbed' characteristics.

For the linearized theory of supersonic flow, the characteristics are assumed to have fixed direction (independent of the solution), and only the higher approximations involve the 'warping' of the characteristic lines.

Scanning methods are essential features of the television technique, and they can be quite readily adapted to generate the characteristic lines. A spot moving on the screen of a cathode-ray tube can sweep according to a scanning programme of arbitrary complexity. Present commercial television uses a scan pattern that consists of one family of parallel straight lines (usually in the horizontal direction from left to right) which are formed sequentially in time.

If a scanning programme is devised so that the ordinary television scan is performed twice, first tilted with a positive then with a negative angle, two families of fixed characteristics can be generated. For practical reasons it is more convenient to generate the two sets of lines as part of a single scan pattern as given in figure 1. By using symmetrical triangular waves for vertical deflection and saw-tooth waves for horizontal deflection with only slightly differing frequencies, one obtains a dense scan pattern. The scan lines also appear to be 'reflected' from the top and bottom edges of the scanned area.

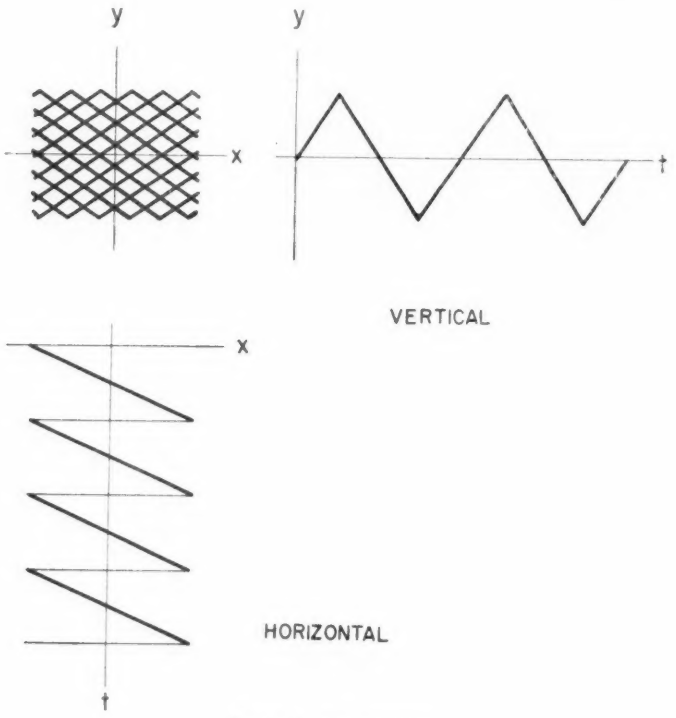

Figure 1. Scan pattern.

By choosing the light intensity of the cathode-ray screen as the dependent variable, solutions to the linear wave equation can be obtained by simply holding the light intensity constant during each scan stroke, but varying it in an arbitrary manner between scan strokes.

The assignment of light intensity for each scan stroke depends on the boundary conditions, and a simple method can be devised for introducing such boundary conditions. Suppose the light intensity is the integral of a function which is zero in the field, but not on the boundary. The spot will

have constant intensity after it leaves the boundary and this constant can be set at the boundary. Pictures were obtained with the use of two cathode-ray tubes as indicated in figure 2. Identical scan patterns were applied to the two tubes. The first one, labelled *SCANNER*, sweeps in front of a cut-out mask giving light only when crossing the diamond-shaped slit. The light intensity is picked up by a phototube, and is integrated by an integrating circuit. The integrand is different from zero only when the scan spot passes the cut-out area. The value of the integral is displayed on the second tube labelled *DISPLAY*. The light intensity is constant along scan lines outside of the 'body'. Figure 3 (plate 1) shows the results of such an experiment.

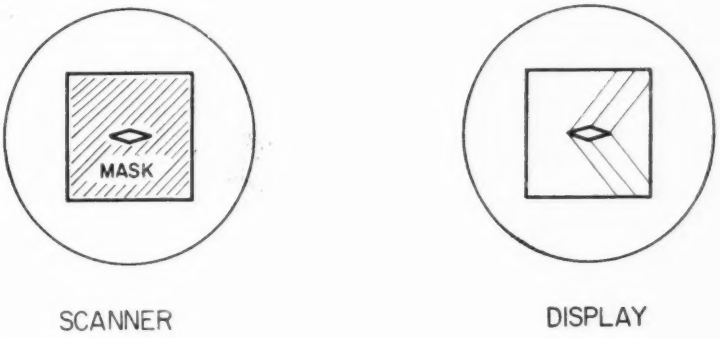

Figure 2. Two cathode-ray tubes.

The integrator can either be reset to zero at the extreme values of the vertical scan (figure 3(*a*), plate 1), or permitted to hold its value and be reset only when returning to the left vertical edge (figure 3(*b*), plate 1). This gives a different set of 'wall' boundary conditions.

In an actual flow problem, the boundary conditions are imposed by the slope of the surface and not by the integral of body thickness as in the above example. However, it is quite possible to construct masks so that the integrated values of light transmittance inside the body contour are proportional to the slopes of the contour.

The analogue for the linearized supersonic flow problem as described above appears to be quite trivial, and the interest in this method was mainly due to the fact that a certain amount of non-linear behaviour is rather easily introduced. If the disturbances are small but not infinitesimal, the principal effect of the non-linearity is to warp the characteristics by changing their local angle (and position) due to the change of the local Mach number and flow direction (see Lighthill 1954). In the analogue the simplest way to alter the characteristic angle is by changing one of the

scan velocities. For example, the horizontal velocity of the cathode-ray spot can be altered by an amount proportional to the magnitude of the disturbance. Since the scan is obtained by integration, this change in velocity also modifies the position of the scan line.

For the non-linear operation, the boundary conditions are introduced in the same manner as for the linearized problem, namely, by scanning a mask as shown in figure 2. The video signal obtained from the phototube

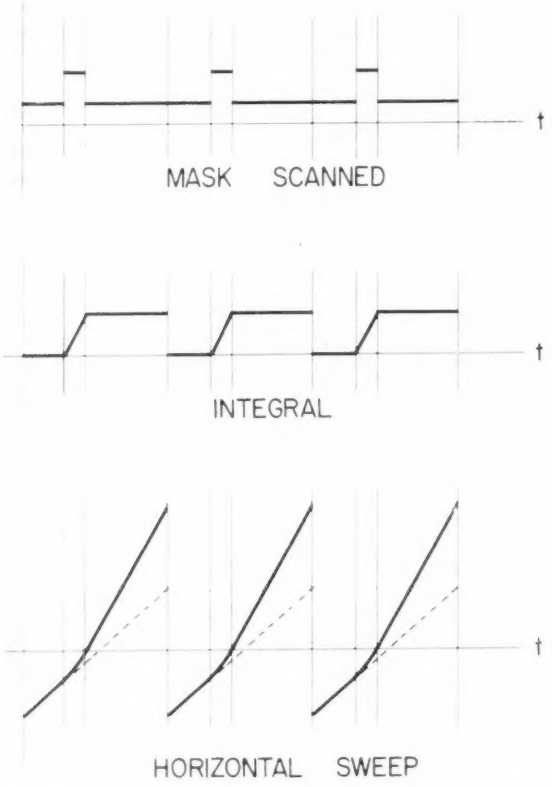

Figure 4. Formation of the horizontal sweep for non-linear operation.

by scanning the cut-out mask is integrated, and this integrated signal is considered as the 'disturbance' function. This signal can be used to modify either or both the horizontal scan velocity and the light intensity of the cathode-ray spot on the *DISPLAY* tube. Figure 4 shows the modifications of the horizontal scan by such an arrangement. Figure 5 shows a three-tone mask for a diamond aerofoil giving the correct boundary conditions when used with an integrator. Since the slope can be both

positive and negative, the background is a neutral grey, and there are both positive (light) and negative (dark) areas contributing to the integral that represents the slope of the surface.

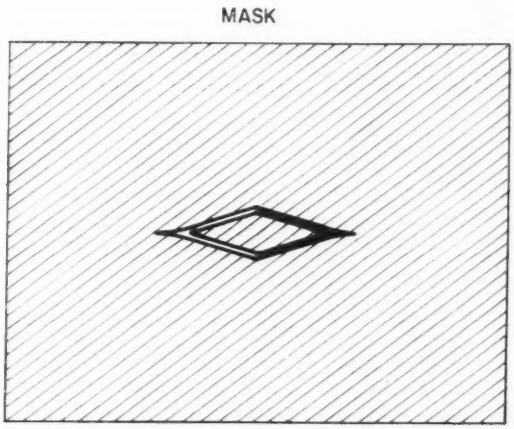

Figure 5. Proposed three-tone mask for introducing proper boundary conditions in case of diamond aerofoil.

Analysis

1. *The second-order equation*

The steady two-dimensional flow of a perfect gas has been the subject of extensive theoretical studies during the last hundred years. If the flow is assumed to be isentropic and the viscosity and heat conduction are neglected, the assumption of potential flow is justified.

Let us introduce the following quantities:

x, y, Cartesian coordinates,
$\phi(x, y)$, velocity potential,
$u(x, y)$, $v(x, y)$, velocity components in the x- and y-directions,
$q(x, y)$, absolute magnitude of the velocity,
c, local speed of sound,
$q_{\max}$, maximum possible velocity of the gas,
γ, ratio of the specific heats.

The local speed of sound depends only on the absolute magnitude of the local velocity,

$$c^2 = \tfrac{1}{2}(\gamma-1)(q_\infty^2 - q^2); \tag{1}$$

also

$$c_0 = \left(\frac{\gamma-1}{2}\right)^{1/2} q_\infty. \tag{1a}$$

The governing equation of the flow is (see, for example, Howarth 1953)

$$(c^2-\phi_x^2)\phi_{xx} - 2\phi_x\phi_y\phi_{xy} + (c^2-\phi_y^2)\phi_{yy} = 0. \tag{2}$$

This second-order non-linear partial differential equation is designated as 'quasi-linear' because the highest-order derivatives ($\phi_{xx}, \phi_{xy}, \phi_{yy}$) all occur linearly, and only lower-order derivatives occur non-linearly.

The equation is elliptic where the flow is subsonic, i.e.

$$c^2 > q^2 = \phi_x^2 + \phi_y^2,$$

and hyperbolic where the flow is supersonic, i.e.

$$c^2 < q^2 = \phi_x^2 + \phi_y^2.$$

There are few exact solutions of this equation.

Let us introduce the concept of an undisturbed flow and a superimposed small perturbation

$$\phi(x,y) = U_1 x + c_1\psi(x,y); \tag{3}$$

then

$$u = U_1 + c_1\psi_x,$$

and

$$v = c_1\psi_y,$$

where $c = c_1$ when $\psi_x^2 + \psi_y^2 = 0$. It is also convenient to use $M_1 = U_1/c_1$, the Mach number of the undisturbed flow. From equation (1) we find that

$$c^2 = c_1^2[1 - \tfrac{1}{2}(\gamma-1)(2M_1\psi_x + \psi_x^2 + \psi_y^2)]. \tag{4}$$

By substituting c from (4) and ϕ from (3) into (2), we obtain a still exact equation for the disturbance potential ψ:

$$\begin{aligned}[(M_1^2-1) + \tfrac{1}{2}(\gamma+1)(2M_1+\psi_x)\psi_x + \tfrac{1}{2}(\gamma-1)\psi y^2]\psi_{xx} + \\ + 2\psi_y(M_1+\psi_x)\psi_{xy} - \\ - [1 - \tfrac{1}{2}(\gamma+1)\psi_y^2 - \tfrac{1}{2}(\gamma-1)(2M_1+\psi_x)\psi_x]\psi_{yy} = 0.\end{aligned} \tag{5}$$

Equation (5) can be simplified by eliminating certain higher-order terms. Keeping only second-order terms and introducing $\beta_1^2 = M_1^2 - 1$, we obtain

$$[\beta_1^2 + (\gamma+1)M_1\psi_x]\psi_{xx} - [1-(\gamma-1)M_1\psi_x]\psi_{yy} = -2M_1\frac{\partial}{\partial x}(\psi_x^2). \tag{6}$$

Dividing through by $1-(\gamma-1)M_1\psi_x$, and again retaining only second-order terms in the expansion, we obtain

$$[\beta_1 + \kappa M_1\psi_x]^2\psi_{xx} - \psi_{yy} = -M_1\frac{\partial}{\partial x}(\psi_y^2), \tag{7}$$

where $\kappa = [(\gamma+1)+\beta_1^2(\gamma-1)]/2\beta_1$. Equation (7), which is exact up to the second order, is in a convenient form for our present purpose. The right-hand side is proportional to $v\,\partial v/\partial x$, and it vanishes as a second-order quantity when the x-axis is turned into the direction of the local flow. Since the purpose of the present analysis is to demonstrate the effect of non-linearity, the right-hand side of (7) is neglected and a modified second-order equation used:

$$[\beta_1+\kappa M_1\psi_x]^2\psi_{xx}-\psi_{yy}=0. \tag{8}$$

If we introduce

$$\epsilon(x,y)=\kappa M_1\psi_x, \tag{9}$$

this becomes

$$(\beta_1+\epsilon)^2\epsilon_{xx}-\epsilon_{yy}=-2\beta_1\epsilon_x^2. \tag{10}$$

2. *The linearized equation*

The linearized equation for the present problem is the well-known wave equation

$$\beta_1^2\psi_{xx}-\psi_{yy}=0. \tag{11}$$

The general solution is

$$\psi(x,y)=F(x+\beta_1 y)+G(x-\beta_1 y) \tag{12}$$

where F and G are arbitrary functions.

The pressure disturbance is computed in the following manner. For polytropic changes we have

$$p\rho^{-\gamma}=\text{const.}, \tag{13}$$

and the equation of state takes the form

$$\gamma p/\rho=c^2(q). \tag{14}$$

We see that all thermodynamic properties are unique functions of the absolute velocity q. The pressure takes the form

$$p=p_0(1-q^2/q_\infty^2)^{\gamma/(\gamma-1)}. \tag{15}$$

In the linearized approximation, we have

$$p=p_1-\tfrac{1}{2}\rho_1 U_1^2(2\psi_x/M_1) \tag{16}$$

$$\rho=\rho_1-\rho_1 M_1\psi_x. \tag{16a}$$

If the wave equation is solved for a supersonic flow over a solid boundary $y=f(x)$, the boundary conditions are imposed in the form that the flow direction must follow the tangent of the solid boundary; thus

$$\frac{v}{u}=\frac{dy}{dx}=f'=\frac{\psi_y}{M_1+\psi_x}\doteq\frac{\psi_y}{M_1}. \tag{17}$$

If the oncoming flow is undisturbed, only one family of characteristics carries a signal ($G=0$, or $F=0$). One then obtains

$$\psi_y=\pm\,\beta_1\psi_x, \tag{18}$$

(the sign depends on whether F or G vanishes), and

$$p=p_1-\tfrac{1}{2}\rho_1 U_1^2(2f'/\sqrt{(M^2-1)}). \tag{19}$$

This shows that the local pressure disturbance is proportional to the local slope of the boundary.

The lines $\xi = x + \beta_1 y = \text{const.}$ and $\eta = x - \beta_1 y = \text{const.}$ are the characteristics, and they form a fixed network of oblique lines (Mach lines) along which the disturbances 'propagate'. The linearized theory improves as the disturbance becomes smaller (very slender body), and is really valid only for the limiting case of infinitesimal disturbances.

3. *The analogue system*

Two families of lines are generated, and they are regarded as two sets of characteristics. With the use of a finite number of scan lines, there will be only discrete values of ξ and η.

The coordinates of the cathode-ray spot during the nth stroke are given as a function of time by

$$X(t) = X_0 + (t - t_0)\dot{X}, \tag{20}$$

$$Y(t) = (t - t_0)\dot{Y}. \tag{21}$$

In general $\dot{X}$ and $\dot{Y}$ are arbitrary functions of the time; X_0 and t_0 are arbitrary constants. By making a total of N strokes, the two sets of characteristics can be obtained in the following way.

Choose for the nth stroke

$$\left.\begin{aligned} X_0 &= \xi_n \quad \text{for } n \text{ even}, \\ &\eta_n \quad \text{for } n \text{ odd}, \end{aligned}\right\} \tag{22 a}$$

$$t_0 = n\,\Delta t, \tag{22 b}$$

where Δt is the period of one scan stroke, also

$$\left.\begin{aligned} \dot{X} &= V(\beta_1 + \epsilon_n) \quad \text{for } n \text{ even}, \\ &V(\beta_1 + \delta_n) \quad \text{for } n \text{ odd}, \end{aligned}\right\} \tag{22 c}$$

$$\dot{Y} = (-1)^n V. \tag{22 d}$$

Here ϵ_n and δ_n are numbers for $0 < n < N$, and they are introduced by the boundary conditions. For convenience, one can choose equal steps in ξ_n and η_n, i.e. $\xi_n = n\rho$, and $\eta_n = n\rho$. Using a dense set of lines, the subscript can be dropped, and ξ, η as well as δ, t can be considered as continuous variables. Thus

$$\xi = x - \beta_1 y - \epsilon(\xi)\, y, \tag{23 a}$$

$$\eta = x + \beta_1 y + \delta(\eta)\, y. \tag{23 b}$$

Observe that if $\epsilon = 0$ and $\delta = 0$, then $\xi = \text{const.}$, and $\eta = \text{const.}$ become the characteristics for the linearized problem.

If $\epsilon(x, y)$ and $\delta(x, y)$ are regarded as the dependent variables, it is easy to verify that they obey the first-order partial differential equations

$$(\beta_1 + \epsilon)\epsilon_x + \epsilon_y = 0, \tag{24}$$

$$(\beta_1 + \delta)\delta_x - \delta_y = 0. \tag{25}$$

The variables $\epsilon(x, y)$ and $\delta(x, y)$ each also obey the following second-order equation:

$$(\beta_1+\epsilon)^2\epsilon_{xx}-\epsilon_{yy} = -2\epsilon_x^2\beta_1-2\epsilon\epsilon_x^2, \tag{26}$$

$$(\beta_1+\delta)^2\delta_{xx}-\delta_{yy} = -2\delta_x^2\beta_1-2\delta\delta_x^2. \tag{27}$$

Naturally, these equations are valid separately, each for one family of simple waves only. By comparing (26) with (10), it is found that they agree for all except the last term on the right-hand side, but that is of the third order. This agreement can be interpreted in the following way.

The analogue generates simple wave solutions of the second-order hyperbolic partial differential equations (26) or (27). They are also simple wave solutions of the simplified second-order equation for the flow problem if a third-order term is disregarded. The dependent variable in both cases is the disturbance in the characteristic angle. For simple waves, the relation between ϵ and the flow angle θ is monotonic. This can be seen as follows.

Using only the linearized approach from (18), we find (taking the upper half-plane)

$$\psi_y = -\beta_1\psi_x. \tag{28}$$

The increment in the absolute magnitude of the velocity vector becomes

$$dq/q = -d\theta/\beta_1; \tag{29}$$

from (1), we get

$$dc/c = -\tfrac{1}{2}(\gamma-1)M_1^2\,dq/q; \tag{30}$$

and, from the definition of Mach number,

$$dM/M = dq/q-dc/c, \tag{31}$$

or

$$dM/M = -(1+\tfrac{1}{2}(\gamma-1)M_1^2)\,d\theta/\beta_1. \tag{32}$$

Also, the change in the cotangent of the characteristic angle with respect to flow direction becomes

$$d\beta = -M^2(1+\tfrac{1}{2}(\gamma-1)M_1^2)\,d\theta/\beta_1^2. \tag{33}$$

The characteristic makes an angle α with the x-axis given by

$$\cot\alpha = \beta_1+\epsilon, \tag{34}$$

$$\alpha = \mu+d\theta. \tag{35}$$

After linearization, this becomes

$$\beta_1+\epsilon = \beta_1+d\beta-M_1^2\,d\theta, \tag{36}$$

$$\epsilon = d\beta-M_1^2\,d\theta, \tag{37}$$

$$\epsilon = -\frac{M_1^4}{M_1^2-1}\frac{\gamma+1}{2}d\theta. \tag{38}$$

Equation (38) indicates that the disturbance to be imposed at the beginning of each scan stroke must be proportional to the surface slope, and the ratio constant is a function of the nominal Mach number of the flow.

Since the value of ϵ is constant during a scan stroke, the simplest way of imposing its value at the boundary is by integration. An integrating circuit holds the value of ϵ during the scan. It is reset after each stroke.

The signal is built up before the cathode-ray spot leaves the body contour The boundary condition can be introduced as a variable opacity or variable thickness of a zone within the body.

Figure 5 shows one simple method for introducing the right boundary condition.

4. *Light intensity of the screen*

The solution is obtained in the form of a photograph taken from the screen of the display cathode-ray tube. The light intensity on the cathode-ray tube is however, not proportional to $\epsilon(\xi)$, but depends on both the luminosity of the spot and on the duration the spot spends in the local area.

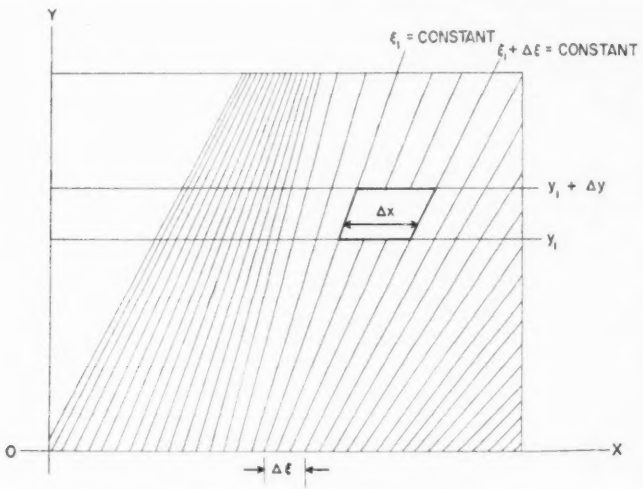

Figure 6. Light intensity relations.

In order to find the relations between ϵ and the screen intensity, introduce $i(t)$, the instantaneous luminous intensity of the cathode-ray spot, and $I(x, y)$, the average luminous intensity per unit area of the screen. The intensity is held constant during a single stroke but varies from stroke to stroke. Note that $i(t)$ and $I(x, y)$ do not have the same dimensions. Introduce for convenience

$$I_0(\xi) = \frac{i(t)T}{ab}, \tag{39}$$

where ab is the total scanned area and T is the time of the entire scan cycle. The local intensity obeys the equation of conservation of (luminous) energy

$$I(x, y)\,\Delta x\,\Delta y = i(t)\sum \Delta T, \tag{40}$$

where $\sum \Delta T$ is the sum of time intervals the spot spends in the area $\Delta x\,\Delta y$. The luminous intensity $I(x, y)$ can be expressed as shown in figure 6. The small quadrangle is bounded by $\xi_1 = \text{const.}$, $\xi_1 + \Delta\xi = \text{const.}$, $y_1 = \text{const.}$,

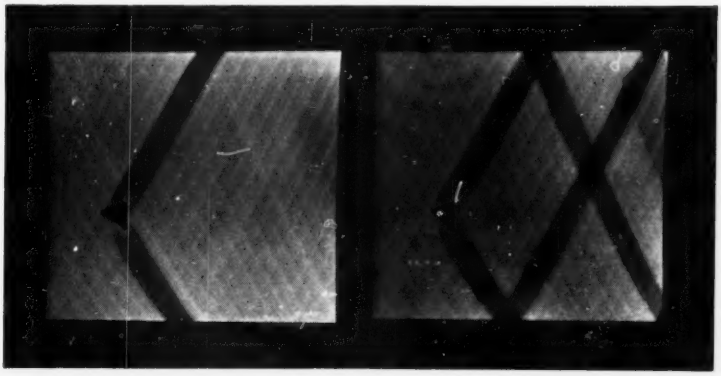

(*a*) (*b*)

Figure 3. Linear operation. (*a*) Integrator reset both at the end of each vertical and horizontal scan stroke. (*b*) Integrator reset only at the end of horizontal scan stroke.

(*a*)

(*b*)

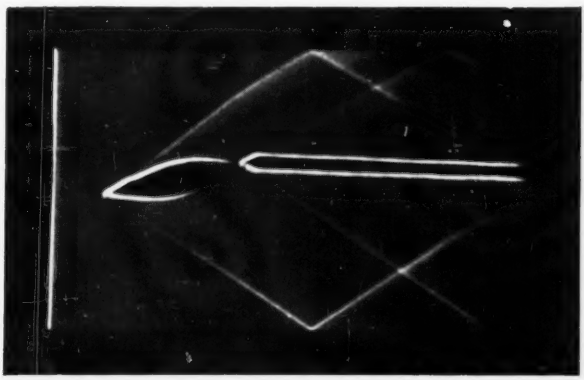

Figure 9. Non-linear analogue for supersonic flow. (*a*) Mask scanned. (*b*) Picture obtained on display.

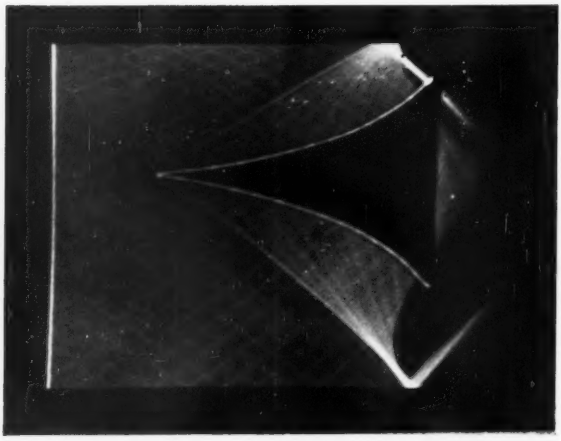

Figure 8. Crowding of characteristics over concave surface.

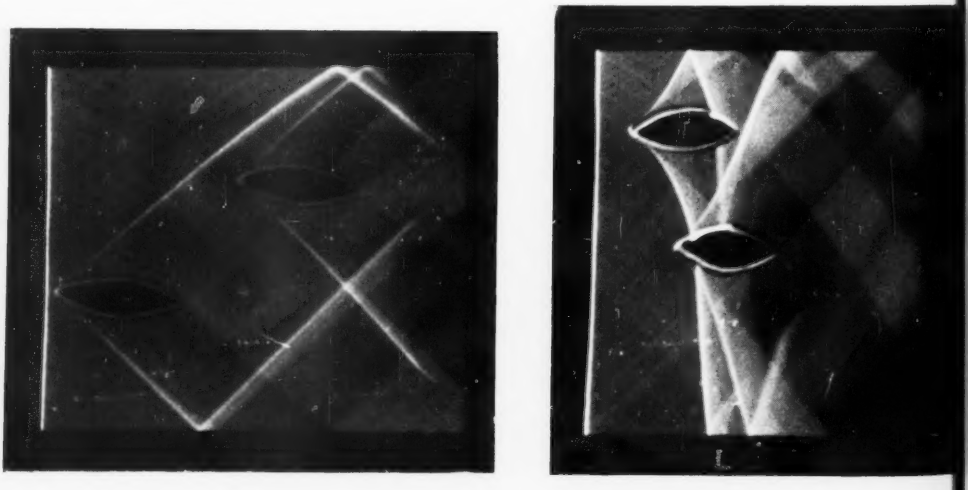

(*a*) (*b*)

Figure 10. Different degrees of non-linear effect. (*a*) Weak non-linear effect. (*b*) Strong non-linear effect.

and $y_1 + \Delta y = \text{const}$. Let us assume successive scan lines correspond to equal increments in ξ (they are equidistant on the x-axis). The fraction of the number of scan lines that pass through the area is $\Delta\xi/2a$ (the factor 2 is due to the fact that there are two families of scan lines during a full scan cycle). The fraction of the time the spot spends within the area during a single stroke is $\Delta y/b$ (the vertical velocity is constant), so that

$$\frac{\sum \Delta T}{T} = \frac{\Delta\xi\,\Delta y}{2ab}.$$

Substituting this value in (40), we obtain

$$2I_0(\xi)\,\Delta\xi = I(x,y)\,\Delta x,$$

or

$$I(x,y) = \tfrac{1}{2} I_0(\xi)\frac{\partial\xi}{\partial x}. \tag{41}$$

If the light intensity is modulated in intensity so that

$$I_0(\xi) \doteq \frac{d\epsilon}{d\xi}, \tag{42}$$

the luminous intensity of the screen becomes

$$I(x,y) \doteq \frac{d\epsilon}{d\xi}\frac{\partial\xi}{\partial x} = \frac{\partial\epsilon}{\partial x}. \tag{43}$$

This is a significant result since it was previously shown that ϵ is analogous to pressure (or density) within the range of linear approximation. In wind-tunnel experiments, the x derivative of the density is made visible optically by the schlieren method. This is the most common visualization method used in routine wind-tunnel work. If the luminosity of the spot (intensity modulation, or 'Z-axis') is varied according to the change of ϵ from scan stroke to scan stroke, schlieren pictures result.

Experiments

The experiments were carried out only to indicate feasibility of the method, and were not pursued to any degree of perfection. A flying-spot scanner previously described by Kovasznay & Joseph (1955) was modified for the present purpose, and many of the limitations of the original equipment determined the experiments that could be attempted. The block diagram of the equipment is shown in figure 7.

The flying-spot generator produces a video signal corresponding to the transparent and opaque areas of the mask. A real image is formed in the plane of the mask by an objective lens and the signal obtained at the phototube is of the 'yes or no' type. A bi-stable trigger quantizes the phototube signal into a definite two-level signal (0 or 1). The reset integrator integrates the signal during one scan stroke. The integrator is reset to zero either at the end of the horizontal strokes or only at the end of both vertical and

and $y_1 + \Delta y = \text{const}$. Let us assume successive scan lines correspond to equal increments in ξ (they are equidistant on the x-axis). The fraction of the number of scan lines that pass through the area is $\Delta\xi/2a$ (the factor 2 is due to the fact that there are two families of scan lines during a full scan cycle). The fraction of the time the spot spends within the area during a single stroke is $\Delta y/b$ (the vertical velocity is constant), so that

$$\frac{\sum \Delta T}{T} = \frac{\Delta\xi\,\Delta y}{2ab}.$$

Substituting this value in (40), we obtain

$$2I_0(\xi)\,\Delta\xi = I(x,y)\,\Delta x,$$

or

$$I(x,y) = \tfrac{1}{2} I_0(\xi)\frac{\partial\xi}{\partial x}. \tag{41}$$

If the light intensity is modulated in intensity so that

$$I_0(\xi) \doteq \frac{d\epsilon}{d\xi}, \tag{42}$$

the luminous intensity of the screen becomes

$$I(x,y) \doteq \frac{d\epsilon}{d\xi}\frac{\partial\xi}{\partial x} = \frac{\partial\epsilon}{\partial x}. \tag{43}$$

This is a significant result since it was previously shown that ϵ is analogous to pressure (or density) within the range of linear approximation. In wind-tunnel experiments, the x derivative of the density is made visible optically by the schlieren method. This is the most common visualization method used in routine wind-tunnel work. If the luminosity of the spot (intensity modulation, or 'Z-axis') is varied according to the change of ϵ from scan stroke to scan stroke, schlieren pictures result.

Experiments

The experiments were carried out only to indicate feasibility of the method, and were not pursued to any degree of perfection. A flying-spot scanner previously described by Kovasznay & Joseph (1955) was modified for the present purpose, and many of the limitations of the original equipment determined the experiments that could be attempted. The block diagram of the equipment is shown in figure 7.

The flying-spot generator produces a video signal corresponding to the transparent and opaque areas of the mask. A real image is formed in the plane of the mask by an objective lens and the signal obtained at the phototube is of the 'yes or no' type. A bi-stable trigger quantizes the phototube signal into a definite two-level signal (0 or 1). The reset integrator integrates the signal during one scan stroke. The integrator is reset to zero either at the end of the horizontal strokes or only at the end of both vertical and

horizontal strokes. In the former case, the waves 'reflect' from the vertical edges of the scan pattern (see figure 3, plate 1); in the latter they do not. If the masks were cut in such a way that the transparent portion along the scan line corresponded to the slope of the boundary, the signal obtained after integration becomes proportional to the ϵ disturbance. In the analogue for the linearized problem, we can simply modulate the light intensity with this signal. Figure 3 (plate 1) was obtained in such a way (with the switch, shown in figure 7, set on *INTENSITY CONTROL*). For non-linear operation, however, the horizontal scan velocity must be modified according to ϵ. This is obtained by the variable velocity sweep. This circuit is essentially a second reset integrator. In absence of a velocity control signal, it integrates a constant and $\dot{X} = \beta_1 V$, and it is reset at equal intervals. The velocity control signal is added to the integrand, forming $\dot{X} = V\beta_1 + V\epsilon$ as required by (22 c).

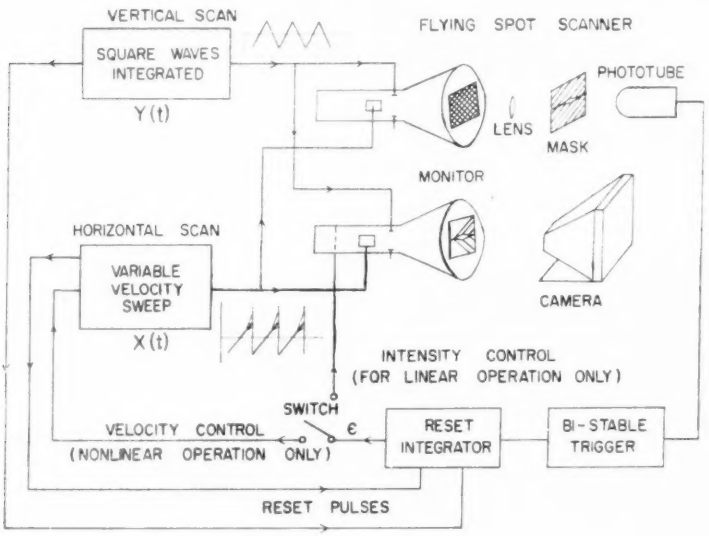

Figure 7. Block diagram of equipment.

In the present experiments, the light intensity I_0 was not varied according to (42), but was kept constant. In this way the flow pictures do not actually correspond to schlieren pictures.

A more serious defect of the present experimental set-up is that the boundary conditions were not introduced correctly. The masks were simply cut out of black paper, thus giving two levels of the video signal. Every smooth closed body contour, however, has both positive and negative slopes. In order to form both positive and negative disturbances, one needs at least a three-level discriminator instead of the bi-stable trigger, and this

was not available at the time of the experiments. There is really one exception to this comment. Figure 8 (plate 2) represents a concave 'body', and the slope is approximately proportional to the local thickness so in this particular example the proper boundary conditions were applied. (A wedge with exponential contour satisfies the requirement that thickness is proportional to slope.)

To modulate the light intensity in accordance with (42) would have required the use of a memory circuit to retain the value of ϵ from the previous scan stroke, hence to form $d\epsilon/d\xi \doteq \epsilon(\xi_n) - \epsilon(\xi_{n-1})$.

It should be emphasized that both of these improvements (proper boundary conditions by use of three-level discriminator and light-intensity modulation according to (42)) require only standard electronic design, and were not attempted only for lack of time available for the work.

Figure 8 (plate 2) clearly shows the crowding of characteristics into the formation of an envelope. Figure 9 (plate 1) shows the photographic print of the cut-out mask and the 'flow picture' thus obtained. Since the period of scan cycle is constant and the horizontal scan velocity is variable, the right edge of the picture is irregular as the total x distance is varying with the disturbance. In order to render the pictures more 'life-like', a small artifice was introduced. On the display cathode-ray tube intensity grid, a linear combination of the video signal and its time derivative was imposed. The negative value of the video signal from the phototube produced darkness in the interior of the body and the time derivative of the video signal gave a sharp outline of the body contours. Without this artifice the body contours would not even have been visible.

Figure 10 (plate 2) shows two objects. In the picture in figure 10(*a*) the non-linearity is 'weak', having low amplification of the disturbance signal. In the other picture, the non-linear effect is strong.

As a possible extension of the method, the analogue for axisymmetric supersonic flows seems to be quite feasible. A more speculative proposition is the use of iteration. Using iterative processes, the first flow picture would be obtained by scanning a cut-out mask representing the boundary conditions. The display would be photographed and would be introduced into the scanner to obtain a second approximation. In this way, the interaction between the two families of characteristics would be introduced.

The extension to the one-dimensional unsteady problem, where the cathode-ray face would represent the x, t plane, is also obvious. It is interesting to note that in this case the analogue becomes exact for $\gamma = 3$, as shown in the Appendix.

The present work was carried out in the National Bureau of Standards, Washington, D.C., under a cooperative programme of basic instrumental research and development while the author was a consultant. The author acknowledges the enthusiastic help of Mr H. M. Joseph and Mr N. Newman. Thanks are due to Dr B. T. Chu of Brown University for contributing the special case given in the Appendix.

Appendix

The one-dimensional unsteady flow of a compressible gas presented on an (x, t)-plane has a qualitative similarity to the steady two-dimensional flow. The governing equations for an isentropic perfect gas are:

Conservation of mass,
$$\frac{\partial \rho}{\partial t} + u\frac{\partial \rho}{\partial x} + \rho\frac{\partial u}{\partial x} = 0. \tag{A 1}$$

Conservation of momentum,
$$\frac{\partial u}{\partial t} + u\frac{\partial u}{\partial x} + \frac{c^2}{\rho}\frac{\partial \rho}{\partial x} = 0. \tag{A 2}$$

By eliminating ρ, one obtains the pair of equations

$$\frac{\partial}{\partial t}\left(u + \frac{2}{\gamma-1}c\right) + (u+c)\frac{\partial}{\partial x}\left(u + \frac{2}{\gamma-1}c\right) = 0, \tag{A 3}$$

$$\frac{\partial}{\partial t}\left(u - \frac{2}{\gamma-1}c\right) + (u-c)\frac{\partial}{\partial x}\left(u - \frac{2}{\gamma-1}c\right) = 0. \tag{A 4}$$

Introduce the characteristic lines $\xi = \text{const.}$ and $\eta = \text{const.}$, i.e. with $\xi = \xi(x, t)$, $\eta = \eta(x, t)$, so that

$$d\xi = dx - (u+c)\,dt, \qquad d\eta = dx - (u-c)\,dt. \tag{A 5}$$

Along these lines the characteristic relations are obtained:

$$\text{Along} \quad \xi = \text{const.}, \qquad u + 2c/(\gamma-1) = \text{const.}$$

$$\text{Along} \quad \eta = \text{const.}, \qquad u - 2c/(\gamma-1) = \text{const.}$$

The characteristic relations can be conveniently written as

$$c + \tfrac{1}{2}(\gamma-1)u = c_0 + \epsilon(\xi), \qquad c - \tfrac{1}{2}(\gamma-1)u = c_0 + \delta(\eta), \tag{A 6}$$

where $\epsilon(\xi)$ and $\delta(\eta)$ are arbitrary functions of their arguments. In general the characteristics will be curved lines. However, if $\gamma = 3$,

$$u + c = c_0 + \epsilon(\xi), \qquad u - c = -c_0 - \delta(\eta). \tag{A 7}$$

Consequently, the equations (A 5) can be independently integrated, giving, for instance,

$$\xi = x - [c_0 + \epsilon(\xi)]t, \qquad \eta = y + [c_0 + \delta(\eta)]t. \tag{A 8}$$

These equations represent two 'non-interacting' sets of characteristics.

Unfortunately all gases have $\gamma < 5/3$. It is worth mentioning that shallow water flow has properties analogous to a two-dimensional gas flow with $\gamma = 2$ (see Courant & Friedrichs 1948).

References

Courant, R. & Friedrichs, K. O. 1948 *Supersonic Flow and Shock Waves.* New York: Interscience.

Higgins, T. J. 1956 Electroanalogic Methods. *Applied Mech. Rev.* **9**, 1.

Howarth, L. (Ed.) 1953 *Modern Developments in Fluid Dynamics: High Speed Flow.* Vol. I, p. 64. Oxford University Press.

Kovasznay, L. S. G. & Joseph, H. M. 1955 Image processing. *Proc. Inst. Radio Engrs.* **43**, 560.

Lighthill, M. J. 1954 Higher Approximations, Section E of *General Theory of High Speed Aerodynamics* (Ed. W. Sears). Princeton University Press.

On the stability of plane shock waves

By N. C. FREEMAN
*Department of Mathematics, University of Manchester**

(*Received* 13 *February* 1957)

SUMMARY

The decay of small perturbations on a plane shock wave propagating along a two-dimensional channel into a fluid at rest is investigated mathematically. The perturbations arise from small departures of the walls from uniform parallel shape or, physically, by placing small obstacles on the otherwise plane parallel walls. An expression for the pressure on a shock wave entering a uniformly, but slowly, diverging channel already exists (given by Chester 1953) as a deduction from the Lighthill (1949) linearized small disturbance theory of flow behind nearly plane shock waves. Using this result, an expression for the pressure distribution produced by the obstacles upon the shock wave is built up as an integral of Fourier type. From this, the shock shape, ξ, is deduced and the decay of the perturbations obtained from an expansion (valid after the disturbances have been reflected many times between the walls) for ξ in descending power of the distance, ζ, travelled by the shock wave. It is shown that the stability properties of the shock wave are qualitatively similar to those discussed in a previous paper (Freeman 1955); the perturbations dying out in an oscillatory manner like $\zeta^{-3/2}$. As before, a Mach number of maximum stability (1·15) exists, the disturbances to the shock wave decaying most rapidly at this Mach number. A modified, but more complicated, expansion for the perturbations, for use when the shock wave Mach number is large, is given in § 4.

In particular, the results are derived for the case of symmetrical 'roof top' obstacles. These predictions are compared with data obtained from experiments with similar obstacles on the walls of a shock tube.

1. INTRODUCTION

The ability of plane shock waves, propagating into a stationary fluid, to retain their shape when subjected to small disturbances was considered theoretically in a previous paper (Freeman 1955). This property has been called 'stability'. It was realized however that the model used to demonstrate

*Now at the National Physical Laboratory Teddington.

this, namely, a perturbation to the shock wave produced by moving a plane piston impulsively from rest at constant speed into the stationary fluid, would be difficult to reproduce in the laboratory. In order to overcome this disadvantage another model is here studied. In this model, a plane shock wave propagating down a uniform channel into a fluid at rest is disturbed by small protuberances on the channel wall. This model bears a close resemblance to actual experimental conditions when the shock is produced, as is usually the case, in a shock tube, and, in fact, such experiments have been performed by Mr K. C. Lapworth in the Manchester University shock tube. It will be shown that the shock wave qualitatively exhibits similar properties to those described in the preceding paper (Freeman 1955).

Chester (1953) has already considered the problem of a shock propagating along a two-dimensional channel which begins to diverge slowly, and has extended this result to obtain the change in strength of a shock propagating along a channel which changes from one uniform cross-section to another. The solution given below will be a further development of this work obtained, essentially, by considering higher order terms in the expansion given by Chester. In its turn, the Chester solution is a development of the problem, investigated by Lighthill (1949), of a shock wave propagating along a plane wall which suddenly changes in direction by a small angle δ. The fluid is assumed inviscid except in a thin region comprising the shock wave across which the variables of the flow change discontinuously in a manner determined by the Rankine–Hugoniot relations. The disturbances produced at the corner are assumed to be small enough for the equations of the flow behind the shock wave to be linearized. The shock wave is disturbed from its plane form within a region cut off by a cylindrical wavefront, which originating at the corner, expands with the speed of sound behind the undisturbed shock wave and is translated bodily with the velocity of the fluid behind the undisturbed shock wave (see figure 1). When the corner is concave to the flow, this becomes the familiar Mach reflection. Under the conditions stated above, the pressure satisfies the wave equation with constant sound speed and the solution can be obtained in terms of the 'conefield' variables by the use of the Busemann transformation and conformal mapping techniques. Chester has shown that the presence of another wall can be accounted for by considering a system of images in the wall. The solution is rather complicated, being a sum of Lighthill solutions. After the disturbances produced have undergone a sufficiently large number of reflections at the walls, however, an asymptotic expansion for the pressure on the shock wave can be obtained in descending powers of the time. The first term of this expansion is used by Chester in his solution for a change in cross-section of the channel. Further higher order terms, which decay with time, are neglected. It is these terms that we shall consider here. In the case when the channel is uniform along its length, except over a finite range, after which it returns to its original cross-section, the decaying terms alone remain.

We, therefore, consider the propagation of a plane shock wave along a uniform two-dimensional channel with walls a fixed distance apart except over a finite length where the channel width varies slowly in some prescribed manner. Following Chester, we will concern ourselves with the behaviour at large time, that is, after many reflections have taken place at the channel walls. It will also be assumed that sufficient time has elapsed for the shock to have travelled a distance large compared with the length of the non-uniform section of the channel.

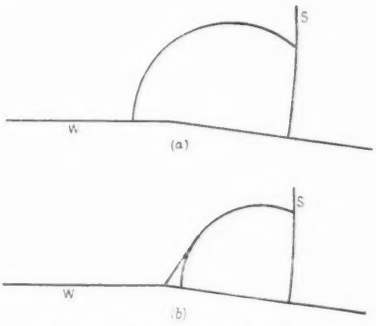

Figure 1. The configuration in the Lighthill problem.
S, shock; *W*, wall. (*a*) Subsonic; (*b*) Supersonic.

The perturbations to the flow arising from each element of the disturbing wall are propagated, as pointed out in the previous paper (Freeman 1955), at the speed of sound behind the undisturbed shock as cylindrical waves convected with the fluid. The velocity of the disturbances along the shock wave is the velocity component of these wavefronts along the shock. To the linearized approximation, the velocity of the wavefront of the cylindrical wave produced by a particular element of wall is $a_1\sqrt{\{1-([U-u]/a_1)^2\}}$ $(=a_1\sin\psi$, say) along the shock, where a_1 is the velocity of sound behind the undisturbed shock and $U-u$ is the velocity of the undisturbed shock relative to the fluid behind it. As these waves are cylindrical in character, we expect a singularity like $\sqrt{\{1-(r/a_1t)^2\}}$ where r is the distance from the centre of the disturbance produced by the particular element under consideration, and t is the time measured from the instant at which the shock strikes it. But, as has been shown previously (Freeman 1955), the strength of this wavefront is forced to vanish at the shock by the form of the boundary condition there, and the singularity is of higher order. The effect of the non-uniformity of the channel wall is then the sum of all these cylindrical waves and is obtained as a Fourier transform of the individual solutions. At large time, the behaviour of this integral is dominated by the singularity at the cylindrical wavefront. Thus, the shock is perturbed on passing the non-uniformity by disturbances which travel along it with a speed $a_1\sin\psi$. Due to the singularity at the wavefront, the disturbances decay in an oscillatory manner like $\zeta^{-3/2}$ where ζ is the distance travelled

past the obstacle. This rate of decay varies with shock Mach number, decreasing rapidly both for strong and very weak shocks. Between these extremes there lies a Mach number of maximum stability where the perturbations to the shock wave decay most rapidly with the distance travelled by the shock. This has been calculated as $M = 1{\cdot}15$ approximately, which is very close to the value 1·14 given for the first model (Freeman 1955).

An interesting phenomenon occurs when we consider the particular case of symmetrical 'roof top' obstacles placed on the upper and lower walls of the channel (see figure 2). Then, together with the above variation in Mach number, there is a variation with the length of the 'roof top' due to cancellation or reinforcement in varying degrees of the disturbances produced at the corners and vertices. A similar effect occurs in linearized aerofoil theory of supersonic flow for the so-called 'Busemann Biplane'. When the shock wave strikes the 'roof tops', disturbances propagate outwards along it and are reflected at the opposite walls. At the ends of the 'roof top', the corners being concave to the flow, the disturbances will

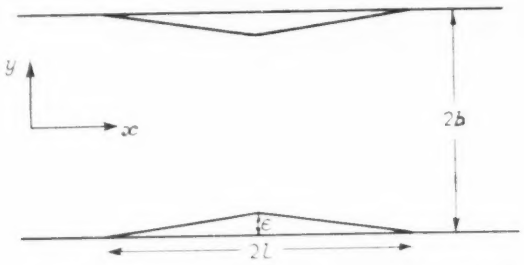

Figure 2. The 'roof top' obstacles in position in the channel.

be compressive ones, whereas at the vertex, the corner being convex to the flow, the disturbance will be expansive. The latter disturbance, according to linear theory, is opposite in sign and twice the magnitude of either of the former. On this account, should the length of the 'roof top' be such that the time taken for the shock to travel between corner and vertex is an integral number of times that for the disturbances on the shock to travel across the channel, cancellation of these disturbances will occur and the decay will be faster than indicated above. In a similar manner, maximum disturbance is produced when the time taken for the shock to move from corner to corner is an odd integral multiple of that for the disturbances to cross the channel. These conditions may be written $Ub/a_1 l \sin\psi = 2n$ and $Ub/a_1 l \sin\psi = 2n+1$, where n is an integer, U is the velocity of the shock wave, $2l$ is the length of the 'roof top' and $2b$ the width of the channel.

In § 5, the results obtained by Lapworth (1956) from experiments on 'roof top' obstacles situated on the walls of a shock tube are briefly discussed. These results indicate that the theory developed in this paper gives a good qualitative picture of actual conditions. The oscillatory nature of the

perturbations and their rate of decay are in good agreement although the actual magnitude of the perturbation is somewhat less than predicted. This discrepancy might be expected however since the present theory is only a linear approximation to the true state of affairs.

In conclusion, a comparison of the present model with the one discussed previously (Freeman 1955) makes it clear that the behaviour of the shock wave is to some extent independent of conditions prevailing in the flow field behind. A theory making this assumption has been put forward by Whitham (1957) to take into account non-linear effects.

2. Extension of Chester solution

The theory of Lighthill (1949) has shown that the flow behind a plane shock moving along a plane wall which changes in direction by a small angle δ is disturbed within a circle expanding with the velocity of sound behind the shock and whose centre moves with the velocity of the fluid behind the shock originally being situated at the corner (see figure 2). These velocities are, to this approximation, constant and equal to their value behind the undisturbed shock wave. In the case of supersonic flow behind the shock, there is an additional region of disturbance bounded by the tangent from the corner to this circle (figure 2(*b*)). The shock is disturbed from its plane form in the region cut off by this circle.

The pressure within the circle is given by

$$(p_1 - p_0)\,\delta p(X, Y), \tag{2.1}$$

where

$$\frac{\partial p}{\partial y_1} + i\frac{\partial p}{\partial x_1} = \frac{C[D(z_1 - 1 + \gamma^2) - 1]\sec\psi}{(z_1^2 - 1)^{1/2}(z_1 - 1 + \gamma^2)(\alpha - i(z_1 - 1)^{1/2})(\beta - i(z_1 - 1)^{1/2})} \tag{2.2}$$

with $\cos\psi = [(M^2+5)/(7M^2-1)]^{1/2}$. The constants α, β, γ, C and D are functions of M defined by Lighthill (1949). M is the Mach number of the shock; a_0, p_0, ρ_0 and a_1, p_1, ρ_1 are the sound speed, pressure and density in front and behind the shock respectively. The $z_1(= x_1 + iy_1)$-plane is related to the physical (x, y)-plane with origin at the corner and x-axis in the direction of propagation by

$$z_1 = -\frac{1}{2}\left[\left\{\frac{\rho e^{i(\theta+\psi)} - 1}{\rho e^{i\theta} - e^{i\psi}}\right\}^2 + \left\{\frac{\rho e^{i\theta} - e^{i\psi}}{\rho e^{i(\theta+\psi)} - 1}\right\}^2\right] \tag{2.3}$$

and

$$\frac{x - q_1 t}{a_1 t} + i\frac{y}{a_1 t} = X + iY = \frac{2\rho e^{i\theta}}{1+\rho^2},$$

where q_1 is the velocity of the fluid behind the undisturbed shock wave. The disturbed region in the (x, y)-plane is mapped into the upper half plane. The disturbed shock, which is given by $x = Ut$ or $X = \cos\psi$, becomes

$$x_1 = \frac{1 + (Y/\sin\psi)^2}{1 - (Y/\sin\psi)^2}, \qquad y_1 = 0, \tag{2.4}$$

with

$$0 < Y < \sin\psi.$$

The point $x_1 = 1$, $y_1 = 0$ is the intersection of the shock and wall and $x_1 = \infty$, $y_1 = 0$ the intersection with the circular wavefront. From (2.2),

$$\frac{\partial p}{\partial x_1} = \frac{C[D(x_1 - 1 + \gamma^2) - 1](\alpha + \beta)\sec\psi}{(x_1+1)^{1/2}(x_1 - 1 + \gamma^2)(x_1 - 1 + \beta^2)(x_1 - 1 + \alpha^2)} \tag{2.5}$$

on the shock.

Chester (1953) has shown that the problem of a shock moving along a channel of width $2b$ which begins to diverge uniformly at a small angle 2δ can be solved in terms of this solution. The effect of enclosing the shock between two walls is to reflect the waves produced at the corners repeatedly between the two walls. Since this wave motion is already of order δ, however, the effect of the divergence of the walls will be a second order effect in δ in the reflections, and hence these reflections may be considered to take place at plane walls. Suitable images can be placed outside the walls to produce the required reflections. The number of these images that influence the shock will grow with time. The pressure in the case of a channel can therefore be written

$$\delta(p_1 - p_0)P(x, y, t),$$

with

$$P = \sum_n \left\{ p\left(\frac{x - q_1 t}{a_1 t}, \frac{(2n+1)b - y}{a_1 t}\right) + p\left(\frac{x - q_1 t}{a_1 t}, \frac{(2n+1)b - y}{a_1 t}\right)\right\}, \tag{2.6}$$

where x is measured along the channel and y from the centre of the channel, the summation being taken over all the images that influence the shock. By using Dirichlet's summation formula, Chester writes this, in a form more convenient for asymptotic estimation, as

$$\begin{aligned} P = {} & \tfrac{1}{2}p(X, (b-y)/a_1 t) + \tfrac{1}{2}p(X, (b+y)/a_1 t) + \\ & + \frac{a_1 t}{2b} \sum_{n=-\infty}^{\infty} \left[\int_{(b-y)/a_1 t}^{(1-X^2)^{1/2}} (-1)^n p(X, Y) e^{n\pi i(a_1 tY + y)/b}\, dY + \right. \\ & \left. + \int_{(b-y)/a_1 t}^{-(1-X^2)^{1/2}} (-1)^n p(X, Y) e^{n\pi i(a_1 tY - y)/b}\, dY, \right. \end{aligned} \tag{2.7}$$

where $p(X, Y)$ is given by (2.2).

If we now consider pressure variations on the shock alone, then

$$\begin{aligned} P = {} & \tfrac{1}{2}p\left(\cos\psi, \frac{b-y}{a_1 t}\right) + \tfrac{1}{2}p\left(\cos\psi, \frac{b+y}{a_1 t}\right) + \\ & + \frac{a_1 t}{2b} \sum_{n=-\infty}^{\infty} \left\{ \int_{(b-y)/a_1 t}^{\sin\psi} (-1)^n p(\cos\psi, Y) e^{n\pi i(a_1 tY + y)/b}\, dY \right. \\ & \left. + \int_{(b-y)/a_1 t}^{-\sin\psi} (-1)^n p(\cos\psi, Y) e^{n\pi i(a_1 tY - y)/b}\, dY \right\}. \end{aligned} \tag{2.8}$$

It will be sufficient to consider the behaviour of this function for large time.

The behaviour of the first two terms will simply be determined by expanding p as a function of Y. The integrals within the sum will however be dominated by the singularities of p in the range of integration. It will be shown as in the previous paper (Freeman 1955) that the singularity at the shock-wavefront intersection is dominant.

Let us now consider the function $p(\cos\psi, Y)$ in more detail. Near the wall, when $Y = 0$, $x_1 = 0$, (2.5) together with (2.4) states that

$$p = \text{const.} + O(Y^2).$$

Thus $\partial p/\partial Y = 0$ at $Y = 0$ and also

$$p(\cos\psi, (b \pm y)/a_1 t) = \text{const.} + O((b \pm y)^2/a_1^2 t^2). \tag{2.9}$$

At the shock–wavefront intersection $Y = \sin\psi$, or $x_1 = \infty$, then, from (2.5),

$$\frac{\partial p}{\partial x_1} \sim \frac{CD(\alpha+\beta)\sec\psi}{x_1^{5/2}}. \tag{2.10}$$

Consider now a general term of the sum in (2.8). For $n \neq 0$ we have

$$\begin{aligned} J_n &= \frac{a_1 t}{2b} e^{\pm in\pi y/b} \int_{(b\mp y)/a_1 t}^{\sin\psi} (-1)^n p(\cos\psi, Y) e^{in\pi a_1 tY/b}\, dY \\ &= \frac{(-1)^n}{2n\pi i}\left\{ A - e^{\pm in\pi y/b} \int_{(b\mp y)/a_1 t}^{\sin\psi} \frac{\partial p}{\partial Y} e^{in\pi a_1 tY/b}\, dY \right\} + O\left(\frac{1}{t^2}\right), \end{aligned} \tag{2.11}$$

using (2.9) and (2.5), where A is a constant. Also, since $\partial p/\partial Y = O(Y)$ as $Y \to 0$, it follows that

$$J_n = B_n - \frac{(-1)^n e^{\pm in\pi y/b}}{2n\pi i} \int_0^{\sin\psi} \frac{\partial p}{\partial Y} e^{in\pi a_1 tY/b} + O\left(\frac{1}{t^2}\right), \tag{2.12}$$

where B_n is a constant and the integration is now along the shock from the wall to the wavefront. It follows also that the above integral is dominated by the singularity at the upper limit. The integrand is

$$\begin{aligned} &\frac{\partial p}{\partial x_1}\left(\frac{dx_1}{dY}\right)_{\text{shock}} e^{in\pi a_1 tY/b} \\ &\sim CD(\alpha+\beta)\sec\psi\,\operatorname{cosec}\psi(1 - Y\operatorname{cosec}\psi)^{1/2} e^{in\pi a_1 tY/b} \end{aligned} \tag{2.13}$$

near $Y = \sin\psi$, and so the integral may be written

$$CD(\alpha+\beta)\sec\psi\,\operatorname{cosec}\psi \int^{\sin\psi} (1 - Y\operatorname{cosec}\psi)^{1/2} e^{in\pi a_1 tY/b}\, dY + O\left(\frac{1}{t^2}\right).$$

Using the formula for the asymptotic expansion of a Fourier integral (see, for example, Freeman 1955), we obtain

$$\begin{aligned} J_n \sim B_n + \frac{(-1)^n CD(\alpha+\beta)\sec\psi}{4n\sqrt{\pi}} \left| \frac{b}{n\pi a_1 t \sin\psi} \right|^{3/2} \times \\ \times \exp\left[\frac{in\pi}{b}\{a_1 t \sin\psi \pm y\} + \frac{i\pi}{4}\theta_n \right], \end{aligned} \tag{2.14}$$

where

$$\begin{aligned} \theta_n &= -1 \qquad (n > 0), \\ &= +1 \qquad (n < 0), \end{aligned}$$

for t large. Substituting in (2.8), we have

$$\begin{aligned} P = \frac{a_1 t}{b} \int_0^{\sin\psi} p(\cos\psi, Y)\, dY + B + \\ + \frac{CD(\alpha+\beta)\sec\psi}{2\pi^2} \left[\left(\frac{b}{a_1 t \sin\psi} \right)^{3/2} \sum_{n=-\infty}^{\infty}{}' \frac{(-1)^n}{n^{5/2}} \times \right. \\ \left. \times \exp\left\{ \frac{in\pi a_1 t \sin\psi}{b} + \frac{i\pi}{4}\theta_n \right\} \cos\frac{n\pi y}{b} \right] + O\left(\frac{1}{t^2}\right), \end{aligned} \tag{2.15}$$

where $\sum'$ denotes that there is no term $n = 0$ in the summation, and B is a constant. The integral has been calculated by Chester, who denotes it by $K(U/a_1)$, and hence

$$P = \frac{KUt}{b} + B + \frac{CD(\alpha+\beta)\sec\psi}{\pi^2}\left(\frac{b}{a_1 t\sin\psi}\right)^{3/2} \times$$
$$\times \sum_{n=1}^{\infty} \frac{(-1)^n}{n^{5/2}} \cos\left(\frac{n\pi a_1 t\sin\psi}{b} - \frac{\pi}{4}\right)\cos\frac{n\pi y}{b} + O\left(\frac{1}{t^2}\right). \quad (2.16)$$

Now, let us consider a channel of more general cross-section defined by $y = b + f(x)$, $y = -b - f(x)$, where $f(x)$ is non-zero for some range of x and $f'(x)$ is small. In fact, we will consider the case of $f(x)$ non-zero only in a finite range, that is, the effects of change in shock strength due to changes in width of channel, which have already been studied by Chester, will not be considered. The solution of the problem in which the channel begins to diverge uniformly can now be generalized to this new channel shape by considering a change of slope $df'(\eta)$ at time $t = \eta/U$ and distance $x = \eta$. Thus the value of P for the new problem will be

$$P_1 = \int P\left(t - \frac{\eta}{U},\ y\right) df'(\eta), \quad (2.17)$$

the integral being taken over the range in which f is non-zero. For sufficiently large distances away from the obstacle in the channel, the powers of $t-(\eta/U)$ become t and thus,

$$P_1 = \frac{CD(\alpha+\beta)\sec\psi}{\pi^2}\left(\frac{b}{a_1 t\sin\psi}\right)^{3/2}$$
$$\times \sum_{n=1}^{\infty}{}' \int \frac{(-1)^n}{n^{5/2}} \cos\left[\frac{n\pi a_1\sin\psi}{b}\left(t - \frac{\eta}{U}\right) - \frac{\pi}{4}\right] \times$$
$$\times \cos\frac{n\pi y}{b}\, df'(\eta) + O\left(\frac{1}{t^2}\right). \quad (2.18)$$

Now if ξ is the perturbation of the shock wave from its plane form, then the perturbation to the pressure is $\frac{5}{3}Ma_0\rho_0(\partial\xi/\partial t)$, to a linear approximation, from the shock equation ($\gamma = 1{\cdot}4$). Hence the perturbation to the shock shape may be written

$$\frac{\xi}{b} = \frac{3CD(\alpha+\beta)}{5\pi^3 M\cos\psi\sin\psi}\left(\frac{p_1 - p_0}{a_1 a_0\rho_0}\right)\left(\frac{b}{a_1 t\sin\psi}\right)^{3/2} \times$$
$$\times \sum_{n=1}^{\infty}{}' \int \frac{(-1)^n}{n^{7/2}} \sin\left[\frac{n\pi a_1\sin\psi}{b}\left(t - \frac{\eta}{U}\right) - \frac{\pi}{4}\right]\cos\frac{n\pi y}{b}\, df'(\eta) + O\left(\frac{1}{t^2}\right). \quad (2.19)$$

This result indicates, as has been shown previously (Freeman 1955), that the perturbations to the shock wave decay at a rate proportional to the inverse three-halves power of the time, or, alternatively, of the distance travelled by the shock wave past the obstacle. The variation of the coefficient in (2.19) with Mach number will be discussed in more detail in § 3.

In passing, it might be observed that the modification to equation (2.19) for the case of a channel which increases in width by a small amount 2ϵ is obtained by adding a term

$$-\frac{3(p_1-p_0)K_\epsilon}{5\rho_0 U^2 b}\cdot\frac{Ut}{b}$$

to the right-hand side.

3. The 'roof top' disturbance

In order to obtain more detailed knowledge of this phenomenon, we will now study a particular form of the function $f(x)$—the so-called 'roof top' (see figure 2). Let

$$\left.\begin{aligned} f(\eta) &= -\left(1+\frac{\eta}{l}\right)\epsilon \qquad (-l<\eta<0),\\ &= -\left(1-\frac{\eta}{l}\right)\epsilon \qquad (0<\eta<l). \end{aligned}\right\} \tag{3.1}$$

Then, using (2.17), we obtain

$$P_1 = \frac{\epsilon}{l}\left\{2P(t,y)-P\left(t-\frac{l}{U},\ y\right)-P\left(t+\frac{l}{U},\ y\right)\right\}. \tag{3.2}$$

The total disturbance is made up of a sum, therefore, of the individual disturbances at the corners and vertex of the 'roof top', due regard being taken of their origin in time. Hence, using (2.19) and (3.2),

$$\begin{aligned}\frac{\xi}{b} = \frac{\epsilon}{l}\Omega_1\left(\frac{b}{a_1 t\sin\psi}\right)^{3/2}\times\\ \times\left[2E\left(\frac{\pi}{b}(a_1 t\sin\psi+y)\right)+2E\left(\frac{\pi}{b}(a_1 t\sin\psi-y)\right)-\right.\\ -E\left(\frac{\pi}{b}(a_1\sin\psi\{t+(l/U)\}+y)\right)-E\left(\frac{\pi}{b}(a_1\sin\psi\{t+(l/U)\}-y)\right)-\\ \left.-E\left(\frac{\pi}{b}(a_1\sin\psi\{t-(l/U)\}+y)\right)-E\left(\frac{\pi}{b}(a_1\sin\psi\{t-(l/U)\}-y)\right)\right],\end{aligned} \tag{3.3}$$

where

$$E(z)=\sum_{n=1}^{\infty}\frac{(-1)^n}{n^{3/2}}(\sin nz-\cos nz)$$

and

$$\Omega_1=\frac{3CD(\alpha+\beta)(p_1-p_0)}{10\pi^3\sqrt{2M\cos\psi\sin\psi a_1 a_0\rho_0}}.$$

If $\zeta = Ut$, the distance travelled by the shock, then

$$\frac{\xi}{b}=\frac{\epsilon}{l}\frac{\Omega}{(\zeta/b)^{3/2}}\left[F\left(\frac{\pi}{b}\left\{\frac{a_1\sin\psi}{U}\zeta+y\right\}\right)+F\left(\frac{\pi}{b}\left\{\frac{a_1\sin\psi}{U}\zeta-y\right\}\right)\right],$$

where

$$F(z)=2E(z)-E\left(z+\frac{\pi a_1 l\sin\psi}{Ub}\right)-E\left(z-\frac{\pi a_1 l\sin\psi}{Ub}\right) \tag{3.4}$$

and

$$\Omega=\left(\frac{U}{a_1\sin\psi}\right)^{3/2}\Omega_1.$$

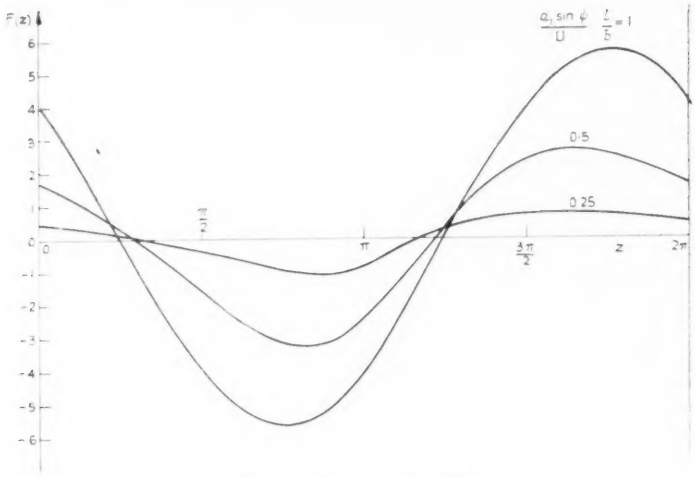

Figure 3. The function $F(z)$.

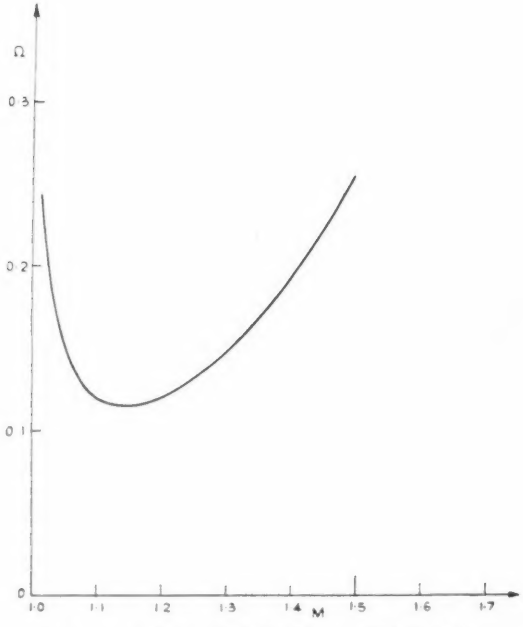

Figure 4. The coefficient Ω as a function of M.

The function $E(z)$ was computed by making use of the relation

$$\sum_{n=1}^{\infty} \frac{e^{inx}}{n^{s+1}} = \frac{1}{s!}\int_0^{\infty} \frac{z^s\,dx}{e^{z-ix}-1}. \tag{3.5}$$

The function $F(z)$ is plotted in figure 3 for various values of $la_1 \sin\psi/Ub$. $F(z)$ is periodic with period 2π. For $la_1 \sin\psi/Ub = 2n$, where n is an integer, the function is identically zero. This condition may be written $l/U = (2b/a_1 \sin\psi)n$, which states that the time taken for the shock to travel between a corner and the vertex of the 'roof top' is an integral multiple of the time taken for a disturbance to travel along the shock across the channel. If this is so, the initial term of our expansion will vanish and higher order terms will dominate, the shock perturbations decaying more rapidly. The function F is a maximum for values of $(a_1 l \sin\psi/Ub)$ at which $(l/U) = (b/a_1 \sin\psi)(2n+1)$. These values correspond to configurations in which the disturbances produced at the vertex and corners reinforce each other. The coefficient Ω is shown in figure 4. The similarity between this figure and figure 5 of the earlier paper (Freeman 1955) is immediately obvious. The minimum at $M = 1{\cdot}15$ is very close to the one shown there. The perturbations to shock waves of this Mach number decay most rapidly with the distance travelled by the shock wave.

4. The variation at high Mach number

The behaviour of the various constants for large Mach number M may be summarized as follows:

$$\cos\psi \sim \sqrt{(\tfrac{1}{7})}, \qquad \sin\psi \sim \sqrt{(\tfrac{6}{7})}, \qquad \alpha \sim 2\sqrt{(\tfrac{2}{7})}M^2, \qquad \beta \sim \sqrt{(\tfrac{7}{2})},$$
$$\gamma \sim \sqrt{(\tfrac{7}{2})}, \qquad C \sim 35\sqrt{(\tfrac{6}{7})}M^2/\pi, \qquad D \sim \tfrac{1}{5}. \tag{4.1}$$

The correct approximation to equation (2.5) for large M and large x_1 is, therefore,

$$\frac{\partial p}{\partial x_1} \sim \left(\frac{CD}{\alpha}\right)\frac{[1+(\beta/\alpha)]\sec\psi}{x_1^{3/2}\{1+[(x_1-1)/\alpha^2]\}}, \tag{4.2}$$

since α is no longer small. It will be observed that as $\alpha \to \infty$ then $(\partial p/\partial x_1) \sim x^{-3/2}$ and the form of the singularity that dominates the integral (2.13) has changed. When α is large but finite, we must consider a form of expansion in which the pole $x_1 = -\alpha^2$ lies close to the branch point. The method used is due to Clemmow (1950). From (4.2),

$$\frac{\partial p}{\partial x_1} \sim \frac{\Theta z^{5/2}}{z+\alpha^{-2}} \tag{4.3}$$

near $z = 0$, where $z = 1-(Y/\sin\psi)$ and $\Theta = CD(\alpha+\beta)\sec\psi/\alpha^2$. Whence, using (2.4),

$$\frac{\partial p}{\partial Y} \sim \frac{\Theta z^{1/2}}{\sin\psi(z+\alpha^{-2})}, \tag{4.4}$$

and thus for large M,

$$\frac{\partial p}{\partial Y} \sim \frac{\Theta}{\sin\psi\{1-(Y/\sin\psi)\}^{1/2}}$$

as opposed to $$\frac{\partial p}{\partial Y} \sim \frac{\alpha^2\Theta}{\sin\psi\{1-(Y\sin\psi)\}^{1/2}}$$

for smaller M. This in turn would give a slower decay, like $t^{-1/2}$, to the shock perturbations for large M. For large M, therefore, we require an expression for

$$\int_0^{\infty} \frac{z^{1/2}}{z+\alpha^{-2}} e^{in\pi a_1 tz\sin\psi/b}\, dz \tag{4.5}$$

in place of the expansion of (2.13) since, as before, the main contribution will come from near $z=0$. Thus, as in § 2, the pressure due to a slightly diverging channel is

$$P = -\frac{KUt}{b} + B + \Theta \sum_{n=-\infty}^{\infty}{}' \frac{(-1)^n}{n\pi i}\left[\int_0^{\infty} \frac{z^{1/2}}{z+\alpha^{-2}} e^{in\pi a_1 t\sin\psi z/b}\, dz\right] e^{-in\pi a_1 t\sin\psi/b} + O\left(\frac{1}{t^2}\right). \tag{4.6}$$

The integral enclosed in the square brackets may be written

$$\left(\frac{b}{na_1 t\sin\psi}\right)^{1/2} I^*\left(\frac{n\pi a_1 t\sin\psi}{\alpha^2 b}\right) e^{\frac{1}{4}i\pi} \quad \text{for } n>0$$

and

$$\left(\frac{b}{n\,a_1 t\sin\psi}\right)^{1/2} I\left(\frac{n\,\pi a_1 t\sin\psi}{\alpha^2 b}\right) e^{-\frac{1}{4}i\pi} \quad \text{for } n<0,$$

where * denotes the complex conjugate and

$$I(z) = 1 - \sqrt{(\pi z)} e^{iz}\left\{e^{\frac{1}{4}i\pi} - \frac{2i}{\sqrt{\pi}}\int_0^{\sqrt{z}} e^{-iv^2}\, dv\right\}. \tag{4.7}$$

As in (2.19), the shock shape is then given, for a channel varying in width, by

$$\frac{\xi}{b} = \frac{\Lambda}{(\zeta/b)^{1/2}} \sum_{n=1}^{\infty} \frac{(-1)^n}{n^{3/2}} \cos\frac{n\pi y}{b} \times \times \int\left[I^*\left(\frac{n\pi a_1 \sin\psi}{\alpha^2 b}\left\{t-\frac{\eta}{U}\right\}\right) e^{-in\pi a_1(t-\eta/U)/b - \frac{1}{4}i\pi} - I\left(\frac{n\pi a_1\sin\psi}{\alpha^2 b}\left\{t-\frac{\eta}{U}\right\}\right) e^{in\pi a_1(t-\eta/U)/b - \frac{1}{4}i\pi}\right] df'(\eta), \tag{4.8}$$

where Λ is given in table 1. And, in a similar manner to § 3, the solution for a 'roof top' obstacle can be obtained.

M	Λ
1·5	0·102
2·0	0·128
3·0	0·168
∞	0·234

Table 1.

5. Experimental results

The model discussed in the previous section bears a close resemblance to actual experimental conditions in a rectangular shock tube when 'roof top' protuberances are placed on two opposite walls. Such experiments have been undertaken by Mr K. C. Lapworth (1956) in the shock tube at the Mechanics of Fluids Department, Manchester University. The original intention was to make a comprehensive study of the results obtained from the preceding theory. However, the results obtained so far fall somewhat short of this ideal due to the inability to reproduce the theoretical model as closely as would be desired.

In theory, the perturbations to the shock wave are assumed infinitesimally small—a consequence of the linearization of the problem. In practice, it is necessary to produce disturbances which are large enough to be measured. Since the perturbations are decaying all the time, this will always limit the distance downstream at which one can observe the perturbations to the shock wave. As the theoretical result is given by an asymptotic expansion in inverse powers of the distance, this can seriously limit any comparison between theory and experiment by not allowing time for the regime in which this expansion is valid to be set up. In fact, however, the main features of the asymptotic form of decay would seem to be apparent earlier than one might expect theoretically, at least for Mach numbers not too small.

Also, in the theoretical considerations viscous effects are neglected entirely except in so far as they occur in the idealized form of the shock wave. In practice, viscous effects are important especially around the corners of the 'roof tops', producing separation and the formation of a wake from the vertex. As any viscous effects produced at the wedges will take time to develop after the shock has passed, it will take time for such disturbances to grow large enough to influence the shock. It is thought that it is this which puts an even greater restriction on the distance downstream at which measurements of the perturbations under theoretical flow conditions can be made. For, after a time, the perturbations start to increase due probably to the wake formation influencing the shock wave.

The experiments were made at three shock Mach numbers, 1·60, 1·41 and 1·16. The shock wave was photographed using Schlieren techniques at various distances after passing the 'roof top' system. As it was difficult to decide where the undisturbed position of the shock wave would be and hence to measure ξ directly, a measure of the perturbation which was independent of this was used. This will be called 'the total perturbation' and denoted by ξ_T. ξ_T is the sum, without regard to sign, of the maximum and minimum values of ξ along the shock wave at any particular time. The Mach numbers 1·41 and 1·60 give disturbances to the shock wave which are near the maximum for the 'roof top' system considered, and hence, for these, it is sufficiently accurate to approximate the function $F(z)$ by a sinusoidal function of the appropriate amplitude and period. The total perturbation ξ_T can then be written in the form

$$\frac{\xi}{2b} = \frac{G}{(\zeta/2b)^n} |\sin(mx+p)|, \tag{5.1}$$

from equation (3.4), where the values of n, G, m and p are functions of Mach number and are given in table 2.

For the Mach number 1·16, it was found difficult to compare the values with theory in any way. This may be due to the fact that the asymptotic behaviour will take a longer time to establish itself for lower Mach numbers and those results will therefore not be discussed further. For the two Mach numbers 1·41 and 1·60, Lapworth (1956) has attempted to fit the experimental results for a formula of the type (5.1). Estimates of m and p are obtained from the zeros of the function ξ_T and then G and n are obtained by applying a least squares fit. In order to decide at what point the perturbations began to be influenced by the disturbances in the flow produced by separation at the roof tops, the data were analysed using varying numbers of results dispensing one at a time with the later results until a fairly consistent set of values on n and G were obtained. An average of these values is given in table 3.

M	n	m	p	G
1·41	1·5	3·39	−3·91	0·157
1·60	1·5	3·44	−3·91	0·273

Table 2.

M	n	m	p	G
1·41	1·45	3·31	−2·3	0·066
1·60	1·65	3·31	−1·9	0·090

Table 3.

A comparison of tables 2 and 3 shows that even with the difficulties encountered, the decay of the perturbations is in fair qualitative agreement with theoretical predictions. The actual perturbations are two to three times smaller than those predicted but this might be expected from a linear theory. Non-linear effects would interfere with the reinforcement or cancellation of the sets of disturbances from the two roof tops and also cause the disturbances to interact among themselves. The compressive disturbances would tend to concentrate themselves into shock waves whereas the expansive ones would spread out and interact with these waves. A non-linear theory, such as that developed by Whitham (1957), would be required to describe these effects. The resulting perturbations would thus be reduced by a further cancelling of the individual disturbances. The poor agreement of the phase difference p may again be due to the non-asymptotic nature of the flow.

In view of the reason for the breakdown of the theoretical flow conditions in practice, it would seem difficult to modify this model in any simple way to overcome this defect. To make any more detailed study of the phenomena, it would seem that a different shaped obstacle not so prone to separation difficulties would have to be used.

I would like to express my sincere thanks to Professor M. J. Lighthill for his help and encouragement in the preparation of this paper, and to members of the Departments of Mathematics and Fluid Mechanics with whom this work has brought me into contact, in particular Mr K. C. Lapworth, Dr D. Blackburn and Dr F. Goldsworthy.

I am grateful to the Department of Scientific and Industrial Research for a grant during the period of this research.

References

Chester, W. 1953 *Quart. J. Mech. Appl. Math.* **6,** 440.

Clemmow, P. O. 1950 *Quart. J. Mech. Appl. Math.* **3,** 241.

Freeman, N. C. 1955 *Proc. Roy. Soc.* A, **228,** 341.

Lapworth, K. C. 1956 Ph.D. Thesis, Manchester University.

Lighthill, M. J. 1949 *Proc. Roy. Soc.* A, **198,** 454.

Whitham, G. B. 1957 *J. Fluid Mech.* **2,** 145.

REVIEWS

Relaxation Methods in Theoretical Physics, Volume II, by R. V. SOUTHWELL. Oxford : Clarendon Press, 1956. 274 pp. 55*s*.

It is not often that a scientific treatise is at once a comprehensive account of the subject and a record of much of the professional career of the author. But Sir Richard Southwell has made the subject of relaxational methods peculiarly his own, and the work reviewed here fits the dual description.

Anticipations or hints by early writers usually make it impossible to set precisely the date of invention of an idea. In 1924 Hardy Cross introduced one of the major concepts of the relaxational approach in conjunction with his ' moment distribution ' method for the calculation of the forces in statically indeterminate structures. Thom's device for solving Laplace's equation (1928) differs from what we now call relaxation only by a small yet important technicality. Be this as it may, the concept and use of the relaxational technique as a systematic device for obtaining numerical solutions to physical problems of all descriptions derives from the investigations of Southwell beginning in 1935. Since that time he has been the high priest of relaxation : a faithful worker, an enthusiastic proponent of its virtues, and, in a small way, the founder of a school. The major part of the literature on the subject is by Southwell and by younger men who entered the field under his tutelage.

This, the second volume of *Relaxation Methods in Theoretical Physics*, appears ten years after publication of the first. The two together make a whole, and they have been so treated for the purpose of this review. In the preface to the first volume, Southwell conceived the work to be " of less concern to engineering than to theoretical physics ", in contradistinction to his 1940 volume on *Relaxation Methods in Engineering Science*. Either Southwell has misjudged the situation, or in the meantime the scope of engineering has grown mightily, for most of the problems he deals with are of first-rate significance in engineering. The stated aims of the two volumes are to set out the underlying theory in a coherent and detailed manner, to describe the various techniques of computation proved by experience, and to convey the rather different atitude conferred by the approach to a physical problem through relaxation. All this Southwell has done in a lucid if rather formal manner.

Both volumes are concerned with physical problems of the classical continuum type. With one minor digression, the range of problems is confined to those having two independent variables : either two space coordinates, or one space and one time coordinate. The first volume begins with a statement of certain aspects of the calculus of finite differences, as a preliminary to the reformulation of partial differential equations as algebraic difference equations. About half of this volume is concerned

with the numerical solution of Laplace's equation in the plane, including conformal mapping by numerical methods, and with the quasi-plane-potential problem. The first volume closes with ' free surface ' problems involving boundaries or interfaces not initially known. The second volume continues with more difficult problems, many of which were still classified when the first volume appeared. It deals principally with the biharmonic equation; with eigenvalue problems; with non-linear problems of large elastic distortions, viscous fluid motions, and plastic straining; and it concludes with a brief resumé of recent innovations in relaxation.

When a differential equation purporting to describe a physical phenomenon does not yield to analysis, relaxation, with its entirely different outlook, may be used to advantage. The relaxer does not think in terms of independent and dependent variables as such. He fastens attention on the *numerical* values of the wanted quantity at the nodal points of a finite net in the plane (or the space) of the independent variables. Relaxation comprises a systematic method for determining these numerical values so that they satisfy the finite-difference version of the differential equation. Once the problem has been formulated in terms of relaxation operations indicating the steps required to liquidate the residues (or errors) of the finite-difference equation, its numerical solution requires only simple arithmetical calculations.

Southwell quite rightly brings in much physical argument, for this helps the relaxer to get on with his job. But the reviewer is not the first to be irritated and distracted by Southwell's insistence on thinking of so many problems in terms of the analogy of the force-displacement system in a net made up of strings. This does in fact permit one to revive in a rather strained form the original meaning of the term ' relaxation ', that is, the systematic relaxation of artificial constraints at the joints of a redundant structure, until, all such artificial constraints having been relaxed, the solution sought for is at hand. But while the string-net analogue may somehow illuminate for Southwell problems in, say, potential fluid motion, it interferes with clarity of presentation for others.

Relaxation has a brute force quality which makes it possible, at least in principle, to solve numerically any problem that can be quantitatively formulated in terms of algebraic, differential or integral equations. The wielder of the pencil need know no mathematics beyond arithmetic. Nevertheless mathematical skill and physical insight are assets which usually greatly reduce the time required to effect a solution. Above all, the calculator should have the qualities of an accountant—patience, neatness, and an empathy for numbers. While the arithmetical operations are simple enough, the whole process proceeds rapidly only after a certain amount of experience has been gained. On new and exceptionally difficult problems, the circumstances are often such that various bits of analysis must be invented *ad hoc* as the calculations proceed, and the formulator of the problem may easily find himself in the position of doing the tedious arithmetic. After the few weeks or months required to complete his

problem, he has become an expert relaxer, but unless he is one of those for whom relaxation possesss a special fascination, he may thenceforth avoid it like the plague.

The present position of relaxation methods so far as the differential equations of mathematical physics are concerned is that it has indeed demonstrated its ability to solve problems before which more orthodox mathematical methods fail. From a practical point of view, these may be classified in two categories. In one class, e.g., Laplace's equation for plane, irrotational motion of an incompressible fluid, the calculations are so straightforward and progress so rapidly toward a solution that the method is perfectly feasible for the engineering office or for almost any circumstance where, say, a day's labour is not excessive. The other class, e.g., the motion of compressible gases at high speed, or the viscous motion of fluids when inertia cannot be ignored, contains problems requiring the labour of weeks or even months, with the frequent application of analytical thinking. Such problems demand a determined and motivated individual who can spend the necessary time without distraction. One need hardly say that such is not likely to be the case in an engineering office. But the solutions of even a few such problems may settle certain crucial questions arising in a research effort, and each problem solved may exemplify some phenomenon in such manner as to enlarge greatly our understanding if not our capacity to deal quantitatively with it.

An enumeration of titles from the " Index of Problems Solved " delineates the range of problems in fluid mechanics that have yielded to relaxational methods :

Conformal transformation of an area into a circle;
Conformal representation of the region external to an airscrew section into the region external to a circle;
Oil pressure-distribution in a plane slider bearing;
Oil pressure- and temperature-distributions in a partial-journal bearing;
Flow of gas through a convergent-divergent nozzle;
Percolation through an earth wall;
Laminar flow through a two-dimensional Borda mouthpiece;
Orifice plate in a circular tube;
Free jet falling under gravity (' waterfall ');
Slow motion of viscous fluid through a two-dimensional nozzle;

Only a fraction of the book is concerned with problems of fluid mechanics, however. Major sections deal with elasticity, plasticity, and vibrations, and a few problems in heat conduction and electricity are discussed.

The final chapter of Volume II, apparently written after the main body went to press, gives brief accounts of two recent ideas, both due to D. N. de G. Allen. The first employs the device of isometric representation on a single sheet of paper to effect a three-dimensional relaxation solution, a feat which would strain the sanity of any one attempting it on multiple

leaves of paper. The second converts a ' marching ' type of problem to one of ' jury ' type, thereby making the problem accessible to relaxation methods. The trick here is to effect a substitution of variables which yields an equation of higher order; since the actual number of physical boundary equations is unaltered, one or more boundary conditions in the substituted variable becomes free both in its value and in its location, and the problem expressed in the substituted variable may thus be framed in the jury form. By this device the parabolic differential equations of unsteady heat conduction, for instance, may be solved by relaxation.

Although Southwell's single-minded enthusiasm might lead one to believe otherwise, there are few circumstances in which a relaxation solution would be preferred to an analytical solution. Questions of computation time aside, the analytical solution possesses two decisive advantages. A single analytical solution in closed form actually comprises many solutions by reason of the parametric constants which appear. And, of great importance to the applied physicist and engineer, it exhibits in condensed form certain patterns of physical behaviour which no mere collection of sheets of relaxation solutions, each with its own array of numbers, can possibly evoke.

Southwell's presentation of the subject incorporates a balance between the physical, the mathematical, and the computational sides. Much of the subject matter is discussed in reference to specific physical problems, and many complete numerical solutions are displayed elegantly and clearly. However, one looks in vain for any critical assessment of the physical models employed, or for meaningful interpretations of the results. Southwell considers the problem ' solved ' when the numerical solution is completed. This should be taken as an observation rather than a criticism, for the book is really concerned with relaxation *methods* and not with physical problems. The mathematical aspects are given their full share of attention, with the thought that this would be one of the more useful items for those who might wish to apply relaxation to an as yet unsolved problem. The various labour-saving tricks of computation and schemes for economically organizing the work are discussed to the point where further elaboration would not be as useful as actual practice on the part of the reader.

It is disappointing that, in a book concerned with numerical methods of solution, there is no discussion of the relationship of relaxation methods to the recent flourishing progress in high-speed machine computation. Relaxation calculations for differential equations with two or three independent variables pose difficulties for a high-speed machine because information must be remembered at a great many net points. Several questions come to mind. Having regard for the special characteristics of digital computers, how can the relaxation procedure be adapted to use best the machine's limited memory but great speed ? Is it feasible or desirable to use many fewer net points in conjunction with higher-order terms in the Taylor-series expansion about a central point ? Is it better

for the machine to search for the largest residual or to relax the residuals at the net points in some fixed geometrical sequence? The reviewer would have welcomed reflections along these lines.

Finally, brief mention may be made of two other books on relaxation methods*. These are both much shorter books dealing with the whole of the subject in the sense that algebraic equations and ordinary differential equations, as well as partial differential equations and eigenvalue problems, are treated. Shaw's book omits all discussion of physical problems, and is focussed on the mathematical theory underlying relaxation and on the computational procedures. Allen's book is more akin to Southwell's in its description and illustration of the subject through the medium of physical problems.

For the novice to the subject, Allen's book is, in the opinion of this reviewer, the easiest and best organized introduction to the subject. Southwell's book is the definitive treatise on the subject, giving extensive details of the physical, mathematical, and computational sides, and constituting a compendium of the significant types of problems accessible to relaxation. And Shaw's book seems best suited as an introduction for those interested only in the mathematical and computational aspects of relaxation.

A. H. SHAPIRO

Proceedings of the 8th International Congress on Theoretical and Applied Mechanics (Istanbul, 1952). Published by the Faculty of Science of the University of Istanbul. Vol. 1, 1953; 529 pp. Vol. 2, 1955; 203 pp. £3 15*s.* 0*d.* for the two volumes.

These two volumes providing a record of the 8th International Congress for Applied Mechanics, held at Istanbul in August 1952, are now available in Britain and U.S.A. The first volume contains the list of members of the congress, the scientific programme, the addresses read at the opening and closing sessions, and summaries (a page or two in length) of the 336 papers read at the congress. The second volume contains extended accounts of most of the seven general lectures and ten sectional addresses.

* *An Introduction to Relaxation Methods*, by F. S. Shaw. New York: Dover, 1953. *Relaxation Methods*, by D. N. de G. Allen. New York: McGraw-Hill, 1954.

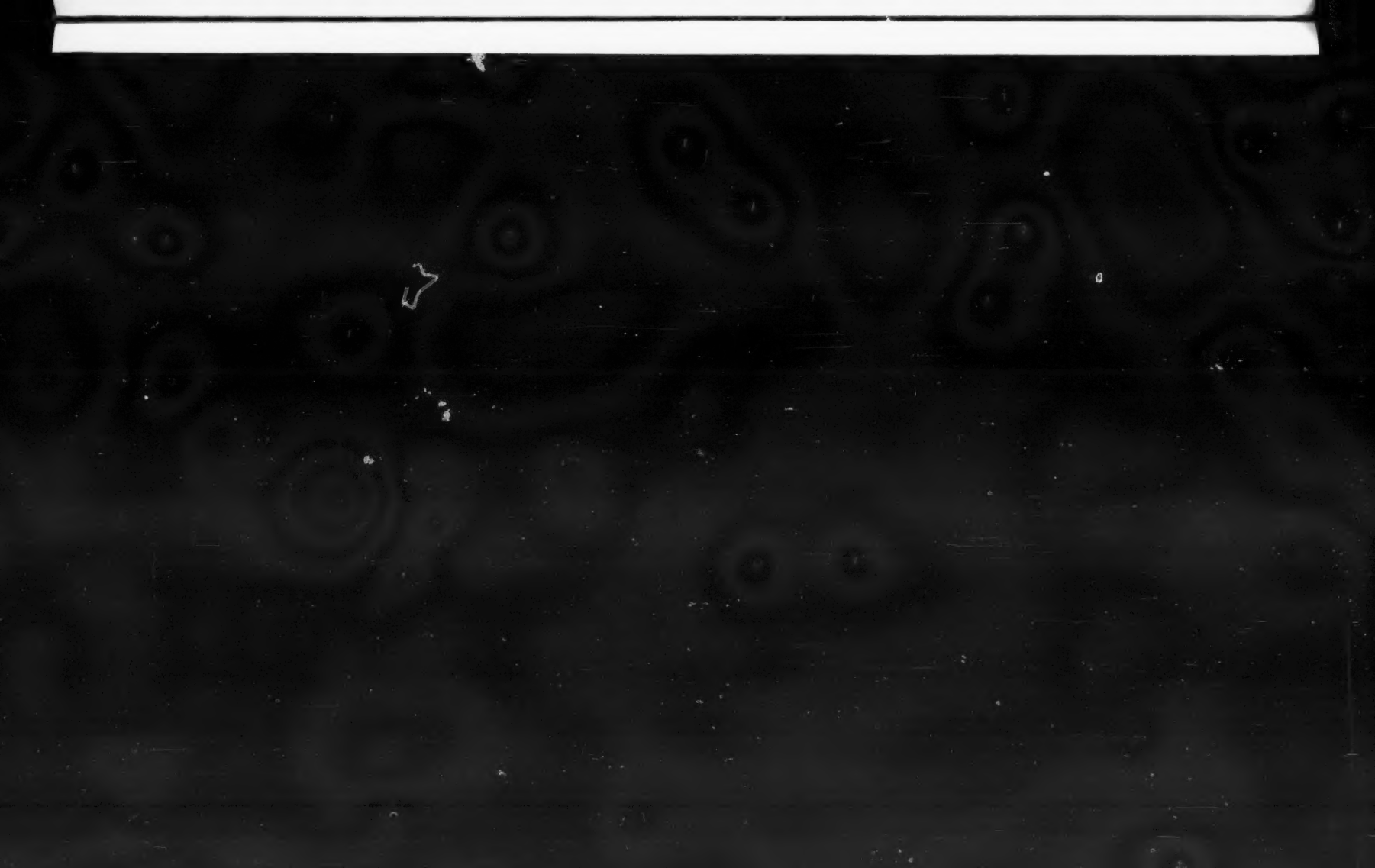

JOURNAL OF
FLUID MECHANICS

—o—

Orders originating

in

UNITED STATES OF AMERICA

and

CANADA

should be sent to the sole agents

ACADEMIC PRESS INC.

111 Fifth Avenue,

New York, 3,

N.Y., U.S.A.

JOURNAL OF FLUID MECHANICS
Volume 2, Part 4 June 1957

CONTENTS

Space-time double correlations and spectra in a turbulent boundary layer
by A. J. FAVRE, J. J. GAVIGLIO and R. DUMAS 313

On the hydrodynamic stability of two viscous incompressible fluids in parallel uniform shearing motion
by SAUL FELDMAN 343

Oscillations of tide and surge in an estuary of finite length
by J. PROUDMAN 371

An electronic analogue for supersonic flow
by LESLIE S. G. KOVÁSZNAY 383

On the stability of plane shock waves
by N. C. FREEMAN 397

Reviews 412